Doctoral theses at NTNU, 2021:412

Evelina Folkesson

A Study of Models for Prediction of Treatment Response in Cancer

Doctoral thesis

NTNU
Norwegian University of Science and Technology
Thesis for the Degree of
Philosophiae Doctor
Faculty of Medicine and Health Sciences
Department of Clinical and Molecular Medicine

NTNU
Norwegian University of
Science and Technology

Evelina Folkesson

A Study of Models for Prediction of Treatment Response in Cancer

Thesis for the Degree of Philosophiae Doctor

Trondheim, December 2021

Norwegian University of Science and Technology
Faculty of Medicine and Health Sciences
Department of Clinical and Molecular Medicine

NTNU

Norwegian University of
Science and Technology

NTNU
Norwegian University of Science and Technology

Thesis for the Degree of Philosophiae Doctor

Faculty of Medicine and Health Sciences
Department of Clinical and Molecular Medicine

ISBN 978-82-326-6092-6 (printed ver.)
ISBN 978-82-326-5440-6 (electronic ver.)
ISSN 1503-8181 (printed ver.)
ISSN 2703-8084 (online ver.)

Doctoral theses at NTNU, 2021:412

Printed by NTNU Grafisk senter

Abstract in Norwegian

Kreft kjennetegnes av molekylære forandringer som resulterer i unormal og høy celledeling. Opp gjennom årene har et vesentlig antall kjemoterapier rettet mot å hemme denne celledelingen blitt godkjent for bruk i behandling av kreft. Anvendelsen av disse har ført til generelt forbedrede prognoser for kreftpasienter, men fortsatt er det slik at langt fra alle pasienter responderer på slik behandling, og i tillegg opplever mange bivirkninger. For å øke effekten av kreftbehandling, fokuserer mye av dagens forskning på mulighetene for mer målrettet behandling ved å spesifikt angripe de molekylære endringene som gir opphav til sykdommen. Denne behandlingsformen antas å være gunstig av flere grunner, blant annet ved at bivirkningene blir mindre, og ved at mulighetene for persontilpasset behandling blir større. Selv om målrettet behandling i teorien er en lovende strategi, er det også flere utfordringer. En av disse utfordringene er knyttet til plastisiteten til kreftceller, der endringer i kreftcellenes molekylære signalertrafikk ofte gir opphav til behandlingsresistens. Bruken av medikamentkombinasjoner har vist seg å være en effektiv strategi for å omgå resistens, men på grunn av det astronomiske antallet mulige kombinasjoner som må undersøkes eksperimentelt, har relativt få blitt vurdert, godkjent, og nådd klinisk bruk. I tillegg antas mangler i den biologiske likheten mellom mange av dagens eksperimentelle kreftmodeller og virkelige svulster å føre til lite samsvar mellom eksperimentelle og kliniske responser.

Med hovedmål om å øke kunnskapen om hvordan kreftbehandling kan effektiviseres, var arbeidet i denne doktorgraden spesielt rettet mot å undersøke 1) hvordan bruk av mer avanserte eksperimentelle kreftmodeller, med antatt økt klinisk relevans, kan brukes i høykapasitets-utprøving av mange medisiner, og 2) hvordan datamodeller kan brukes som verktøy i søket etter effektive medikamentkombinasjoner. Gjennom en storskala studie som studerte effekten av 21 medikamentkombinasjoner i klassiske (2D) og mer avanserte (3D) eksperimentelle kreftmodeller, ønsket vi å finne forskjellene i medikamentrespons forårsaket av forskjeller i den tredimensjonale oppbyggingen av kreftsvulster. Resultatene fra studien viste signifikante forskjeller i kombinasjonseffekt mellom kreftmodeller, som igjen belyser viktigheten av å nøye vurdere den kliniske relevansen av ulike modeller ved design av eksperimentelle studier. Av de 21 medikamentkombinasjonene som ble testet i studien, ble en betydelig andel funnet å være ineffektiv i begge modellene. For å vise at datakraft kan brukes til å forutsi medikamentrespons og dermed fungere som et verktøy for effektivisering av eksperimentelle studier, designet vi en datamodell basert på medikamentene som er inkludert i kombinasjonsstudien vår. Datamodellen ble oppdatert basert på eksperimentelle funn, og kunne deretter brukes til å identifisere en rekke nye

medikamentkombinasjoner med mulig høyere effekt. Alle disse ble bevist riktige i en oppfølgingsstudie, som viser kraften i å bruke datamodeller for å effektivisere eksperimentelle studier av medikamentkombinasjoner. Avslutningsvis, rettet mot å ytterligere øke den kliniske relevansen av eksperimentelle kreftmodeller, utviklet vi en metode for medikamentresponsstudier i primære pasientderiverte kreftmodeller (sfæroider). Denne studien viste klare forskjeller i respons mellom sfæroider fra forskjellige pasienter, som igjen understreker relevansen av persontilpasset behandling av kreft.

Table of Contents

Abstract

Cancer is characterised by molecular alterations that lead to abnormal and excessive cellular proliferation. Over the years, a considerable number of chemotherapies, aimed to prevent proliferation by inducing cell death, have been approved for treatment of cancer. The use of such therapies has led to an overall increase in the quality of life and survival of cancer patients, but far from all patients respond to treatment. In addition, many patients experience side-effects to therapies. Seeking to increase the effect of cancer therapies, today's research has turned towards the possibility of treating cancer using strategies that more specifically target the molecular alterations that are the assumed cause of the disease. Treating cancer by specific targeting of aberrant molecular mechanisms is believed to be beneficial from several points of view. As treatments are designed to specifically target cancer cells, the risk for side-effects is supposedly lower. Also, based on evidence of large molecular heterogeneity between cancer patients, targeted therapy is a promising strategy for personalising cancer treatment. Although a promising strategy in theory, the reality of targeted therapy however faces multiple challenges, including, 1) molecular signalling of cancer cells, which is highly adaptive and often results in treatment resistance. While resistance may be circumvented by administrating drugs in combinations 2) identifying such combinations is challenging due to the large combinatorial space that experimentally needs to be explored. In addition, 3) biological discrepancies between in vitro cultures and tumours in vivo are large, which may contribute to low clinical translatability of therapies identified as successful in vitro.

Ultimately seeking to contribute to increased knowledge on how to improve cancer treatment, the work of this thesis was aimed at investigating 1) how drug response can be assayed in more complex culture models that more closely mimic a clinical setting, and 2) how computational models can be employed in the search for synergistic drug combinations.

By performing an unbiased high-throughput screen of 21 drug combinations in planar (2D) and spheroid (3D) cultures of colorectal cancer cell lines, we studied the impact of culture complexity on drug combination effects. We found that drug synergy in general was more pronounced in 2D-cultivated cells, but also noticed that 3D-cultivated cells were more sensitive and showed greater synergistic response to specific combinations. Altogether the results from the study hence indicated that already at the cell line level, culture complexity has a significant impact on drug response, which in turn highlights the importance of careful selection of the most clinically relevant in vitro culture system when seeking to make the most possible out of drug response data. To take 3D models as a tool for in vitro screening one step

closer to a clinical scenario we also developed a procedure for drug testing in patient-derived tumour spheroids. Doing so, we were able to show that by studying just a small group of samples we could capture sample-heterogeneity in terms of growth rate and drug response. These results highlight the relevance of tailoring cancer treatment to individual patients. Both the combination screen and evaluation of response in patient-derived tumour spheroids were performed in an exhaustive design testing all potential drug combinations. To show that computational modelling can be used for prediction of drug response and hence guiding of drug screens, we constructed a mechanistic computational model encompassing signalling pathways known to be dysregulated in multiple cancers. By adjusting the model to increase its predictive capacity for pairwise combinations, we next used it for prediction of synergistic third and fourth-order combinations. The model identified three synergistic third-order combinations, out of which all were confirmed in a subsequent screen. Altogether the results point towards the benefits of using computational tools when designing large-scale experiments.

To summarise, this thesis presents a thorough study of models and strategies available for preclinical testing of drugs and drug combinations. As investigated models span over a wide range of application areas, the study is expected to cover many of the aspects of preclinical drug testing; from early computational simulations of drug response to in vitro screening of clinically approved agents in patient-derived tumour cultures.

Acknowledgements

I would like to express my sincerest gratitude to my supervisor, Dr. Åsmund Flobak, for having stood by my side and supported me since day one of this PhD. In May 2017 I came to Trondheim as a young scientist, with quite a limited set of skills and with a clearly defined, and very small, professional comfort zone. Today, thanks to your excellent supervision and your ways of always encouraging me, I feel more confident and capable than I have ever done before. You have believed in me at times when I have not believed in myself, and if I ever get the chance to supervise a student on my own, I will remember all the time and encouragement you have invested in me and pay it forward.

I would also like to thank my co-supervisors Professor Astrid Lægreid, Professor Liv Thommesen and Dr. Geir Klinkenberg for great supervision and support. Thank you for contributing with your invaluable knowledge and perspectives on science, and for always making my work feel valuable.

To my collaborating authors Barbara Niederdorfer, Vu To Nakstad, Cristoffer Sakshaug, Andrea Draget Hoel, Tonje Husby Haukaas, Margrét Sylvía Sigfúsdóttir, Torkild Visnes, Arne Wibe, Liv Thommesen, Astrid Lægreid, and Åsmund Flobak; thank you for excellent collaboration, communication and for all the fun we have had together in the lab, lunchrooms and meetings.

Also, thanks to all current and former collaborators within the DrugLogics Initiative. Thank you for great discussions, for always contributing with new and interesting perspectives on science and for showing me that if we are to succeed within medical science, working interdisciplinary is the way forward.

I would also like to thank my colleagues at Gastrosenteret, Kunnskapssenteret, and Laboratoriesenteret at St. Olav's Hospital, Trondheim. Thank you for all the assistance in the lab, for always meeting me with a smile, and not least for all the laughs and relaxing discussions in the lunchroom. Additionally, I would like to thank the surgical teams that I have met when collecting tumour samples at Gastrosenteret's Dagkirurgi, St. Olav's Hospital. Thank you for your helpfulness and kindness, and for your interest in contributing to our research.

To personnel at SINTEF Biotechnology and Nanomedicine, with whom I have spent most of my lab time during the past four years; thank you for always making me feel like I was one of you, for your endless support in the lab and for all the fun we have had together. Working with you has been an absolute honour!

To my Trondheim friends, thanks for your endless support and for making me feel that I will forever have a home away from home. A special thanks to Kathleen Heck and Barbara Niederdorfer for letting me be a part of your lives and for showing me that it is possible to be colleagues and great friends at the same time. Getting to know you was for sure the best part of this PhD.

I would also like to express my gratitude towards my friends and family back home in Sweden. Although I have not been much around for some time, you have always made sure that I have felt involved in your lives and your faith in me has never ceased. Mum and Dad, thank you for your love and support, for always emphasizing the value of getting a good education, and for encouraging me to follow my dreams. To my sister Malin, thank you for being my best friend, for sharing my sense of humour, and for always caring more about how I am, than about my performances.

At last, Filip, thank you for your love and support and for encouraging me to go on this adventure although I know how deeply you wanted me to stay. Deciding to move so far away from you was the hardest decision of my life and knowing that I would one day come back to you for good has been my strongest motivation to keep going during these past four years.

List of Papers

The PhD thesis is based on the following original manuscripts, two with a joint first authorship and one as first author:

Paper 1: High-throughput screening reveals higher synergistic effect of MEK inhibitor combinations in colon cancer spheroids. Evelina Folkesson*, Barbara Niederdorfer*, Vu To Nakstad, Liv Thommesen, Geir Klinkenberg, Astrid Lægreid, Åsmund Flobak. 2020. *Scientific Reports*. doi: 10.1038/s41598-020-68441-0.

* Joint first authorship

Paper 2: Synergistic effects of complex drug combinations in colorectal cancer cells predicted by logical modelling. Evelina Folkesson, Baard Cristoffer Sakshaug, Andrea Draget Hoel, Geir Klinkenberg, Åsmund Flobak. 2021. Manuscript submitted.

Paper 3: Growth and treatment response of colorectal cancer spheroids evaluated with imaging. Evelina Folkesson*, Baard Cristoffer Sakshaug*, Tonje Husby Haukaas, Margrét Sylvía Sigfúsdóttir, Torkild Visnes, Arne Wibe, Liv Thommesen, Astrid Lægreid, Geir Klinkenberg, Åsmund Flobak. 2021. Manuscript.

* Joint first authorship

Abbreviations

DNA	Deoxyribonucleic acid
5-FU	5-Fluorouracil
ATP	Adenosine triphosphate
CDK	Cyclin-dependent kinase
CRC	Colorectal cancer
DDR	DNA-damage response
DSB	Double-strand break
KEGG	Kyoto Encyclopedia of Genes and Genomes
mAb	Monoclonal antibody
ODE	Ordinary differential equation
PARP	Poly (ADP-ribose) polymerase
PDTS	Patient-derived tumour spheroid
PKN	Prior knowledge network
SMI	Small molecule inhibitor
SSB	Single-strand break

Introduction

Each year accounting for the death of millions of people worldwide[1], cancer constitutes a growing threat to global health. While decades of research have been aimed at uncovering universal treatment options for the disease, most of the findings point in the same direction: cancer is a highly heterogeneous disease, both in terms of progression and treatment response[2]. Consequently, researchers have turned their focus towards the possibility of adapting cancer treatment to better fit individual patients; a strategy called *personalised medicine*[3].

Today, we are for certain cancer subtypes partly there, as several examples of successful applications of personalised medicine have been brought into the light during the past two decades[4,5]. However, despite the overall promise of this treatment strategy, personalised medicine is still faced by multiple challenges. Some of them relate to the economic aspects of individualising treatment, others to the ethical issues[6,7]. Some of the more practical challenges are related to the selection of the most efficient treatment strategy for each patient, a process that, before advancing to the clinical setting, requires systematic procedures for testing large numbers of therapeutic options in clinically relevant in vitro and in silico models[8,9]. By investigating the landscape of such preclinical models available for evaluation of cancer treatment response, the greater aims of the work presented in this thesis are to contribute to scientific progress within the field of personalised medicine in general, and to streamlining treatment selection in particular.

In the subsequent introductory text, I aim to give the reader a theoretical background to the main topics of the thesis: (1) drug combinations as means to individualise cancer treatment and counteract development of resistance to cancer therapy, (2) high-throughput screening as a tool for evaluating the effect of drugs in vitro, and (3) computational modelling as a tool for prediction of the effect of anti-cancer therapy in silico. I will start by giving a general background to the development of cancer, by highlighting the multitude of dysfunctional events that ultimately lead up to the transformation of normal cells into cancer cells. In the light of cancer as a multifaceted and adaptive signalling disease, I then introduce the concepts of cancer systems biology and combination therapy and describe how these can be employed in cancer therapy. Parts three and four give the reader an overview of strategies for high-throughput screening and computational modelling of signalling networks and describe how such methods can be implemented for prioritization of therapeutic agents. The objectives of the thesis are outlined in *Objectives of the study*.

The Development of Cancer

Cell Proliferation throughout Life

The human body is a complex organism, consisting of trillions of cells. Every human life however starts with a single cell, and for the complex structures of you and me to develop, a significant amount of cell proliferation is needed. Proliferation takes place during the early development and is characterised by a cell's growth and division to produce daughter cells. As cells formed during the early development eventually gain specialised skills and find their functional context in different tissues and organs, their proliferation rate usually decreases, but with large variations between tissues, from tissues where most cells are in a resting state, to tissues with a high turnover due to tissue renewal. Apart from a few cells which never divide again, most cells retain the capability to start proliferating whenever they need to. The latter is the case when cell replacement is needed due to e.g., tissue injury or loss due to normal wear and tear[10,11]. When new cells are needed by the body, resting cells are stimulated to start proliferating. Upon this stimulation, the cell leaves an arrested state and enters the cell cycle. The cell cycle consists of the four stages G1, S, G2 and M, whose collective task is to, for each lap in the cycle, produce two new cells, identical to the mother cell[12,13]. A cell's progression through the cell cycle is closely monitored by multiple molecular surveillance systems, and decision to continue is assessed at multiple points throughout the cell cycle[14]. These checkpoints serve to guarantee that proliferation is carried out in a way that is influenced by both cues from neighbouring cells and cues that are cell-intrinsic. In particular, several of the checkpoints ensure the integrity of DNA, a highly important task, as abnormal cellular proliferation threatens the integrity of both the cell and the organism. For each cell division there is a small but not negligible risk of introducing alterations to the DNA, called mutations. With accumulation of mutations the growth capacity of the cell can be influenced to neither take cues from the neighbouring cells, nor to ensure continued integrity of DNA.

A Cancer Cell Arises

Uncontrolled proliferation is a key feature of cancer, enabled by defects in multiple systems that are supposed to regulate cellular growth[15]. Molecular defects resulting in the growth advantage of cells are often considered as hallmarks of cancer. In January 2000, Douglas Hanahan and Robert Weinberg published the paper *The Hallmarks of Cancer* presenting a thorough literature study of factors that govern the transformation of normal cells into cancer cells[16]. With this study, the authors aimed to show that most, if not all, cancers share a relatively small number of traits, so-

called acquired capabilities, which collectively support tumour growth[16]. The six hallmarks originally presented by Hanahan and Weinberg are summarised below.

- **Self-sufficiency in growth signals.** To be able to grow and divide, all cells are dependent on receiving signals that tell them to do so. Such signals are often received by membrane-bound receptors, which transmit the signal across the cell membrane, where then other molecules take over the role as intracellular signalling mediators[17–21]. In normal cells, the transduction of pro-proliferative signals is tightly regulated to ensure that cells only commit to cell division when they receive exogeneous growth stimulation[17]. Most cancers, however, depend less on such stimulation as they have invented strategies for how to produce growth-promoting signals themselves. This may occur by multiple different means, out of which mutations resulting in overexpression of intracellular components responsible for transducing the signals probably is the most common[22–29].

- **Insensitivity to anti-growth signals.** Just as much as growth-promoting signals encourage cells to proliferate, growth-inhibiting signals prevent the proliferation from being excessive[17]. Normally, unwanted cellular growth is prevented by growth-inhibitory proteins of the cell cycle, such as the retinoblastoma protein and p53, which particularly govern the transition from G1 to S phase[30,31]. In many types of cancers, one or both of these and other growth-inhibiting proteins are lost, consequently resulting in the constant activation of the cell cycle[32–35].

- **Evading apoptosis.** The apoptotic program, comprising a series of events by which cells may undergo regulated death, is present in latent form in virtually all cells in the human body. Under normal conditions, this program ensures that cells that do not display enough capacity for life do not continue to be a potential source of proliferation[36]. Upregulation of anti-apoptotic proteins, as well as downregulation of pro-apoptotic proteins are frequently observed in cancer, which altogether has been found to render cancer cells insensitive to conditions which normally would be associated with regulated cell death[37–41].

- **Limitless replicative potential.** All the above-mentioned acquired capabilities provide cancer cells with a replicative advantage. Normally, the acquisition of one or several of these traits would however not constitute that much of a threat, as healthy cells carry a program which prevents them from undergoing too many replication cycles[42]. Not surprising, cancer cells have acquired the capability to continue replicating far beyond what is normal for

non-cancerous cells; a trait which in 85-95% of all cancers has been found to be enabled by an upregulation in an enzyme, telomerase, which ensures the constant rebuilding of chromosomes[43–45].

- **Sustained angiogenesis.** During the development of tissues and organs, the increased need for oxygen and nutrients is met by an increased formation of blood vessels; a process called angiogenesis[46]. As organs become fully developed, the formation of new blood vessels eventually ceases, and in order to grow large, tumours must at some point, acquire the capability to reactivate angiogenetic capacity[47]. In most cancers, the latter is enabled by altered expression of angiogenetic inducers and inhibitors, which in turn results in a change in the balance between these factors and a push towards angiogenesis[48].

- **Tissue invasion and metastasis.** Eventually most untreated tumours acquire the capability to invade surrounding tissue and spread to distant parts of the body where new tumours, metastases, are formed. Tissue invasion and metastasis have been found to be the results of changes in the physical coupling of cancer cells to each other and to their microenvironment, which eventually allows the cells to detach from the primary tumour. Alterations in cell adhesion molecules (CAMs) are frequently observed in metastatic tumours, and are believed to be some of the key steps to metastasis[49,50].

In 2011, Hanahan and Weinberg revisited the topic and extended the list of hallmarks based on the recognition that the acquisition of the previous six hallmarks is made possible by additional *enabling characteristics*[51]. The development of genomic instability was highlighted as the most prominent enabling characteristic and is referred to as a higher mutational frequency in cancer cells compared to normal cells, a feature that in turn enables the acquisition of the substantial number of mutations needed for the other hallmarks to occur. The authors highlighted that the development of genomic instability arises from either or both of 1) increased sensitivity to mutagenic agents and 2) breakdown of components in the genomic maintenance machinery where p53 is considered to play a major role. Further, tumour-promoting inflammation was highlighted as another enabling characteristic, whereas reprogramming of metabolism and evasion of immune destruction were considered as *emerging hallmarks.*

Treatment of Cancer

While the number of acquired capabilities accounting for the transformation of normal cells into cancer cells is relatively small, one must remember that the acquisition of each one of the traits often depends on molecular alterations in multiple components involved in proper execution of affected cellular functions. In addition, distinct combinations of molecular alterations may lead up to each of the cancer hallmarks, which altogether makes cancer a highly heterogeneous disease. Despite this, cancer has traditionally often been treated as a uniform disease, using methods aimed at targeting general cellular targets or traits.

DNA-Damaging Therapies: Chemotherapy and Radiotherapy

History

For almost a century, chemotherapy and radiotherapy have been two of the leading modalities for treatment of cancer, in addition to the surgical approaches[52,53]. The era of cancer chemotherapy began in the early 1940s with the observation of the anti-tumoral effects of an alkylating agent, nitrogen mustard, in lymphoma patients[54,55]. The use of radiation to treat cancer is considered to have started multiple decades earlier, with reported use as early as in the late 1800s[56]. The early use of these treatment methods was associated with modest efficacy and severe side-effects, in large due to a lack of understanding of the molecular effects of the treatments on *all* cells in the body[54,56]. An increased understanding of these effects as well as of the inherent responding mechanisms of our cells has led to improvement of both chemotherapy and radiotherapy[52,57].

General Mechanism of Action

While strikingly different to their physical nature, chemotherapy and radiotherapy share multiple properties that make them suitable for treatment of cancer. Especially, both treatment modalities exert their anti-tumoral effects by inducing direct or indirect DNA damage in cells[52]. Depending on the type of the induced damage, the cells respond by activating various DNA damage response (DDR) pathways, whose main purpose is to either activate mechanisms for repair of DNA, or, if the damage is too large, induce apoptosis[58]. Distinct types of DDR pathways have been found to be activated upon treatment with various types of chemo and/or radiotherapeutics. Altogether this stems from the fact that various treatments have been found to compromise DNA integrity in distinct ways[52]. As an example, the two

chemotherapeutic agents oxaliplatin and 5-fluorouracil (5-FU), which are both used for treatment of advanced colorectal cancer (CRC), induce DNA damage by strikingly different means. The platinum-based compound oxaliplatin exerts its DNA-damaging effect by forming intra- or inter-strand crosslinks (ICLs)[59], whereas the antimetabolite 5-FU, on the other hand, induces DNA damage by either inhibiting synthesis of thymidine, one of the major building blocks of DNA, or by outcompeting thymidine in DNA strands. These are events which ultimately lead to the induction of either single-strand breaks (SSBs) and/or double-strand breaks (DSBs)[52].

Treatment Resistance

The implementation of oxaliplatin, 5-FU and a range of other chemotherapies and radiotherapies has improved the prospects for cancer patients, but despite this positive trend, many cancer patients still fail to respond to treatment or are found develop treatment resistance over time. Resistance to especially chemotherapy can occur at many levels, whereof changes in the processing of treatment-induced damage and evasion of apoptosis are two that also apply to radiotherapy resistance[60]. Resistance due to changes in the processing of DNA damage may occur if these changes lead to increased activity of pathway(s) responsible for repairing the damage[60,61]. Resistance due to evasion of apoptosis may on the other hand arise if proteins involved in regulating the onset of apoptosis are dysfunctional. Here, the tumour suppressor protein p53 is considered to have a major role, as the protein normally promoting onset of apoptosis upon irreparable DNA damage[62–64].

To increase the effect of especially chemotherapeutic agents, a great deal of the last decades' research within cancer therapy has been focused on developing agents that specifically target and inhibit damage repair pathways and other cellular components contributing to resistance[52]. In particular, it has been shown that cancers with compromised DNA repair, which is a way of enabling a cancer-beneficial higher mutation rate, can be targeted with drugs that increase DNA damage beyond the point where cancer cells can benefit from the high mutation rate: poly (ADP-ribose) polymerase (PARP) protein inhibitors[4,65]. By inhibiting these proteins, which have a vital role in the repair of especially SSBs, PARP inhibitors have been found to potentiate the effect of both therapy-induced and natural DNA damage[52,66]. Due to their role in the repair of DNA damage, PARP inhibitors are often referred to as DDR modulators, but they also belong to a class of cancer therapy called *targeted therapy*.

Cancer-Signalling Therapies: Targeted Therapies

Concept

Targeted therapy, or molecularly targeted therapy, constitutes a treatment method where chemical agents are used in order to specifically target molecules involved in promoting cancer growth and progression[67]. Examples of such molecular targets are proteins involved in pro-proliferative signal-transduction, and those mediating resistance to apoptosis[68]. Due to their target specificity, as well as low toxicity to cells that proliferate by mechanisms other than the intended mechanism, targeted therapies are often considered advantageous over chemotherapy and other broadly acting therapies[3,68,69].

Targeted therapies are typically designed to act on specific molecules that, due to e.g., mutations, predominantly feature in cancer cells and drive cancer growth. Genetic mutations that give rise to a selective growth advantage of cancer cells are labelled driver mutations. Scientific discoveries over the past few decades in genetic sequencing and bioinformatics has enabled the discovery of a considerable number of driver mutations, which has opened new possibilities for targeted treatment of cancer[70].

Types of Targeted Therapies

There are two main classes of targeted therapy: monoclonal antibodies and small molecule inhibitors. Monoclonal antibodies (mAbs) constitute a class of targeted therapy that exhibits high specificity to extracellular proteins such as receptors, to which antibodies bind and thereby interfere with normal receptor-ligand interaction. Targeted therapy using mAbs may induce a range of different effects, including immune system-mediated antibody-dependent cellular cytotoxicity, inhibition of signal transduction pathways, as well as induction of apoptosis[69]. Compared to the other main class of targeted therapy, the small molecule inhibitors, mAbs usually exhibit higher target specificity, but are, due to their large size, typically around 150 kDa, limited to interacting with extracellular targets[71]. Due to the inability of mAbs to target intracellular molecules, which are of main interest in this thesis, I will from now on focus on small molecule inhibitors in the discussion of targeted therapy.

Compared to mAbs, small molecule inhibitors (SMIs) have considerably lower molecular weight, typically less than 1 kDa, and can possess the ability to penetrate cell membranes to reach intracellular targets. SMIs have been found to interact with, and inhibit, a wide range of intracellular targets, whereof kinases has been a long term focus of research[69]. Kinases are protein enzymes that catalyse the transfer of

phosphate groups from ATP-donating molecules to receiving protein target molecules, a biochemical process called phosphorylation. The protein target that is phosphorylated will typically have a shift in its surface charge, which induces a conformational change that can change the enzymatic activity of the target protein. Such phosphorylation regulation accounts for a significant part of pro-proliferative signal transduction. Mutations represent another mechanism by which proteins can have a similar shift in surface charge, for instance in a mutation of a hydrophobic amino acid to a hydrophilic amino acid. Such phospho-mimetic mutations can cause dysregulation with constant activation of kinases that may result in increased proliferation. Altogether this makes kinases attractive targets for SMIs. Kinase inhibitors exert their inhibiting effect by competitively binding to catalytic sites of kinases, thereby preventing ATP from binding to these sites. As the binding of ATP is crucial for the catalytic activity of a kinase, the act of SMIs results in inactivation of the drug-targeted kinase. A list of some examples of clinically approved SMIs is presented in Table 1.

Table 1. Examples of small molecule inhibitors approved for treatment of cancer.

Small molecule	**Target**	**Target type**	**Approved for cancer type**	**Ref.**
Erlotinib	EGFR	Kinase	Non-small cell lung cancer	[72]
Idelalisib	PI3Kδ	Kinase	Chronic lymphocytic leukaemia	[73]
Lapatinib	HER2/EGFR	Kinase	HER2 positive breast cancer	[72]
Sorafenib	VEGFR/KIT/FLT3/PDGFR	Kinase	Renal cancer Hepatocellular carcinoma	[72]
Trametinib	MEK1/2	Kinase	BRAF-mutated melanoma	[74]
Vemurafenib	BRAF	Kinase	BRAF V600E-mutated melanoma	[75]
Olaparib	PARP	PARP	BRCA-mutated advanced ovarian cancer	[76]
Palbociclib	CDK4/6	CDK	Metastatic breast cancer	[77]
Venetoclax	BCL-2	Anti-apoptotic protein	Chronic lymphocytic leukaemia Small lymphocytic lymphoma Acute myeloid leukaemia	[78–80]

Strategies to Increase the Effect of Cancer Treatment

Predictive Biomarkers

As targeted therapies are designed to inhibit specific cellular proteins, stratification of patients to targeted therapy is today to a large degree dependent on our knowledge of the mutational status of proteins that can either be targeted by inhibitors or predict the response of inhibition of other proteins. For example, for the clinical use of the BRAF inhibitor vemurafenib, BRAF V600E mutation, where the hydrophobic amino acid valine (V) at position 600 is replaced by the hydrophilic glutamate (E), is used as a positive predictor of response to this drug for some cancer types (Table 1). The predictive capacity of this mutation stems from the fact that vemurafenib blocks activity of the mutated BRAF protein with a much higher affinity than active wild type BRAF proteins[81]. Likewise, mutated BRCA1/2 is used as predictor of sensitivity to the PARP inhibitor olaparib (Table 1). Here, BRCA1/2 mutation implies non-functional homologous recombination, a feature which makes these cells more dependent on another pathway, base-excision repair, for repair of DNA damage. Base excision repair relies on the presence of functional PARP – hence, inhibition of this protein will render even this repair pathway non-functional, ultimately leading to DNA damage overload, and cellular death. BRAF V600E and BRCA mutations are examples of genetic biomarkers that predict drug sensitivity. Apart from BRAF V600E and BRCA mutations as predictors of sensitivity to vemurafenib and olaparib, respectively, a number of mutations have been identified and approved as genetic markers of sensitivity (or lack of sensitivity) to different targeted therapies[82]. Despite this, for many patients no predictive biomarkers are found, and even in the presence of a biomarker, many patients fail to respond to these treatments. This has been attributed to the fact that single mutations rarely alone are responsible for the progression of disease[83]. To better understand how molecular mechanisms and mutations infer sensitivity as well as resistance to targeted therapy, cancer should instead of being studied as a disease arising from dysfunction in isolated signalling entities and pathways, be studied as a disease where signalling pathways are highly integrated in large signalling networks and where the dynamics of the networks influence disease progression and treatment response[84,85].

Cancer Systems Biology

The behaviour of a cell can largely be described by the joint activity of intracellular components, like transcription factors and protein kinases, and their integrated responses to cell internal and external cues. Traditionally, the effects of these components on cellular phenotypes like proliferation and apoptosis have been described by signalling pathways, like the canonical Ras-Raf-MEK-ERK and PI3K-

AKT signalling pathways. The assumption that the signalling events of these pathways occur independently of each other has enabled the study of their proposed effect on cell fate. Today, however, a major shift is taking place in that rather than being isolated from each other, the signalling pathways of cells are studied as a highly interconnected large signalling network. Studying the dynamics of such networks is considerably less trivial compared to studies of isolated signalling pathways and has called for mathematical and computational solutions.

Systems biology is the study of complex biological systems, like signalling networks, aided by computational and mathematical power and has been widely used in multiple contexts within biology for the past 20 years[84,86–88]. These studies have been enabled by the generation of large datasets of genomics, transcriptomics, proteomics etc., as the foundation for computational and mathematical analysis of biological events. Cancer systems biology is a branch of systems biology, specifically focusing on causes and treatment of disease using cancer-specific data and tools, for the purpose of improving cancer diagnosis and treatment prediction – foundations for personalised medicine[88]. A large part of these studies relies on the power of computational models, which will be introduced later in this thesis. By taking on a network-based approach for studies of cancer cell signalling, cancer systems biology has enabled identification of multiple possible mechanistic causes of tumorigenesis and treatment resistance. This has more than ever highlighted the molecular heterogeneity of cancer and the need for more complex treatment options.

Drug Combinations

Combinations of chemotherapeutic agents have a long clinical history within cancer treatment[54]. Today, also some targeted drug combinations have been approved for treatment of cancer. One example is the combination of dabrafenib (BRAF inhibitor) and trametinib (MEK inhibitor) for treatment of non-small-cell lung cancer and malignant melanoma[89].

Drug combinations are believed to be advantageous over monotherapy (i.e., single-drug treatment), both due to the combinations' expected ability to induce larger absolute effects for the same concentration of individual drugs, and by being associated with reduced side-effects[90]. The observation of a larger treatment effect for drugs administered in combination, compared to when these drugs are administered separately, is referred to as synergy. Drugs' ability to act synergistically may account for reduced side-effects if lower concentrations of the individual drugs can be used to induce the same treatment effect as that induced by higher concentrations of the individual drugs. Reduced side-effects of combinations involving particularly targeted drugs can also be ascribed to the even higher specificity by which these combinations can target cancer cells. However, it should

be kept in mind that synergistic toxicity is also conceivable. Using drug combinations for treatment of cancer has also been suggested as a promising approach to overcome resistance to monotherapy. Here, the superiority of drug combinations is ascribed to the combinations' ability to simultaneously interfere with multiple parts of the cancer signalling network and by these means blocking the mechanisms that are normally used by the cell to infer treatment resistance. Targeting multiple pathways jointly, tailored to the experimental cancer system, has also been proposed to allow for higher biological selectivity, which implies that synergistic drug combinations might act more potently on cancer cells than other growing cells in the body, and thus reduce side-effects[91]. Lastly, as drugs can be combined in large number of ways, such combinations hold great promise for personalisation of cancer treatment, where a drug combination can be selected to match the molecular makeup of cancer[92–94].

Identification of Cancer Treatment Effects In Vitro

Increased knowledge of the molecular heterogeneity of cancer as well as the identification of a wide range of druggable targets have increased the demands of parallel testing of large numbers of drugs in large panels of cancer cell cultures. In 1951, the first human cancer cell line HeLa was established from cervical cancer and set the stage for experimentation of cancer drugs without administering these to patients or animals directly[95]. Since then, cancer cell lines from many cancerous tissues have been established and subjected to drug testing in small-scale experiments, and to drug screening in high throughput setups[96,97]. Today, drug screens are typically performed in multi-well plates where each well represents a reaction chamber. The implementation of technology for high-throughput screening has revolutionised the field of drug testing, by providing automated solutions for many of the key steps of in vitro evaluation of drug responses, such as plating of cells in multi-well plates, dispensing of small volumes of drugs to wells, and not least assessment of treatment response. This technological advancement has not only reduced the experimental workload of in vitro drug testing, but also enabled generation of larger amounts of more reproducible data compared to corresponding small-scale experiments. Traditionally, high-throughput drug screens have been performed on 2D-cultivated cell lines, with response assessed using different, mostly viability-based, endpoint readouts assessing ATP content as a surrogate marker for the number of viable cells[98]. The contribution of data from these screens to cancer research has been invaluable – yet the biological relevance of the traditional screening format has been frequently debated, due to e.g., 1) the obvious structural differences between 2D-cultivated cell lines and tumours in vivo[8], 2) possible

limitations stemming from assessment of treatment response at a single timepoint, and 3) the short observation time for drug screens compared to clinical/in vivo tumour growth and responses. Overall, this has led to further advancement of high-throughput screening technology, including implementation of solutions for drug testing in more tumour-like in vitro models and development of phenotypically diverse readouts enabling continuous assessment of response[99].

Culture Formats for High-Throughput Screening

The cell culture constitutes the navel of in vitro drug testing. This is the biological entity which drugs are tested on and whose response lays the foundation for how we evaluate the effect of drugs. Hence, the more extensive the molecular characterisation of these cultures, the more we hope to be able to conclude about the terms of effect of individual and combined drugs. Cell lines constitute one of the most well-characterised in vitro culture models, and due to the ease by which these cells can be cultivated in suspension or on planar plastic surfaces, cell lines are well suited and historically the most widely used culture system for screening in the multi-well plate format[100,101]. However, despite the large number of drug screens performed on traditionally cultivated (2D) cell lines, drugs identified as effective in such screens have often been met by poor clinical translatability[102]. While many different factors may account for the low degree of translatability, the clinical relevance of 2D-cultivated cell lines has been a highly debated topic over the past decades, not least due to the obvious structural differences between cells cultivated on flat surfaces and solid tumours in vivo[8]. An important feature of tumour cells in vivo is the ability of these cells to interact and communicate with each other in all three dimensions - a feature, which to a high degree, is lost in 2D cultures. By maintaining the possibility for cellular interaction in three dimensions, 3D-cultivated cell lines (spheroids) have been suggested to potentially be a biologically more relevant tumour model, compared to 2D cultures[103]. In addition to enabling more extensive cell-cell communication, cell line spheroids have also been found to display several of the gradients frequently observed in tumours in vivo, such as oxygen, nutrient, and proliferation gradients[103,104]. All these are structural characteristics, which may affect how cells respond to drug treatment. While the biological relevance of 3D cultures also has been discussed for almost half a century, their implementation in high-throughput drug screening settings is relatively new. This progress has been enabled by the development of technical solutions for the generation of spheroids in specialized multi-well plate formats, typically employing a U-shaped bottom, and by optimisation of spheroid-specific readout technology for assessment of response[105,106].

While cell lines (2D and 3D) still constitute the most widely used culture system for drug screening and other culture-based applications and has contributed largely to an increased understanding of cancer biology, the relevance of cell lines in personalised drug screening is unclear. This stems in part from these cultures' proposed inability to reflect the cellular heterogeneity of tumours, and which may impact treatment response[107]. Patient-derived tumour spheroids (PDTSs), established directly from primary or metastatic tumours of cancer patients, have been suggested as an alternative model for prediction of individual patient response to drug treatment. The response-predictive potential of these cultures has also been demonstrated in clinical studies[108–111]. While the widespread use of PDTSs in high-throughput drug screens is limited due to the, compared to cell lines, smaller amounts of material typically available, screening of such cultures can, when the quantity of material allows, be performed based on the same principles and technology as for cell lines.

Selection of Doses for Screening

Once seeded in the multi-well plate format, cell cultures can be subjected to large-scale drug screening. This step involves the addition of small volumes of drug solution to each well, where the effect of each drug typically is evaluated at multiple different doses and in several technical replicates. While the selection of doses for screening of single-drugs usually is a relatively uncomplicated task, and which can be guided either by the effect of the drugs in other cell lines, or by the sensitivity of the assayed cell line(s) to related drugs, selection of doses for combination screening is a lot more challenging. This stems from the fact that while the synergistic effect of two (or more) drugs could be considered as an effect irrespective of doses or dose ratios, observed synergies tend to vary in strength across the combinatorial landscape of doses[112]. Whether or not we will be able to observe synergistic effects of a given drug combination in drugs screens will therefore be influenced by the doses at which we decide to combine the drugs. Multiple different strategies for combining of doses for drug combination screening have been reported in the literature[113–115]. One commonly used design is the anchor drug design, where one drug is applied at a fixed dose, whereas the other is used at multiple continuous doses[115]. Drugs can also be combined in a ray design where the doses of both drugs (for pairwise combinations) are varied and combined according to an equimolar or equipotent ratio[114,116]. The most complex form of drug combination screening is to combine drugs according to a matrix design, in which each dose of one drug is combined with each dose of the other[113,117,118]. However, even with the matrix design, the doses tested typically are non-continuous, meaning that the sparsity of the data will also here influence what synergies will be observed. While the matrix design strategy offers the largest coverage of the dose landscape per drug combination it also

constitutes the most challenging method screening-wise, due to the large number of conditions to test per such combination. As an example, while a 4-dose ray screen of 21 drug combinations in three cell lines would result in testing of a total of 252 conditions, a corresponding matrix screen would require testing of 1008 conditions. Regardless of which strategy one aims to use for combining drugs on the dose level, the individual doses of the drugs should be selected with the intention of not inducing too large effect on their own, as this would prevent synergistic effects from being detected (and conversely for drug antagonism).

Assessment of Treatment Response

To be able to evaluate the effect of a drug or drug combination on cells, we need to measure the cellular response to treatment. This is commonly done 24-96 hours after drug exposure initiation, depending on the design and purpose of the study[96,97]. Cellular response to treatment is often assessed by indirect measurement of phenotypes such as viability, proliferation, and cell death (apoptosis). The choice of phenotypic measurement often depends on the intention of the study, and while drug effect usually is assessed by measuring cellular viability, toxic effects are commonly quantified by assessment of cell death. As phenotypes are not intrinsically measurable, we make use of different phenotypic surrogate markers to quantify cellular response. Examples of such markers are ATP concentration for viability, and caspase 3/7 protein expression for apoptosis[119–121]. Quantification of surrogate markers is often done using cell-based assays. A wide range of cell-based assays have been developed for assessment of cellular phenotypes, but overall, they rely on the same basic principle, a principle where the surrogate marker is allowed to interact with specific components of an added assay reagent, which in turn leads to the generation of measurable, often optical, signals, such as luminescence and fluorescence. One example of such an assay is the CellTiter-Glo viability assay, in which ATP catalyses the conversion of the added reagent luciferin to oxyluciferin, whereof the latter component produces a measurable luminescent signal[122]. In the case of CellTiter-Glo, luminescence is therefore proportional to the level of ATP and hence the number of viable cells. Due to the simple use of cell-based assays, such as CellTiter-Glo and the corresponding assay for 3D-cultivated cells (CellTiter-Glo 3D), many of these are employed for assessment of cellular response to treatment in high-throughput drug screens[123]. This allows the generation of large amounts of data within a relatively short timeframe and without too much manual effort. Unfortunately, CellTiter-Glo and many other cell-based assays have the limitation of being endpoint assays, which stems from the fact that in order for indicated cellular reactions (such as the conversion of luciferase) to take place, cells need to be lysed and thereby terminated. This prevents valuable time-course studies of response (unless multiple plates are prepared in parallel), as well as retrieval of

cellular material following finished treatment. To enable continuous assessment of treatment response, multiple less invasive and even label-free detection assays have been developed for high-throughput screening[124]. Some examples are NucView and CellTox Green, which both enable fluorescence-based continuous assessment of cell death. In addition, repeated imaging constitutes a valuable method for generation of continuous data on treatment response.

Assessment of Drug Synergy

When screening for the effect of single-drugs, a screen can be regarded as relatively finished when response has been assessed and data analysed. In drug combination screening, however, the most important step remains at this point: the quantification of expected drug combination effects, to which the observed drug responses is compared in order to identify drug synergies. Quantification of expected drug combination effects is done mathematically, by the integration of drug response data according to one or several reference models[125]. While there is a disagreement within the research community about what constitutes the most valid way of quantifying the expected drug combination effects, it is generally agreed that the total observed effect of a drug combination AB (E_{AB}) comprises an expected effect (E_{A+B}) that can be calculated based on the effect of each individual drug A (E_A) and B (E_B), and an additional interaction effect (I_{AB}):

$$E_{AB} = E_{A+B} + I_{AB}$$

Based on this principle, a combination AB will generally be classified as synergistic, when the total observed effect of the combination is larger than the expected effect (i.e., $E_{AB} > E_{A+B}$). According to the same principle, a combination for which $E_{A+B} > E_{AB}$, will be classified as antagonistic, whereas combinations for which $E_{AB} = E_{A+B}$ will be regarded as additive[125].

Different models have been developed for quantification of expected drug combination effect, whereof the highest single agent (HSA), Bliss independence, and Loewe additivity models constitute some of the most widely adopted methods[126].

The HSA model provides the simplest classification of drug synergy, by stating that the expected effect of a combination equals the effect of the most effective single-drug, i.e.,

$$E_{A+B} = \max(E_A, E_B)$$

According to this definition, a combination AB is therefore classified as synergistic as soon as its total observed effect (E_{AB}) exceeds that of the most effective single-drug.

Compared to the HSA model, the Bliss independence model provides stricter synergy classification. In the Bliss independence model, the expected effect of two drugs A and B is the product of the two single-drug effects. Bliss independence assumes that the drugs act by independent probabilistic mechanisms, by assuming that the two drugs cannot both act on the same population of cells (or, analogously, both on the same drug target). Therefore, given that drug A acts on a fraction of the cells, drug B can only act on the fraction of cells which have been left unaffected by drug A. According to probabilistic theory, this assumption renders the following definition of the expected effect of drugs A and B,

$$E_{A+B} = E_A + E_B - E_A \cdot E_B$$

According to the Bliss independence model, a combination will be classified as synergistic when $E_{AB} > E_A + E_B - E_A \cdot E_B$.

In this thesis the HSA and Bliss independence metrics were used. A third commonly used reference framework is Loewe additivity. Briefly, the principle of Loewe additivity relies on the assumption that if an effect E can be obtained by either administering a drug A at concentration X or a drug B at concentration Y then drug B can substitute drug A fully or partially along an additive line. Example: If drug A induces 50% growth inhibition at a dose of 1 µM, and drug B induces 50% growth inhibition at a concentration of 5 µM then a combination of drug A and B, can for instance comprise drug A at 0.5 µM and drug B at 2.5 µM. If the effect of this combination is retained at level E the combination is classified as additive. If the effect is greater than E, the doses of drugs A and B can be lowered until the effect level E is produced, and a drug synergy is called.

One limitation of the Loewe additivity model is that a dose response relationship is needed to evaluate synergy for a combination, and that the effect of a combination cannot supersede the maximum effect of each individual drug. Given these two constraints, the HSA and Bliss independence metrics are more commonly used for assessment of drug synergy in high throughput experiments, and in particular for targeted therapies, for which it is not always possible to observe an effect of individual drugs, even though such targeted therapies can interact synergistically.

Identification of Cancer Treatment Effects In Silico

The use of drug combinations has been proposed as a promising strategy to increase the effect of treatment both for patient groups and for individual patients, but despite the advancements within high-throughput drug screening, it is virtually impossible to explore more than a fraction of all available treatment options in vitro. Taking

tumour response heterogeneity, which most likely calls for tumour-specific screens for the identification of effective drug combinations, into account, it is obvious that non-guided screening for identification of the most suitable treatment option for a patient will not be feasible. To increase the relevance of future drug screens we need to be able to prioritise what drugs and combinations to test in these screens. This can be done by computer assisted drug screens. Computational methods to this end are typically divided into two major branches: data-driven and model-driven (also called physics-driven) approaches[127]. Data-driven approaches relate to data analysis with fewer assumptions of underlying mechanisms as basis for the model. Model-driven approaches typically assume particular mechanisms and combine these to larger models, where prior knowledge on biology forms the foundation for the model. In reality, the boundary between these two main approaches is often blurred.

For model-driven approaches to drug testing, this can be done by computationally simulating the effect of treatment options of interest, model the recoded behaviour, whereafter options predicted to be effective can be selected for further validation by e.g., testing drug responses in vitro. Experiments that are performed via computational simulation are referred to as in silico experiments and engage computational models as the basis for simulation. For model-driven approaches discussed here, these models are designed to represent an abstraction of a system of interest, e.g., the signalling network of a cancer cell. Compared to experiments performed in vitro, in silico experiments have several advantages when it comes to testing capacity, which stems from the fact that while in vitro tests usually take days to perform, a computational simulation evaluating the corresponding effect in silico can be executed within seconds. Another advantage of computational models is the relative ease by which these can be manipulated to enable exploration of conditions that are not even possible or at least complicated to study in vitro. Also, for model-driven approaches that are based on representing mechanisms, any observed behaviour of the model can in principle be computationally studied in order to identify the simulated mechanism responsible for the in silico behaviour, and such proposed mechanisms can form hypotheses for follow-up experiments in vitro.

One use-case for computational cancer modelling has been the study of drug responses[114,128–130]. While computational models can simulate the effect of drug responses, it must be considered that computational models constitute highly simplified representations of reality. Therefore, in order take full advantage of computational models as representations of e.g., a disease, these models must be constructed with high accuracy. For this, prior knowledge of the disease is paramount.

Prior Knowledge Networks

While the mathematical modelling of cell signalling can be performed using multiple strategies, simulations of mechanistically based models are, regardless of modelling approach, preceded by construction of a prior knowledge network (PKN). The PKN aims at describing the molecular interactions between the components of the system that is to be modelled and is constructed based on information about signalling interactions reported in publications and databases (i.e., prior knowledge). Examples of databases which store information about the causative relationship between biological components of cells are Signor and KEGG[131,132].

As the PKN constitutes the topology based on which model simulations will be performed, the network should primarily be constructed around the components (genes, proteins, complexes etc.) considered to be relevant for the purpose of the modelling. E.g., for modelling efforts aimed at simulating the effect of drug perturbation using specific targeted agents, the PKN should be constructed around the molecular targets, and related pathways, of the drugs whose effect is to be studied. If mutational status of specific genes is in addition believed to be of relevance for the effect of drug perturbations, components corresponding to these genes/proteins should also be included, and the consequence of the mutation can also be simulated, e.g., constitutive activation or inhibition. In addition, to be able to quantify the effect of in silico perturbations, the PKN also needs to encompass proteins whose activity status will allow us to evaluate the drugs' effect on cellular phenotype(s). For the study of cancer cell growth, central in this thesis, examples of such proteins are those involved in regulation of proliferation (e.g., CDK4/6) and/or apoptosis (Caspase-3/7).

Simulation of Signalling Networks

In order to make use of a PKN for simulation of e.g., drug perturbation or disease development, the network must be converted into a mathematical model. Several mathematical approaches have been described for modelling of signalling networks, both quantitative[133,134] and qualitative[135,136].

ODE Modelling

Quantitative modelling of signalling networks is commonly performed by using ordinary differential equations (ODEs), where the concentration of a component (e.g., a protein) at a given timepoint is described by the rates by which this component is produced and consumed by other components of the system, and where the concentration can take any value on a continuous scale[133]. As such, the signalling network can be described as a set of ODEs, one for each component of the network

and the convergence of signalling can be studied by simultaneously solving the set of ODEs. As the chemical reactions that govern cell signalling are often non-linear, ODE modelling is in theory a highly relevant approach for studies of the dynamical behaviour of such signalling. Commonly, rate parameters of chemical reactions between model components are however unknown and in these cases ODE modelling is not trivial.

Logical Modelling

Logical modelling is a modelling approach where network behaviour is studied qualitatively, without taking detailed reaction kinetics into account. While this principle represents a simplification compared to ODE modelling, the ease by which this modelling strategy can be used, even for systems where kinetic data are lacking, makes the application field wide.

In a logical model, the activity of each component (protein, gene etc.) can be described by a discrete value. For the simplest logical models, the Boolean models, each component can hold two different values, True or False, or conversely, 1 or 0. Here, 1 indicates that the component is active, whereas 0 indicates inactivity. For multileveled logical models on the other hand, one or several components can take on more than two values. Multilevel logical modelling is often employed for studies of components which are known to have different roles depending on their level of activity. In both Boolean and multileveled logical models, the activity state of each component is determined by the activity states of its regulators (given by the PKN) according to a regulatory rule, which in turn is based on the Boolean operators AND, OR, and NOT. For each component in the prior knowledge network, or node, a logical rule is assigned, which unambiguously specifies the integrated influence of the activity states of regulatory components. As an example, where protein A is active in the presence of either protein B or protein C, and in the absence of protein D, the regulatory rule could be:

Protein A = (Protein B OR Protein C) AND NOT Protein D

When regulatory rules have been assigned to all components of a logical model, the global behaviour of the model can be simulated. This is performed by updating the activity state of all components in a series of timesteps and can be done either synchronously (updating of all components simultaneously) or asynchronously (updating of one component at the time). While asynchronous updating usually is to be regarded as a more comprehensive study of the dynamical properties of a model, this updating strategy also calls for larger computational capacity, which makes it less suitable for modelling of large signalling networks.

Applications of Logical Modelling

Many applications of network-based logical modelling of cancer and other conditions have been described in the scientific literature. Developed models have been aimed at studying e.g., cell fate decision mechanisms in the absence or presence of mutations and/or DNA damage, disease progression, and treatment response.

In 2013, Grieco et al., presented a logical model aimed at studying mechanisms governing cell fate decision in urinary bladder cancer[137]. The model was constructed around the mitogen-activated protein kinase (MAPK) signalling network, which is frequently deregulated in cancer. By performing simulations of relevant network perturbations (mutations), the authors found that model results agreed highly with published data for this cancer type. Specifically, their modelling effort demonstrated that EGFR overexpression in the presence of p53 was associated with a proliferative phenotype, which agrees with these alterations' frequent occurrence in aggressive bladder cancer[138].

Logical modelling has also been employed in studies of mechanisms that govern cellular response to DNA damage[139–141]. Based on a logical model encompassing DNA damage signalling pathways involved in regulation of G1/S transition, Mombach et al. studied mechanisms involved in DNA damage-induced onset of the tumour-suppressive phenotype *senescence*[141]. They studied a range of model perturbations corresponding to gene loss- or gain-of-function and found that many predicted phenotypes were comparable to those described for these mutations in vitro. In addition, they identified that loss-of-function alterations to the cell cycle protein CDC25A in the presence of DNA damage enhanced senescence, which highlights inhibition of CDC25A as a potential treatment strategy. In another study by authors from the same group[139], a logical model was constructed to determine the effect of DNA damage on phenotypes senescence, apoptosis, and autophagy in glioblastoma cells. The model suggested that in the absence of other perturbations, DNA damage can stochastically induce either of apoptosis, senescence, or autophagy, with probabilities that decrease in this order. Simulations further implied that induction of the three phenotypes occurred in a p53-dependent manner.

Disease progression in terms of epithelial mesenchymal transition (EMT) has been modelled by several groups[142,143]. In 2015, Cohen et al.[142], presented a logical model aimed for studies of mutations involved in metastatic development. The model was constructed to recapitulate experimentally assessed effects of specific mutations on metastasis and was used for further prediction of other mutations/mutation combinations possibly involved in this process. These predictions specifically suggested that overexpression of the signalling protein Notch in combination with p53 deletion synergistically induces a phenotype capable of metastasis, which was supported by the literature[144].

Multiple models have also been constructed for the purpose of studying treatment response[128,129,145]. In 2020, Eduati et al.[130], presented a study where patient-specific logical models were generated based on data from drug screens on pancreatic tumour biopsies. Generated models were used for studies of mechanisms causing response heterogeneity and for further prediction of patient-specific response to 174 drug combinations. More recently, in 2021, Béal et al.[146], presented a study where logical modelling was employed to study response to BRAF inhibition in multiple melanoma and colorectal cancer cell lines. The model was constructed based on prior knowledge of the MAPK pathway and factors involved in mediating resistance to BRAF inhibition and was calibrated to cell lines by integrating cell line-specific omics data. The authors found that cell line-specific predictions of BRAF inhibition well matched responses observed for corresponding cell lines in vitro.

Objectives of the Study

Cancer is a multifaceted disease, requiring multifaceted tools and strategies for efficient treatment. The aim of this thesis was to gain an increased understanding of the complexity of cancer and what tools we can make use of in the search for treatments for the disease. The project is part of the DrugLogics Initiative at NTNU, Trondheim, an interdisciplinary research initiative with the overall objective *"to investigate and demonstrate how Systems Medicine can deliver a well-constructed pipeline for rational screening for synergistic drug combinations and become a foundation for clinical decision-making for anti-cancer combination therapies under the precision oncology vision."* More specifically, the objectives of the thesis were to develop methods to study cancer treatment response *in vitro* and *in silico* and compare the different methods to gain increased understanding of the dynamics and responses to therapy of cancer. The thesis is constructed around three subprojects, each contributing to fulfilling the overall study objectives.

Sub-project 1: 2D vs. 3D screening

The project aimed at identifying drug combinations with synergistic properties in the most widely used *in vitro* culture system; the cell lines. By studying the effect of drug combinations on cell lines cultivated in 2D (monolayer) and 3D (spheroids), we aimed to highlight the complexity of choosing the 'right' cultivation system(s) for screening. The workflow involved 1) optimisation of a procedure for high-throughput screening using several different readouts in both culture formats, 2) screening for the effect of single-drugs in order identify drug-specific dose ranges to be used in combination screening, 3) screening for the effect of combined drugs administered in a 4x4 matrix design, and 4) concluding data analysis, where the effect of drug combinations was evaluated and compared within and across cell lines, as well as within and across culture formats.

Sub-project 2: Computational modelling

The project aimed at providing a theoretical follow-up to the combination screen performed in sub-project 1. In sub-project 2 we aimed to use computational modelling to predict cellular response to treatment with pairwise and higher-order drug combinations (>2 drugs). The workflow involved 1) construction of a prior-knowledge network encompassing all signalling pathways targeted by drugs in sub-project 1, 2) transformation of the signalling network into a Boolean model for study of network dynamics, 3) model reconstruction for improvement of predictive capacity where data from sub-project 1 were used as reference, 4) simulation of network dynamics upon second and higher-order perturbation, and 5) *in vitro* validation of predictions in (4).

Sub-project 3: Patient-derived tumour spheroids

The project aimed at taking 3D cultures as a tool for evaluation of treatment response *in vitro* one step closer to the clinic, by stepping away from the cell line spheroids studied in sub-project 1, towards patient-derived tumour spheroids. With the higher aim of implementing the use of such spheroids as a future tool for clinical decision-support, the objective of this sub-project was to optimise procedures and readouts allowing for rapid and informative drug screening in primary tumour spheroids derived from CRC patients. The workflow included 1) optimisation of sample processing and cultivation parameters, 2) optimisation of image-based multiparametric screening readouts, and 3) initial testing of the robustness of the procedure by screening for the effect of a clinically used treatment regimen in patient-derived tumour spheroids.

Summary of Papers

Paper 1: High-throughput screening reveals higher synergistic effect of MEK inhibitor combinations in colon cancer spheroids

When it comes to tackling drug resistance in cancer therapy, drug combinations are believed to be advantageous over monotherapy. By interfering with the signalling network of cancer cells at multiple points, targeted drug combinations have been shown to overcome some of the resistance frequently developed upon treatment with single agents[147]. However, despite large screening efforts, aimed at identifying synergistic drug combinations *in vitro*, relatively few targeted drug combinations have been approved for clinical use, with the notable exception of combined BRAF and MEK inhibitors, used for several malignancies that contain activating BRAF mutations[113,117]. The inability of traditionally 2D-cultivated cells to recapitulate response *in vivo* has been suggested as a possible explanation to the low translational throughput, and 3D cultures have been mentioned as a physiologically more relevant screening model, since it retains cell-cell contact and physiological gradients that can be assumed to influence drug responses[103]. Few studies have, however, compared the two culture formats in terms of their ability to uncover synergistic drug combinations.

In this work, we sought to study and compare the effect of cell culture format and readout methods on identification of synergistic drug combinations *in vitro*. To accomplish this, treatment response to 7 single agents and 21 drug combinations was assessed for three CRC cell lines (HCT-116, HT-29, SW-620) cultivated in 2D (monolayer) and 3D (spheroids). Drug combinations comprised all pairwise combinations of the single agents and were administered in 4x4 dose matrices. By monitoring growth (imaging) and viability (CellTiter-Glo) of cells in a 48h combination screen we were able to identify synergistic drug combinations shared among cell lines and cell culture formats, but also synergies that were specific to one cell line or culture format. In general, synergy was more pronounced in 2D-cultivated cells, while we noticed that 3D-cultivated cells were more sensitive to combinations involving a MEK inhibitor. Increased sensitivity of 3D cultures to MEK inhibitors has been demonstrated by others before us[148], indicating reproducibility of the method.

Altogether, the results from our study demonstrate that screening in 3D cultures, as well as inclusion of more readouts, hold great promise as support as well as complement to standard viability-based screening in 2D-cultures when searching for synergistic drug combinations *in vitro*.

Paper 2: Synergistic effects of complex drug combinations in colorectal cancer cells predicted by logical modelling

While the use of drug combinations holds great promise as a tool to overcome resistance to cancer therapy, identification of synergistic drug combinations is limited by today's available screening technology. A strategy for decreasing experimental workload, as well as for increasing the efficiency of drug screens, is to make use of computational modelling to design rationalised drug screens. The value of using computational models in preclinical medicine has been highlighted both by the power of models to predict treatment response, and by their ability to uncover molecular mechanisms accounting for treatment response and/or resistance[145]. However, while computational models have frequently been investigated for their capability to predict the effect of single and pairwise perturbations, the effect of higher-order perturbations has rarely been studied *in silico*[149,150].

In this study, we aimed to make use of computational modelling to predict cellular response to treatment with higher-order combinations of drugs evaluated in the pairwise combination screen in Paper 1. Using the software-suite GINsim, we constructed a Boolean model encompassing all signalling pathways targeted by drugs in the combination screen (Paper 1), as well as additional pathways frequently dysregulated in cancer. Following construction, the model topology was updated to increase its predictive capacity of pairwise synergistic drug combinations identified in the screen (Paper 1). The resulting model allowed us to predict additional synergistic effects of three third-order drug combinations, out of which all involved inhibition of PI3K and MEK, as well as induction of DNA damage. All predictions were validated in a high-throughput combination screen, which confirmed synergism of all three combinations, as well as non-synergism of two additional combinations predicted to be non-synergistic.

Overall, our study shows that computational modelling can be used to predict the effect of higher-order perturbations, which is of great importance when seeking to rationalise higher-order drug combination screens.

Paper 3: Growth and treatment response of colorectal cancer spheroids evaluated with imaging

Patient-derived tumour spheroids have been shown to retain tumour heterogeneity of individual patients and are expected to become an important supporting tool within the field of personalised cancer treatment. Several recent studies have pointed at the clinical value of this relatively new *in vitro* model by demonstrating its ability to predict patient response to several clinically used chemotherapeutic agents[108–110]. However, despite the clinical relevance of data obtained with this model, the

generation of such data is still hampered for several reasons. Limited amount of screening material is considered a major contributing factor, as are invasive whole-well readouts, which prevent continuous monitoring of response as well as post-treatment analysis of already limited sample material.

Aiming to increase the amount of screening data obtained for patient-derived tumour spheroids, we developed a method for non-invasive continuous image-based analysis of spheroid growth and shape in the presence and absence of chemotherapeutic perturbation. The method allowed us to assess measures such as total area (covered by spheroids in brightfield images), average spheroid area, diameter, perimeter, and circularity in a high-throughput manner. By using the method to study growth of spheroids from tumour samples in the absence and presence of chemotherapeutic perturbation, we could conclude that while all measures of size (total and average area, diameter, and perimeter) could detect growth and response of spheroids, total area normalised to day one, which we defined as *relative total area*, provided the most robust readout.

To summarise, results from our study demonstrate that growth and response of patient-derived tumour-spheroids can be continuously and robustly assessed by employing *relative total area*, evaluated based on brightfield images, as a readout. The readout and suggested readout method are highly relevant for collection of data on samples for which material is scarce and for which non-invasive readout methods imperative.

Discussion

Despite the fact that most cancers share a number of traits, summarised as *the hallmarks of cancer*[16], which altogether provide cancer cells with a growth advantage, cancer is a highly heterogeneous disease, on both the cellular and molecular levels, and in terms of disease progression and treatment response. Historically, chemotherapy has been the most common treatment modality for metastatic cancer disease. For localised disease, surgery and radiotherapy are important treatment modalities. Overall, chemotherapy and radiotherapy regimens are aimed at inhibiting cancer by inducing direct or indirect DNA damage in cells. Research within both chemotherapy and radiotherapy has therefore benefited largely from the past decades' increased understanding of DNA damage response and repair mechanisms in human cells. Altogether, this has resulted in the development of a considerable number of chemo and radiotherapeutic treatment strategies with significant effect in cancer patients. However, despite the progress, many patients fail to respond to existing cancer therapies. Genetic and other molecular variability between patient tumours is considered to be the main contributors to observed variations in treatment response.

The term "personalised medicine" was introduced to the public in 1999 and has over the years come to be used interchangeably with terms such as "precision medicine" and "stratified medicine"[151]. In short, it refers to a medical model where treatment strategies, including interventions and therapeutic agents, are being tailored to individual patients based on their molecular profile. For the past two decades, genetic profiling of patient tumours has gradually been implemented in the clinic, and today genetic profiling is being established as routine diagnostics to underpin clinical decision-making. In particular, several genetic markers (mutations, amplifications, translocations) are used for guidance for personalisation of cancer treatment. A few of these markers have contributed significantly to improved cancer care, but overall, the use of genetic markers as predictors of clinical treatment response has so far been met by a modest success. It can be speculated that this can be ascribed to these markers' limited ability in describing the dynamics of the signalling networks that are assumed to govern the behaviour of cancer. Protein markers are to some extent analysed by immunohistochemistry, and markers of gene expression for smaller gene panels are used for diagnostics of subtypes of breast cancer[117]. However, large scale assessment of protein expression and protein modifications (proteomics), and large-scale gene expression analysis (transcriptomics), assumed to better reflect the dynamics of disease, are due to the limited knowledge of how to use these data for diagnostic purposes not routinely profiled within the clinical setting today, although the technology for establishing such profiles exists.

Systems biology has provided us with tools to model and analyse the complex dynamical networks of cancer and other diseases computationally and mathematically, and to integrate different data types of proteomics, transcriptomics, genomics, and others in meaningful ways[86]. While the construction of models reflecting the behaviour of molecular interactions between genes, proteins etc., allows us to study progression and treatment of disease on a computationally efficient mathematical basis, we are still challenged by the heterogeneity of cancer between cancer model systems or patients, which calls for the calibration of these models in order to increase their performance for individual cell lines or tumours[154]. Calibration of a model as employed in Paper 2 relies on gathering of activity data for the studied cell line/tumour, followed by model refinement to make the activity profile of the model compliant with data. This is usually a time-consuming process, and efforts have been done to automate this process for these approaches to be suitable tools for treatment-prediction within clinical settings[155].

Accurate modelling of treatment response also challenges our understanding of how drugs target cells and cell signalling processes. While the name of a drug may imply that targeted therapies inhibit a single molecule class, most such agents are associated with a range of additional targets[156]. Such off-target effects of drugs stem from the fact that proteins are evolutionary conserved, and in particular the ATP-binding pocket typically targeted by a drug is similar for many classes of protein kinases[157]. This constitutes a challenge to prediction of treatment response for mechanistic model-based approaches, since the model can only simulate what has been specifically annotated. However, if drug target profiling underpins the claim that the effect on one drug target is more prominent than the influence on other targets, then neglecting the effects on off-target proteins is a pragmatic way of simulating drug responses. After careful selection of which drugs to use in laboratory experiments, simulations can be simplified, as was done in our study in Paper 2, by choosing to neglect off-target effects, while acknowledging that by doing so we also risk loss in predictive capacity due to the impossibility of avoiding off-target effects in living cells. While modelling treatment response without taking off-target effects into account constitutes the most practical modelling approach, there may be occasions when including such effects could be of interest and even crucial. Examples are when an off-target protein is known to be inhibited to the same degree as the primary target or when an off-target protein corresponds to a cancer driver protein. In these cases, multileveled logical modelling could enable simulation of off-target effects by providing a strategy for representation of a partly inhibited component. Here we are, however, challenged by how to model the regulatory effect

of a partly inhibited component as this most likely requires that even its effector components (and likely most of the network components) are assigned a multileveled representation, which increases the state space of simulations significantly, and which is typically not trivial to match with observed data that must be split into a number of value ranges corresponding to the logical levels.

While the effect of pairwise drug combinations has been studied by mechanistic modelling, most modelling approaches to study the effect of higher-order drug combinations have employed data-driven strategies[149,150,158]. In Paper 2, we studied the effect of higher-order drug combinations using a mechanistic approach and were able to predict three synergistic effects out of 35 possible. This could be regarded as a low number, when taking into account that we by studying the same cell line were able to observe 13 synergistic pairwise combinations out of 21 possible in the screen in Paper 1. The low number of predicted synergies in Paper 2 may indicate that mechanistic modelling as a strategy to identify synergistic higher-order combinations might be more restrictive compared to data-driven modelling. Others have found that for higher-order combinations the total number of synergies usually increases with the number of individual drugs in the combination[159]. In the study in Paper 2, we did not perform a full-scale validation screen, but the screen that was performed identified more synergistic combinations than what could be predicted by the model.

Many researchers pursue the use of drug combinations for treatment of cancer. While drug combinations generally are assumed to be associated with lower side-effects, it should be recognised that we by administering combinations comprising multiple different drugs also risk engaging a larger number of off-targets which could also lead to increased side-effects. The benefits of administering higher-order combinations should therefore be closely monitored. In our validation screen in Paper 2, we recognised that when present, synergy of higher-order combinations was relatively week. As the screen was based on a viability readout we could not conclude if cells were apoptotic, but the model suggested that this was the case for these combinations. If higher-order drug combinations are indeed able to induce a more permanent cytotoxic treatment effect by killing cells, there are obvious clinical benefits associated with the use of higher-order combinations. It is further possible that targeted single-agents and pairwise combinations mainly induce temporary growth arrest without necessarily killing cells and that higher-order combinations could be needed in order to induce long-term effects[116]. In the simulations in Paper 2 we concluded that all synergistic pairwise combinations were associated with growth arrest. If this was the case in vitro was not investigated in this study, but in a

long-term study of synergistic effects of pairwise combinations in Paper 1, we could, by measuring confluency, conclude that while the fully targeted combination of the drugs PI-103 and 5Z-7-oxozeaenol (PI3K inhibitor and TAK1 inhibitor, respectively) was synergistic during the first half (48h) of the study, cells over time seemed to overcome the inhibition, which was manifested by increased growth during the second half of the experiment (48-96h). Overall, these results could indicate that targeted inhibitors of at least this combination did not induce a perturbation that resulted in permanent growth arrest or death.

If the superiority of higher-order combinations in relation to pairwise combinations primarily is manifested in a more sustained effect rather than in increased synergy strength, we will need to reconsider how the effect of these combinations is evaluated in validation screens, as conventional screening strategies most likely will not enable study of this. Firstly, if it is true that synergistic higher-order combinations affect the same fraction of cells as synergistic lower order combinations but induce a different phenotype in these (apoptosis instead of growth arrest), we will most likely not be able to evaluate this in a 48-hours screen where viability is employed as measure of response. This stems from the fact that by using viability as a readout we will not be able to distinguish between arrested and apoptotic cells i.e., cytostatic vs cytotoxic effects[160]. Here we would instead need to make use of e.g., readouts of markers reflecting apoptosis, in addition to the viability readout, to determine if the higher-order combinations induce a different phenotype within this time. It is however possible that higher-order combinations manifest their advantage, not by inducing apoptosis but by inducing permanent growth arrest (senescence). This too we will most likely not be able to study in 48-hours screen, but here we will need to employ screens with longer exposure time. How to design in vitro screens is an overall frequently discussed topic within the medical field[161]. Whereas the research community calls for standardisation of screening procedures to deal with poor inter-experiment reproducibility between labs[162], there will always be cases where one will need to design screens for specific purposes. Screens can be varied on multiple different levels, including culture models, exposure times, and readout methods. In this thesis we present several different screening designs for evaluation of treatment response in vitro. By in Paper 1 studying the effect of drug combinations at multiple timepoints, we demonstrate that drug synergies are classified differently depending on the timepoint for readout. In all of Paper 1-3 we further evaluate and compare multiple different readout methods and culture models, for assessment of response to treatment with drug combinations (Paper 1-2) as well as single-drugs (Paper 1-3). Which readout and design that is most apt to identify clinically relevant drug combinations remains to be decided. Depending on the validation setup planned for proposed drug combinations, either a greedy approach, in which any combination

that by any synergy metric is classified as a synergy, can be chosen, or a conservative approach, in which drug combinations classified as synergistic across multiple timepoints and synergy metrics, can be chosen for follow-up experiments.

Viability measurements constitute one of the most widely adopted standardised readouts for assessment of treatment response in drug screens[163]. We used viability, assessed by the assay CellTiter-Glo, as the main readout throughout our screens in Paper 1 and Paper 2, and we were able to observe excellent reproducibility in all studies, which is of high importance in a field where reproducibility generally has been reported to be poor[162,164]. In addition to assessing response based on viability, we made use of image-based readout methods in both Paper 1 and Paper 2. In both studies we observed strong correlation between viability and image-based readout methods, supporting the use of the latter as a powerful backup. While image-based methods generally are more time consuming and labour-intensive compared to whole-well readouts like CellTiter-Glo, they are advantageous in the sense that they enable continuous and non-invasive estimation of response. Here, the latter is of importance for studies of response in samples where the availability of material is limited (e.g., patient material) and where it therefore may be crucial to be able to preserve sample material following finished exposure, in order to perform further molecular analyses. In Paper 3, we highlight the suitability of using image-based readouts for this purpose, by optimising such a method enabling non-invasive continuous analysis of growth and response of PDTSs.

While the choice of exposure times and readout methods are both of importance for the outcome of a screen, the choice of culture model is probably the single largest factor governing treatment outcome. For cell lines vs. PDTSs the differences in treatment response are to be expected, as cell lines have for long been cultivated in an artificial environment, something that in turn has induced clonal selection of cells, while PDTSs originate from an environment with large cellular heterogeneity reflected in their composition of cells[165]. These are differences that most likely result in these models' different responses to treatment. However, even for the same cell line, cells have been found to behave and respond differently to treatment depending on whether they are cultivated in 2D or 3D, and in many studies[103,166,167], including our own (Paper 1) 3D-cultivated cells have overall been found to be less sensitive to treatment compared to their 2D-cultivated counterparts. A part of the reduced sensitivity observed for 3D-cultivated cells can likely be ascribed solely to the structural differences between the models, as in 3D models, a smaller fraction of cells is directly exposed to the drug solution, as the surface cells to some extent can protect bulk cells. Reduced direct exposure does however not explain all responses.

For example, we, and others[148], have found that 3D-cultivated cell lines are more sensitive to MEK inhibition, compared to cells cultivated in 2D. Instead, these results could indicate that 3D-cultivation confers changes in signal transduction pathways[104,168,169]. These changes can be hypothesised to be ascribed to 3D-cultivated cells' increased ability to interact with cells in more than two dimensions, a feature that would further provide a possible explanation to why also we observed clear differences in synergistic effects between 2D and 3D cultures in Paper 1.

The choice of culture model should in large be based on the purpose of the study. If the purpose is to perform a large-scale study of single-drug sensitivity across multiple cancer types, a 2D design, where each cancer type is represented by a panel of cell lines, is probably suitable. If one, on the other hand, aims to perform a large-scale study of the effect of drug combinations, it must be considered that synergies are likely to be differently displayed in 2D and 3D[170]. Here, attention should be paid to which cultivation format that is the most relevant to the cancer type studied. While 3D models generally have been hypothesised to be more clinically relevant, this has also turned out to be dependent on the cancer type studied, and overall 3D models have been found to be superior to 2D models for studies of cancers that form solid tumours[171]. Based on this reasoning, the 3D models studied in Paper 1 can be regarded as superior to the 2D models for the cancer type studied (CRC). Lastly, if the purpose of a study is to provide data for clinical decision-support, it is obvious that a model as similar as possible to the clinical tumour should be studied, e.g., PDTSs[172–174]. Here, it is also of importance that the model can be generated and screened within a clinically relevant timeframe of 4-6 weeks. In our study in Paper 3, we demonstrate that such a study can been performed in less than two weeks from sample collection without relying on expansion of samples. For the purpose of clinical decision-support, it is further supported that a sample processing strategy that maintains the cellular heterogeneity of the sample is adopted. Whether maintained 3D structure is crucial for the clinical relevance of PDTSs is still unclear, and both full-processing (for generation of single cells) and partly processing of samples have been reported in the literature[108,165,173,175]. It is possible that cell-cell interactions, rather than the 3D structure per sé, is of importance for maintaining the tumour heterogeneity in PDTSs. In tumours, multiple different cell types interact and the interplay between these cells will govern the overall response of the tumour when this is subjected to treatment. Even if all cell types are technically represented in a sample for which one chooses to perform full processing, a large part of the cellular interplay will be lost in the regenerated spheroids as these mainly will be clones of a single cell. If one instead does not allow the sample to be fully digested, it is possible that a larger degree of the interaction between different cell types is maintained, which may be of importance for the response and how similar this response will be

compared to that of the tumour. As we in the future hope to be able to use computational models to guide high-throughput screens even for PDTSs, it is however important that future tumour-models will also be compatible with such a screening format.

Conclusions and Future Perspectives

Increased efficiency of future cancer therapy will most likely require a strategy where treatment selection is based on each cancer patient's unique molecular profile. This will in turn increase the demand of systematic analysis of data using computational power and robust experimental methods for evaluation of treatment response. The work of this thesis was aimed at investigating both sides of this coin, as well as their common value.

Treating cancer with combinations of drugs has been proposed as a strategy to improve treatment outcome. The work in this thesis demonstrates that both computationally simulated and experimentally executed drug screens can be employed for identification of combinations whose effect is larger than that of individual drugs. We show that these methods can be integrated in order to economise drug screening. I believe that studies like this will be of high value to the field where approaches to personalise cancer treatment most likely will be dependent on pipelines where drug screens are guided by predictions from patient-specific computational models. The integrated work in Paper 1 and Paper 2 of the thesis is a direct application of this. The patient-relevance of predictions generated by computational models will likely require that models are informed by patient-specific data. This also means that we will need to be able to validate the predictions in culture systems as similar as possible to the unique tumour. For relevance as clinical decision-support, such validation experiments also need to be executable within a clinically meaningful timeframe, i.e., around one month from patient referral to treatment start. In this thesis we have demonstrated that patient-derived tumour cultures can be established and screened within two weeks from sample retrieval, which points at the relevance of this method as a possible tool for clinical decision-support. However, it remains to be assessed how patient-specific tumour cultures should be established in order to be fully valid as predictive tools of patient-specific treatment response. This assessment is important, especially as it has been shown that cells may respond differently to especially combination treatment depending on whether they are cultured in 2D or 3D, which is also highlighted in this thesis. As drug combinations will likely be a part of the personalisation strategy, this will need to be investigated also for patient-derived tumour cultures.

Future approaches for personalisation of cancer treatment will likely rely on the integration of computational and experimental methods for selection of patient-specific treatment options. By studying some of the key steps of this strategy, the work presented in this thesis is aimed at contributing to improved knowledge within this field, which eventually is hoped to lead to increased quality of life of cancer patients.

References

1. WORLD HEALTH ORGANIZATION: REGIONAL OFFICE FOR EUROPE. *WORLD CANCER REPORT: cancer research for cancer development*. (IARC, 2020).
2. Dagogo-Jack, I. & Shaw, A. T. Tumour heterogeneity and resistance to cancer therapies. *Nat Rev Clin Oncol* **15**, 81–94 (2018).
3. Gambardella, V. *et al.* Personalized Medicine: Recent Progress in Cancer Therapy. *Cancers* **12**, 1009 (2020).
4. Bochum, S., Berger, S. & Martens, U. M. Olaparib. *Recent Results Cancer Res* **211**, 217–233 (2018).
5. Meric-Bernstam, F. *et al.* Advances in HER2-Targeted Therapy: Novel Agents and Opportunities Beyond Breast and Gastric Cancer. *Clin Cancer Res* **25**, 2033–2041 (2019).
6. Shabaruddin, F., Payne, K. & Fleeman, N. Economic evaluations of personalized medicine: existing challenges and current developments. *PGPM* **24**, 115–126 (2015).
7. Sharrer, G. T. Personalized Medicine: Ethical Aspects. *Methods Mol Biol* **1606**, 37–50 (2017).
8. Fong, E. L. S., Toh, T. B., Yu, H. & Chow, E. K.-H. 3D Culture as a Clinically Relevant Model for Personalized Medicine. *SLAS TECHNOLOGY: Translating Life Sciences Innovation* **22**, 245–253 (2017).
9. Jeon, M., Kim, S., Park, S., Lee, H. & Kang, J. In silico drug combination discovery for personalized cancer therapy. *BMC Syst Biol* **12**, 16 (2018).
10. Sompayrac, L. *How Cancer Works*. (Jones and Bartlett Publishers, 2004).
11. Krafts, K. P. Tissue repair: The hidden drama. *Organogenesis* **6**, 225–233 (2010).
12. Lodish, H. *et al. Molecular Cell Biology*. (W. H. Freeman, 2000).
13. Patrick, G. L. *Medicinal Chemistry*. (Oxford University Press, 2013).
14. Pack, L. R., Daigh, L. H. & Meyer, T. Putting the brakes on the cell cycle: mechanisms of cellular growth arrest. *Curr. Opin. Cell Biol.* **60**, 106–113 (2019).
15. Cooper, G. M. *The Cell: A Molecular Approach*. (Sinauer Associates, 2000).
16. Hanahan, D. & Weinberg, R. A. The Hallmarks of Cancer. *Cell* **100**, 57–70 (2000).
17. Alberts, B. *et al. Molecular Biology of the Cell*. (Garland Science, 2002).
18. Gilbert, S. F. *Developmental Biology*. (Sinauer Associates, 2002).
19. Weston, C. R. & Davis, R. J. The JNK signal transduction pathway. *Curr. Opin. Cell Biol.* **19**, 142–149 (2007).

20. Chang, F. *et al.* Involvement of PI3K/Akt pathway in cell cycle progression, apoptosis, and neoplastic transformation: a target for cancer chemotherapy. *Leukemia* **17**, 590–603 (2003).
21. Zhang, W. & Liu, H. T. MAPK signal pathways in the regulation of cell proliferation in mammalian cells. *Cell Res* **12**, 9–18 (2002).
22. Sporn, M. B. & Todaro, G. J. Autocrine secretion and malignant transformation of cells. *N Engl J Med* **303**, 878–80 (1980).
23. Cohen, R. B. Epidermal Growth Factor Receptor as a Therapeutic Target in Colorectal Cancer. *Clin. Colorectal Cancer* **2**, 246–251 (2003).
24. Iqbal, N. & Iqbal, N. Human Epidermal Growth Factor Receptor 2 (HER2) in Cancers: Overexpression and Therapeutic Implications. *Mol. Biol. Int.* **2014**, 1–9 (2014).
25. Carvalho, I., Milanezi, F., Martins, A., Reis, R. M. & Schmitt, F. Overexpression of platelet-derived growth factor receptor α in breast cancer is associated with tumour progression. *Breast Cancer Res* **7**, R788 (2005).
26. Sever, R. & Brugge, J. S. Signal Transduction in Cancer. *Cold Spring Harb. Perspect* **5**, a006098–a006098 (2015).
27. Saeed, O. *et al.* RAS genes in colorectal carcinoma: pathogenesis, testing guidelines and treatment implications. *J Clin Pathol* **72**, 135–139 (2019).
28. Alqathama, A. BRAF in malignant melanoma progression and metastasis: potentials and challenges. *Am J Cancer Res* . **10**, 1103–1114 (2020).
29. Martínez-Sáez, O. *et al.* Frequency and spectrum of PIK3CA somatic mutations in breast cancer. *Breast Cancer Res* **22**, 45 (2020).
30. Blomen, V. A. & Boonstra, J. Cell fate determination during G1 phase progression. *Cell. Mol. Life Sci.* **64**, 3084–3104 (2007).
31. Giacinti, C. & Giordano, A. RB and cell cycle progression. *Oncogene* **25**, 5220–5227 (2006).
32. Sherr, C. J. & McCormick, F. The RB and p53 pathways in cancer. *Cancer Cell* **2**, 103–112 (2002).
33. Aerts, I. *et al.* Retinoblastoma. *Orphanet J Rare Dis* **1**, 31 (2006).
34. Sherr, C. J. Principles of Tumor Suppression. *Cell* **116**, 235–246 (2004).
35. Zhu, G. *et al.* Mutant p53 in Cancer Progression and Targeted Therapies. *Front. Oncol.* **10**, 595187 (2020).
36. Elmore, S. Apoptosis: A Review of Programmed Cell Death. *Toxicol Pathol* **35**, 495–516 (2007).
37. Radha, G. & Raghavan, S. C. BCL2: A promising cancer therapeutic target. *Biochimica et Biophysica Acta (BBA) - Reviews on Cancer* **1868**, 309–314 (2017).
38. Scherr, A.-L. *et al.* Bcl-xL is an oncogenic driver in colorectal cancer. *Cell Death Dis* **7**, e2342–e2342 (2016).

39. Wang, H., Guo, M., Wei, H. & Chen, Y. Targeting MCL-1 in cancer: current status and perspectives. *J Hematol Oncol* **14**, 67 (2021).
40. Fernald, K. & Kurokawa, M. Evading apoptosis in cancer. *Trends Cell Biol.* **23**, 620–633 (2013).
41. Osaki, M., Oshimura, M. & Ito, H. PI3K-Akt pathway: its functions and alterations in human cancer. *Apoptosis* **9**, 667–76 (2004).
42. Counter, C. M. The roles of telomeres and telomerase in cell life span. *Mutat Res* **366**, 45–63.
43. Duesberg, P. & McCormack, A. Immortality of cancers: A consequence of inherent karyotypic variations and selections for autonomy. *Cell Cycle* **12**, 783–802 (2013).
44. Shay, J. W. & Bacchetti, S. A survey of telomerase activity in human cancer. *Eur J Cancer* **33**, 787–791 (1997).
45. Trybek, T., Kowalik, A., Góźdź, S. & Kowalska, A. Telomeres and telomerase in oncogenesis (Review). *Oncol Lett* **20**, 1015–1027 (2020).
46. Otrock, Z., Mahfouz, R., Makarem, J. & Shamseddine, A. Understanding the biology of angiogenesis: Review of the most important molecular mechanisms. *Blood Cells Mol. Dis.* **39**, 212–220 (2007).
47. Folkman, J. Role of angiogenesis in tumor growth and metastasis. *Semin. Oncol* **29**, 15–18 (2002).
48. Nishida, N., Yano, H., Nishida, T., Kamura, T. & Kojiro, M. Angiogenesis in cancer. *Vasc Health Risk Manag* . **2**, 213–9 (2006).
49. Takeichi, M. Cadherins in cancer: implications for invasion and metastasis. *Curr Opin Cell Biol* **5**, 806–11 (1993).
50. Hamidi, H. & Ivaska, J. Every step of the way: integrins in cancer progression and metastasis. *Nat Rev Cancer* **18**, 533–548 (2018).
51. Hanahan, D. & Weinberg, R. A. Hallmarks of Cancer: The Next Generation. *Cell* **144**, 646–674 (2011).
52. Reuvers, T. G. A., Kanaar, R. & Nonnekens, J. DNA Damage-Inducing Anticancer Therapies: From Global to Precision Damage. *Cancers* **12**, 2098 (2020).
53. Ashraf, N., Hoffe, S. & Kim, R. Adjuvant Treatment for Gastric Cancer: Chemotherapy Versus Radiation. *The Oncologist* **18**, 1013–1021 (2013).
54. DeVita, V. T. & Chu, E. A History of Cancer Chemotherapy. *Cancer Res* **68**, 8643–8653 (2008).
55. Chabner, B. A. & Roberts, T. G. Chemotherapy and the war on cancer. *Nat Rev Cancer* **5**, 65–72 (2005).
56. Gianfaldoni, S. *et al.* An Overview on Radiotherapy: From Its History to Its Current Applications in Dermatology. *Open Access Maced J Med Sci* **5**, 521–525 (2017).

57. Lillis, C. Survival and chemotherapy success rates for various cancers. *Medical News Today* https://www.medicalnewstoday.com/articles/326031 (2019).
58. Alhmoud, J. F., Woolley, J. F., Al Moustafa, A.-E. & Malki, M. I. DNA Damage/Repair Management in Cancers. *Cancers* **12**, 1050 (2020).
59. Bakkenist, C. J., Lee, J. J. & Schmitz, J. C. ATM Is Required for the Repair of Oxaliplatin-Induced DNA Damage in Colorectal Cancer. *Clin. Colorectal Cancer* **17**, 255–257 (2018).
60. Longley, D. & Johnston, P. Molecular mechanisms of drug resistance. *J. Pathol.* **205**, 275–292 (2005).
61. Baba, H. *et al.* Upregulation of ERCC1 and DPD expressions after oxaliplatin-based first-line chemotherapy for metastatic colorectal cancer. *Br J Cancer* **107**, 1950–1955 (2012).
62. Bunz, F. *et al.* Disruption of p53 in human cancer cells alters the responses to therapeutic agents. *J. Clin. Invest.* **104**, 263–269 (1999).
63. Perego, P. *et al.* Association between Cisplatin Resistance and Mutation of p53 Gene and Reduced Bax Expression in Ovarian Carcinoma Cell Systems'. *Cancer Res* **56**, 556–562 (1996).
64. Dart, D., Picksley, S., Cooper, P., Double, J. & Bibby, M. The role of p53 in the chemotherapeutic responses to cisplatin, doxorubicin and 5-fluorouracil treatment. *Int J Oncol* **24**, (2004).
65. Syed, Y. Y. Rucaparib: First Global Approval. *Drugs* **77**, 585–592 (2017).
66. Matulonis, U. A. & Monk, B. J. PARP inhibitor and chemotherapy combination trials for the treatment of advanced malignancies: does a development pathway forward exist? *Ann. Oncol.* **28**, 443–447 (2017).
67. Zhong, L. *et al.* Small molecules in targeted cancer therapy: advances, challenges, and future perspectives. *Sig Transduct Target Ther* **6**, 201 (2021).
68. Bedard, P. L., Hyman, D. M., Davids, M. S. & Siu, L. L. Small molecules, big impact: 20 years of targeted therapy in oncology. *The Lancet* **395**, 1078–1088 (2020).
69. Lee, Y. T., Tan, Y. J. & Oon, C. E. Molecular targeted therapy: Treating cancer with specificity. *Eur. J. Pharmacol.* **834**, 188–196 (2018).
70. Martínez-Jiménez, F. *et al.* A compendium of mutational cancer driver genes. *Nat Rev Cancer* **20**, 555–572 (2020).
71. Imai, K. & Takaoka, A. Comparing antibody and small-molecule therapies for cancer. *Nat Rev Cancer* **6**, 714–727 (2006).
72. Hoelder, S., Clarke, P. A. & Workman, P. Discovery of small molecule cancer drugs: Successes, challenges and opportunities. *Mol. Oncol.* **6**, 155–176 (2012).
73. Hallek, M. Chronic lymphocytic leukemia: 2020 update on diagnosis, risk stratification and treatment. *Am J Hematol* **94**, 1266–1287 (2019).

74. Odogwu, L. *et al.* FDA Approval Summary: Dabrafenib and Trametinib for the Treatment of Metastatic Non-Small Cell Lung Cancers Harboring *BRAF V600E* Mutations. *The Oncol* **23**, 740–745 (2018).
75. Kim, G. *et al.* FDA Approval Summary: Vemurafenib for Treatment of Unresectable or Metastatic Melanoma with the BRAF ^{V600E} Mutation. *Clin Cancer Res* **20**, 4994–5000 (2014).
76. Kim, G. *et al.* FDA Approval Summary: Olaparib Monotherapy in Patients with Deleterious Germline *BRCA* -Mutated Advanced Ovarian Cancer Treated with Three or More Lines of Chemotherapy. *Clin Cancer Res* **21**, 4257–4261 (2015).
77. Beaver, J. A. *et al.* FDA Approval: Palbociclib for the Treatment of Postmenopausal Patients with Estrogen Receptor–Positive, HER2-Negative Metastatic Breast Cancer. *Clin Cancer Res* **21**, 4760–4766 (2015).
78. Deeks, E. D. Venetoclax: First Global Approval. *Drugs* **76**, 979–987 (2016).
79. FDA approves venetoclax for CLL and SLL. *U.S. Food & Drug Administration* (2019).
80. FDA approves venetoclax in combination for AML in adults. *U.S. Food & Drug Administration* (2018).
81. Kim, A. & Cohen, M. S. The discovery of vemurafenib for the treatment of BRAF-mutated metastatic melanoma. *Expert Opin. Drug Discov* **11**, 907–916 (2016).
82. Ulivi, P. Predictive biomarkers in clinical practice: State of the art and perspectives in solid tumors. *Int J Biol Markers* **35**, 16–19 (2020).
83. Vogelstein, B. *et al.* Cancer Genome Landscapes. *Science* **339**, 1546–1558 (2013).
84. Apweiler, R. *et al.* Whither systems medicine? *Exp Mol Med* **50**, e453–e453 (2018).
85. Yaffe, M. B. The Scientific Drunk and the Lamppost: Massive Sequencing Efforts in Cancer Discovery and Treatment. *Sci. Signal.* **6**, pe13 (2013).
86. Kitano, H. Computational systems biology. *Nature* **420**, 206–210 (2002).
87. Kitano, H. Systems Biology: A Brief Overview. *Science* **295**, 1662–1664 (2002).
88. Werner, H. M. J., Mills, G. B. & Ram, P. T. Cancer Systems Biology: a peek into the future of patient care? *Nat Rev Clin Oncol* **11**, 167–176 (2014).
89. Khunger, A., Khunger, M. & Velcheti, V. Dabrafenib in combination with trametinib in the treatment of patients with BRAF V600-positive advanced or metastatic non-small cell lung cancer: clinical evidence and experience. *Ther Adv Respir Dis* **12**, 175346661876761 (2018).
90. Palmer, A. C. & Sorger, P. K. Combination Cancer Therapy Can Confer Benefit via Patient-to-Patient Variability without Drug Additivity or Synergy. *Cell* **171**, 1678-1691.e13 (2017).

91. Borisy, A. A. *et al.* Systematic discovery of multicomponent therapeutics. *PNAS* **100**, 7977–7982 (2003).
92. Al-Lazikani, B., Banerji, U. & Workman, P. Combinatorial drug therapy for cancer in the post-genomic era. *Nat Biotechnol* **30**, 679–692 (2012).
93. Le Tourneau, C., Borcoman, E. & Kamal, M. Molecular profiling in precision medicine oncology. *Nat Med* **25**, 711–712 (2019).
94. Comte, B. *et al.* Network and Systems Medicine: Position Paper of the European Collaboration on Science and Technology Action on Open Multiscale Systems Medicine. *Network and Systems Medicine* **3**, 67–90 (2020).
95. Lucey, B. P., Nelson-Rees, W. A. & Hutchins, G. M. Henrietta Lacks, HeLa Cells, and Cell Culture Contamination. *Arch Pathol Lab Med* **133**, 1463–1467 (2009).
96. Barretina, J. *et al.* The Cancer Cell Line Encyclopedia enables predictive modelling of anticancer drug sensitivity. *Nature* **483**, 603–607 (2012).
97. Tate, J. G. *et al.* COSMIC: the Catalogue Of Somatic Mutations In Cancer. *Nucleic Acids Res* **47**, D941–D947 (2019).
98. Shoemaker, R. H. The NCI60 human tumour cell line anticancer drug screen. *Nat Rev Cancer* **6**, 813–823 (2006).
99. Madoux, F. *et al.* A 1536-Well 3D Viability Assay to Assess the Cytotoxic Effect of Drugs on Spheroids. *SLAS DISCOVERY: Advancing the Science of Drug Discovery* **22**, 516–524 (2017).
100. Mirabelli, Coppola & Salvatore. Cancer Cell Lines Are Useful Model Systems for Medical Research. *Cancers* **11**, 1098 (2019).
101. Fox, J. T. & Myung, K. Cell-based high-throughput screens for the discovery of chemotherapeutic agents. *Oncotarget* **3**, 581–585 (2012).
102. Seyhan, A. A. Lost in translation: the valley of death across preclinical and clinical divide – identification of problems and overcoming obstacles. *Transl. Med. Commun.* **4**, 18 (2019).
103. Breslin, S. & O'Driscoll, L. The relevance of using 3D cell cultures, in addition to 2D monolayer cultures, when evaluating breast cancer drug sensitivity and resistance. *Oncotarget* **7**, 45745–45756 (2016).
104. Riedl, A. *et al.* Comparison of cancer cells cultured in 2D vs 3D reveals differences in AKT/mTOR/S6-kinase signaling and drug response. *J. Cell Sci.* **130**, 203–218 (2016).
105. Booij, T. H., Price, L. S. & Danen, E. H. J. 3D Cell-Based Assays for Drug Screens: Challenges in Imaging, Image Analysis, and High-Content Analysis. *SLAS DISCOVERY: Advancing the Science of Drug Discovery* **24**, 615–627 (2019).
106. Sant, S. & Johnston, P. A. The production of 3D tumor spheroids for cancer drug discovery. *Drug Discov. Today Technol.* **23**, 27–36 (2017).

107. Gillet, J.-P., Varma, S. & Gottesman, M. M. The Clinical Relevance of Cancer Cell Lines. *JNCI* **105**, 452–458 (2013).
108. Ooft, S. N. *et al.* Patient-derived organoids can predict response to chemotherapy in metastatic colorectal cancer patients. *Sci. Transl. Med.* **11**, eaay2574 (2019).
109. Vlachogiannis, G. *et al.* Patient-derived organoids model treatment response of metastatic gastrointestinal cancers. *Science* **359**, 920–926 (2018).
110. Wang, T. *et al.* Accuracy of Using a Patient-Derived Tumor Organoid Culture Model to Predict the Response to Chemotherapy Regimens In Stage IV Colorectal Cancer: A Blinded Study. *Dis Colon Rectum* **64**, 833–850 (2021).
111. Wensink, G. E. *et al.* Patient-derived organoids as a predictive biomarker for treatment response in cancer patients. *npj Precis. Onc.* **5**, 30 (2021).
112. Meyer, C. T., Wooten, D. J., Lopez, C. F. & Quaranta, V. Charting the Fragmented Landscape of Drug Synergy. *Trends Pharmacol. Sci.* . **41**, 266–280 (2020).
113. O'Neil, J. *et al.* An Unbiased Oncology Compound Screen to Identify Novel Combination Strategies. *Mol Cancer Ther* **15**, 1155–1162 (2016).
114. Flobak, Å. *et al.* A high-throughput drug combination screen of targeted small molecule inhibitors in cancer cell lines. *Sci Data* **6**, 237 (2019).
115. Nair, N. U. *et al. A landscape of synergistic drug combinations in non-small-cell lung cancer*. http://biorxiv.org/lookup/doi/10.1101/2021.06.03.447011 (2021) doi:10.1101/2021.06.03.447011.
116. Horn, T. *et al.* High-Order Drug Combinations Are Required to Effectively Kill Colorectal Cancer Cells. *Cancer Res* **76**, 6950–6963 (2016).
117. Holbeck, S. L. *et al.* The National Cancer Institute ALMANAC: A Comprehensive Screening Resource for the Detection of Anticancer Drug Pairs with Enhanced Therapeutic Activity. *Cancer Res* **77**, 3564–3576 (2017).
118. Tomska, K. *et al.* Drug-based perturbation screen uncovers synergistic drug combinations in Burkitt lymphoma. *Sci Rep* **8**, 12046 (2018).
119. Adan, A., Kiraz, Y. & Baran, Y. Cell Proliferation and Cytotoxicity Assays. *Curr. Pharm. Biotechnol.* **17**, 1213–1221 (2016).
120. Ward, T. H. *et al.* Biomarkers of apoptosis. *Br J Cancer* **99**, 841–846 (2008).
121. Lee, S.-Y., Doh, I. & Lee, D. W. A High Throughput Apoptosis Assay using 3D Cultured Cells. *Molecules* **24**, 3362 (2019).
122. CellTiter-Glo® 2.0 Assay. (2018).
123. Rajalingham, K. Cell-based assays in high-throughput mode (HTS). *bta* **3**, 227–234 (2016).
124. Kessel, S. *et al.* High-Throughput 3D Tumor Spheroid Screening Method for Cancer Drug Discovery Using Celigo Image Cytometry. *SLAS TECHNOLOGY: Translating Life Sciences Innovation* **22**, 454–465 (2017).

125. Greco, W. R., Bravo, G. & Parsons, J. C. The search for synergy: a critical review from a response surface perspective. *Pharmacol Rev* . **47**, 331–385 (1995).
126. Yadav, B., Wennerberg, K., Aittokallio, T. & Tang, J. Searching for Drug Synergy in Complex Dose–Response Landscapes Using an Interaction Potency Model. *Comput. Struct. Biotechnol. J.* **13**, 504–513 (2015).
127. Klie, H. A Tale of Two Approaches: Physics-Based vs. Data-Driven Models. *The Way Ahead* https://jpt.spe.org/twa/a-tale-of-two-approaches-physics-based-vs-data-driven-models (2021).
128. Tsirvouli, E. *et al.* A Middle-Out Modeling Strategy to Extend a Colon Cancer Logical Model Improves Drug Synergy Predictions in Epithelial-Derived Cancer Cell Lines. *Front. Mol. Biosci.* **7**, 502573 (2020).
129. Niederdorfer, B. *et al.* Strategies to Enhance Logic Modeling-Based Cell Line-Specific Drug Synergy Prediction. *Front. Physiol.* **11**, 862 (2020).
130. Eduati, F. *et al.* Patient-specific logic models of signaling pathways from screenings on cancer biopsies to prioritize personalized combination therapies. *Mol Syst Biol* **16**, (2020).
131. Perfetto, L. *et al.* SIGNOR: a database of causal relationships between biological entities. *Nucleic Acids Res* **44**, D548–D554 (2016).
132. Kanehisa, M., Furumichi, M., Tanabe, M., Sato, Y. & Morishima, K. KEGG: new perspectives on genomes, pathways, diseases and drugs. *Nucleic Acids Res* **45**, D353–D361 (2017).
133. Aldridge, B. B., Burke, J. M., Lauffenburger, D. A. & Sorger, P. K. Physicochemical modelling of cell signalling pathways. *Nat Cell Biol* **8**, 1195–1203 (2006).
134. Le Novère, N. Quantitative and logic modelling of molecular and gene networks. *Nat Rev Genet* **16**, 146–158 (2015).
135. Bruggeman, F. J. et al. Modular Response Analysis of Cellular Regulatory Networks. *J. theor. Biol.* **218**, 14 (2002).
136. MacNamara, A., Terfve, C., Henriques, D., Bernabé, B. P. & Saez-Rodriguez, J. State–time spectrum of signal transduction logic models. *Phys. Biol.* **9**, 045003 (2012).
137. Grieco, L. *et al.* Integrative Modelling of the Influence of MAPK Network on Cancer Cell Fate Decision. *PLoS Comput Biol* **9**, e1003286 (2013).
138. Mitra, A. P. & Cote, R. J. Molecular Pathogenesis and Diagnostics of Bladder Cancer. *Annu. Rev. Pathol. Mech. Dis.* **4**, 251–285 (2009).
139. Gupta, S., Silveira, D. A. & Mombach, J. C. M. Towards DNA-damage induced autophagy: A Boolean model of p53-induced cell fate mechanisms. *DNA Repair* **96**, 102971 (2020).
140. Gupta, S., Silveira, D. A. & Mombach, J. C. M. ATM /miR-34a-5p axis regulates a p21-dependent senescence-apoptosis switch in non-small cell lung

cancer: a Boolean model of G1/S checkpoint regulation. *FEBS Lett* **594**, 227–239 (2020).
141. Mombach, J. C., Bugs, C. A. & Chaouiya, C. Modelling the onset of senescence at the G1/S cell cycle checkpoint. *BMC Genomics* **15**, S7 (2014).
142. Cohen, D. P. A. *et al.* Mathematical Modelling of Molecular Pathways Enabling Tumour Cell Invasion and Migration. *PLoS Comput Biol* **11**, e1004571 (2015).
143. Silveira, D. A. & Mombach, J. C. M. Dynamics of the feedback loops required for the phenotypic stabilization in the epithelial-mesenchymal transition. *FEBS J* **287**, 578–588 (2020).
144. Chanrion, M. *et al.* Concomitant Notch activation and p53 deletion trigger epithelial-to-mesenchymal transition and metastasis in mouse gut. *Nat Commun* **5**, 5005 (2014).
145. Flobak, Å. *et al.* Discovery of Drug Synergies in Gastric Cancer Cells Predicted by Logical Modeling. *PLoS Comput Biol* **11**, e1004426 (2015).
146. Béal, J., Pantolini, L., Noël, V., Barillot, E. & Calzone, L. Personalized logical models to investigate cancer response to BRAF treatments in melanomas and colorectal cancers. *PLoS Comput Biol* **17**, e1007900 (2021).
147. Jokinen, E. & Koivunen, J. P. MEK and PI3K inhibition in solid tumors: rationale and evidence to date. *Ther Adv Med Oncol* **7**, 170–180 (2015).
148. Sahu, N. *et al.* Cotargeting of MEK and PDGFR/STAT3 Pathways to Treat Pancreatic Ductal Adenocarcinoma. *Mol Cancer Ther* **16**, 1729–1738 (2017).
149. Zimmer, A., Tendler, A., Katzir, I., Mayo, A. & Alon, U. Prediction of drug cocktail effects when the number of measurements is limited. *PLoS Biol* **15**, e2002518 (2017).
150. Katzir, I., Cokol, M., Aldridge, B. B. & Alon, U. Prediction of ultra-high-order antibiotic combinations based on pairwise interactions. *PLoS Comput Biol* **15**, e1006774 (2019).
151. Jørgensen, J. T. Twenty Years with Personalized Medicine: Past, Present, and Future of Individualized Pharmacotherapy. *The Oncol* **24**, (2019).
152. Gown, A. M. Current issues in ER and HER2 testing by IHC in breast cancer. *Mod Pathol* **21**, S8–S15 (2008).
153. Prat, A. *et al.* Clinical implications of the intrinsic molecular subtypes of breast cancer. *The Breast* **24**, S26–S35 (2015).
154. Read, M. N., Alden, K., Timmis, J. & Andrews, P. S. Strategies for calibrating models of biology. *Brief. Bioinformatics* (2018) doi:10.1093/bib/bby092.
155. Chen, Y. *et al.* CaliBayes and BASIS: integrated tools for the calibration, simulation and storage of biological simulation models. *Brief. Bioinformatics* **11**, 278–289 (2010).
156. Zhang, R. & Loughran, T. P. Off-target effects of tyrosine kinase inhibitors: Beauty or the Beast? *Leuk. Lymphoma* **52**, 556–557 (2011).

157. Munoz, L. Non-kinase targets of protein kinase inhibitors. *Nat Rev Drug Discov* **16**, 424–440 (2017).
158. Zimmer, A., Katzir, I., Dekel, E., Mayo, A. E. & Alon, U. Prediction of multidimensional drug dose responses based on measurements of drug pairs. *Proc Natl Acad Sci USA* **113**, 10442–10447 (2016).
159. Tekin, E. *et al.* Prevalence and patterns of higher-order drug interactions in Escherichia coli. *npj Syst Biol Appl* **4**, 31 (2018).
160. Riss, T. Choosing the right cell-based assay for your research. *IN VITRO TOXICOLOGY* 7 (2003).
161. OECD. *Guidance Document on Good In Vitro Method Practices (GIVIMP)*. (OECD, 2018). doi:10.1787/9789264304796-en.
162. Safikhani, Z. *et al.* Revisiting inconsistency in large pharmacogenomic studies [version 3; referees: 2 approved, 1 approved with reservations]. *F1000Res* . **16**, 46 (2016).
163. Riss, T. L. *et al. Assay Guidance Manual*. (NIH, 2013).
164. Haibe-Kains, B. *et al.* Inconsistency in large pharmacogenomic studies. *Nature* **504**, 389–393 (2013).
165. Kondo, J. *et al.* Retaining cell-cell contact enables preparation and culture of spheroids composed of pure primary cancer cells from colorectal cancer. *PNAS* **108**, 6235–6240 (2011).
166. Vynnytska-Myronovska, B. *et al.* Three-dimensional environment renders cancer cells profoundly less susceptible to a single amino acid starvation. *Amino Acids* **45**, 1221–1230 (2013).
167. Brüningk, S. C., Rivens, I., Box, C., Oelfke, U. & ter Haar, G. 3D tumour spheroids for the prediction of the effects of radiation and hyperthermia treatments. *Sci Rep* **10**, 1653 (2020).
168. Pickl, M. & Ries, C. H. Comparison of 3D and 2D tumor models reveals enhanced HER2 activation in 3D associated with an increased response to trastuzumab. *Oncogene* **28**, 461–468 (2009).
169. Yue, X., Lukowski, J. K., Weaver, E. M., Skube, S. B. & Hummon, A. B. Quantitative Proteomic and Phosphoproteomic Comparison of 2D and 3D Colon Cancer Cell Culture Models. *J. Proteome Res.* **15**, 4265–4276 (2016).
170. Folkesson, E. *et al.* High-throughput screening reveals higher synergistic effect of MEK inhibitor combinations in colon cancer spheroids. *Sci Rep* **10**, 11574 (2020).
171. Han, S. J., Kwon, S. & Kim, K. S. Challenges of applying multicellular tumor spheroids in preclinical phase. *Cancer Cell Int* **21**, 152 (2021).
172. Pasch, C. A. *et al.* Patient-Derived Cancer Organoid Cultures to Predict Sensitivity to Chemotherapy and Radiation. *Clin Cancer Res* **25**, 5376–5387 (2019).

173. de Witte, C. J. *et al.* Patient-Derived Ovarian Cancer Organoids Mimic Clinical Response and Exhibit Heterogeneous Inter- and Intrapatient Drug Responses. *Cell Reports* **31**, 107762 (2020).
174. Kim, M. *et al.* Patient-derived lung cancer organoids as in vitro cancer models for therapeutic screening. *Nat Commun* **10**, 3991 (2019).
175. Jeppesen, M. *et al.* Short-term spheroid culture of primary colorectal cancer cells as an in vitro model for personalizing cancer medicine. *PLoS ONE* **12**, e0183074 (2017).

Paper I

scientific reports

Check for updates

OPEN

High-throughput screening reveals higher synergistic effect of MEK inhibitor combinations in colon cancer spheroids

Evelina Folkesson[1,5], Barbara Niederdorfer[1,5], Vu To Nakstad[3], Liv Thommesen[4], Geir Klinkenberg[3], Astrid Lægreid[1] & Åsmund Flobak[1,2]✉

Drug combinations have been proposed to combat drug resistance, but putative treatments are challenged by low bench-to-bed translational efficiency. To explore the effect of cell culture format and readout methods on identification of synergistic drug combinations in vitro, we studied response to 21 clinically relevant drug combinations in standard planar (2D) layouts and physiologically more relevant spheroid (3D) cultures of HCT-116, HT-29 and SW-620 cells. By assessing changes in viability, confluency and spheroid size, we were able to identify readout- and culture format-independent synergies, as well as synergies specific to either culture format or readout method. In particular, we found that spheroids, compared to 2D cultures, were generally both more sensitive and showed greater synergistic response to combinations involving a MEK inhibitor. These results further shed light on the importance of including more complex culture models in order to increase the efficiency of drug discovery pipelines.

Colorectal cancer (CRC) is the third most common neoplastic malignancy worldwide[1], and although improvements in standard treatments have increased the survival rates over the past 20 years[2], far from all patients benefit from currently available therapies. Targeted therapy, using drugs aimed to target specific molecules involved in tumour growth, is being regarded as a promising tool to increase response rates to cancer therapy. However, the number of such therapies that have made it all the way to the clinic has been limited. This may be explained by lack of therapy response due to adaptive drug resistance, or transient response due to acquired resistance. Drug combinations are being discussed as a promising strategy to overcome the resistance frequently observed upon administration of targeted monotherapy[3,4]. The augmented effect of targeted drug combination treatment is frequently ascribed to the drugs' ability to jointly interfere with the growth-promoting signalling network of cancer cells at multiple points. High-throughput cell line screening platforms have been successfully employed as tools to uncover novel synergistic drug combinations. In the study ALMANAC of the National Cancer Institute (NCI), where a large number of pairwise combinations of FDA-approved cancer drugs were screened in vitro, several novel pairs of synergistic drug combinations were identified, whereof roughly a third also were shown to be efficient and synergistic in vivo[5]. Another example is the Merck Research Laboratories screen, in which 583 combinations of experimental and approved cancer drugs were screened in a panel of cancer cell lines, identifying well-known as well as novel synergistic drug combinations in vitro[6].

Despite large combination screening efforts with successful hits in vitro, putative treatments are challenged by low bench-to-bed translational efficiency. The insufficient ability of cell lines grown on planar surfaces to correctly recapitulate drug response in vivo has been debated as a possible explanation for this[7]. Accompanied by several studies pointing towards signalling and response differences between planar (2D) and spheroid (3D) cultures in vitro[8,9], it has been discussed whether spheroid cultures would offer a more reliable in vitro system. Although different cultivation techniques allow for different levels of complexity of 3D cultures[7], they all share the common characteristic of representing a cellular architecture with physiologically relevant gradients, not present in planar cultured cells[8,10]. These gradients relate to e.g. concentrations of nutrients, growth factors, oxygen

[1]Department of Clinical and Molecular Medicine, Norwegian University of Science and Technology, Trondheim, Norway. [2]The Cancer Clinic, St Olav's University Hospital, Trondheim, Norway. [3]Department of Biotechnology, SINTEF Materials and Chemistry, Trondheim, Norway. [4]Department of Biomedical Laboratory Science, Norwegian University of Science and Technology, Trondheim, Norway. [5]These authors contributed equally: Evelina Folkesson and Barbara Niederdorfer. ✉email: asmund.flobak@ntnu.no

and drugs, which have been shown to mimic corresponding gradients in patient tumours, including chemical gradients set up by the proximity of blood vessels in vivo[8]. In contrast to 2D-cultured cells, where the larger part of the cell population is actively proliferating, 3D cultures are considerably more heterogeneous with respect to the proliferative capacity and have, unlike cells cultured in 2D, been found to contain a non-proliferating quiescent or hypoxic cell population similar to that of tumours in vivo[8]. Clinically, quiescent tumour cell populations constitute a major treatment hurdle, as the quiescent phenotype frequently is associated with resistance to standard therapies[11,12]. Monitoring the effect of drugs considering also non-proliferating cells may therefore be of great significance in order to increase the bench-to-bed translational efficiency. Overall, these considerations are some, among many others, that may partly explain why drugs with documented efficiency in 2D cultures often do not show the same effect in more complex cellular contexts and in vivo.

In the present study, we have performed a high-throughput screen to systematically compare drug combination effects in 2D versus 3D culture models of three CRC cell lines (HCT-116, HT-29 and SW-620). The combinatorial treatments investigated comprised all pairwise combinations of five experimental or approved targeted small molecule inhibitors and two approved chemotherapeutic drugs. Our results show that several drug combination effects are observed in only one of the culture modes as measured by ATP content, a widely used readout for cell viability. Inclusion of cell confluency and spheroid size as additional cell growth readouts identified additional synergistic combinations, although synergistic drug combinations called by the different readouts overall showed high agreement within culture formats. These findings highlight the importance of more advanced screening platforms, encompassing different phenotypic readouts and more so, 3D culture models, for identification of synergistic drug combinations.

Results

Screening procedure. To identify efficacious synergistic drug combinations, we screened five targeted and two chemotherapeutic drugs in 2D and 3D CRC cell line cultures (HCT-116, HT-29, SW-620). Drugs were selected based on approval for clinical use in CRC or other cancer types (5-FU, oxaliplatin, olaparib, palbociclib), and on their ability to target pathways frequently dysregulated in cancer (MAPK/ERK pathway, PI3K/AKT/mTOR pathway and TGF-beta pathway). The combination screen, in which all 21 pairwise combinations were screened in 5 × 5 dose matrices, was preceded by a single-drug screen, where cells were subjected to a broad dose range (0.01–20 μM) of the drugs in single application. Results from the single-drug screen were used to guide the selection of doses for the combination screen (Fig. 1). In line with procedures applied by other drug screen labs[5,6,13,14], we used viability as assessed by ATP content (CellTiter-Glo) as the main readout to gauge drug responses in 2D and 3D cultures. Additional readouts included measurement of confluency (2D), spheroid diameter (3D) and cell death (2D).

MEK and TAK1 inhibitors most strongly compromise cell viability upon single-drug treatment. To evaluate the optimal dose range for the drug combination screen, we performed curve fitting[15] and calculated IC20 and Area Under the Curve (AUC) values (Fig. 2a,b) based on single-drug response viability data (Supplementary Table S1, Supplementary Fig. S4). As shown in Fig. 2a,b, the MEK (MAP2K1, MAP2K2) inhibitor PD0325901 (PD) was found to be the most potent single-inhibitor across all cell lines in both 2D- and 3D-cultured cells, followed by the TAK1 (MAP3K7) inhibitor 5Z-7-oxozeaenol (5Z). Comparison of drug responses between culture formats (2D versus 3D), indicated that HT-29 cells were less sensitive to oxaliplatin (OXA) and palbociclib (PAL) when cultured in 3D, while HCT-116 appeared to be more sensitive to MEK inhibition in the 3D format, compared to planar cultured cells. Although comparison between 2D and 3D cultures revealed general response differences between the two culture formats, no clear trend pointing towards either of them being more sensitive than the other was observed.

Single-drug treatment reduces viability independently of cell death. As the CellTiter-Glo ATP assay provides viability information based on cellular metabolic activity[16] rather than giving an absolute phenotypic outcome, we additionally assessed confluency and cell death[17,18] in 2D-cultured cells and included assessment of spheroid size in 3D-cultured cells[19,20]. Although most drugs showed effect in terms of reduced viability, which was also accompanied by a reduction in relative confluency (Supplementary Figs. S4, S5), increased levels of caspase-3 (NucView) or cellular DNA (CellTox Green) were rarely observed for any of the single-drugs (Supplementary Fig. S6). Out of the seven single-drugs, only the TAK1 inhibitor (5Z) induced cell death detectable by both cell death assays at several concentrations across all cell lines. Apoptotic effects of the TAK1 inhibitor have previously been reported in HeLa and HT-29 cells, where TAK1 inhibition using 5Z-7-oxozeaenol was found to downregulate the apoptosis inhibitor NF-κB in a dose-dependent manner[21]. The overall little effect of single drugs on cell death was also reflected in considerably stronger correlation between cell viability and cell confluency responses compared to the correlation between the viability readout and either of the cell death readouts (Fig. 2c). While none of the treatments reduced confluency compared to start of treatment (Supplementary Fig. S5a), several of the compounds reduced confluency relative to untreated cells upon 48 h exposure (Supplementary Fig. S5b), indicating a cytostatic rather than cytotoxic effect. Spheroid size reported an overall response similar to ATP, with a correlation coefficient of $R = 0.73$, and was found to be only weakly affected by treatment, with the TAK1 inhibitor having the largest effect followed by the MEK inhibitor (Supplementary Fig. S7).

In summary, our results suggest that, at least in 2D cultures, most of the tested single-drugs reduce viability independently of apoptosis. Overall, response in 3D correlated well with 2D response. As only two of the tested compounds induced cell death at doses selected for the combination screen, this readout was omitted in the combination screen.

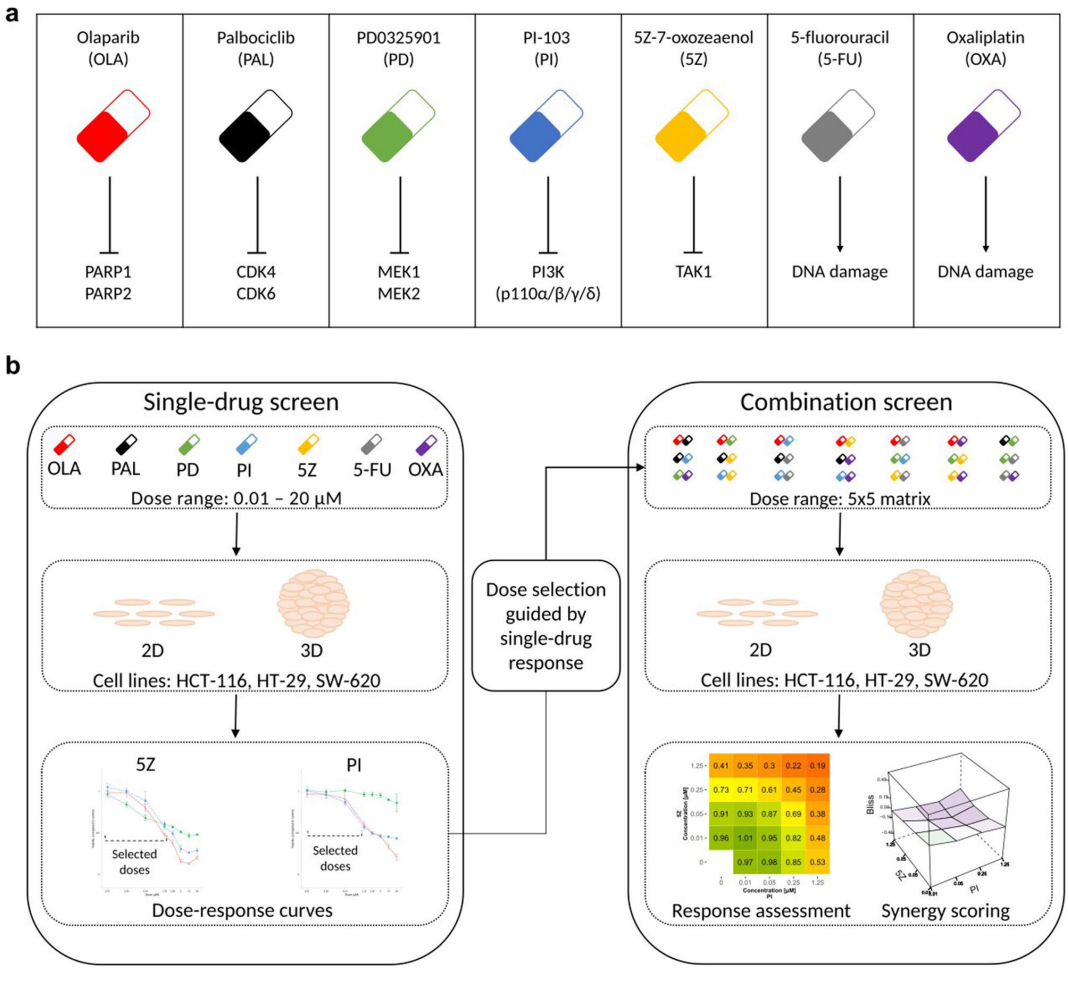

Figure 1. Overview of drugs, targets and screening procedure. (**a**) Drugs included in the study are presented with their full name, abbreviation and target/effect. (**b**) Single-drug screen: cells were treated with each drug in single application in a broad dose range. Combination screen: drugs were combined pairwise in 5 × 5 matrices. Dose selection was guided by single-drug response. In both screens, cells were subjected to drugs or drug combinations for 48 h. Combination effect was calculated using the Bliss independence reference model. Responses in both single and combination screens were assessed by measuring cell viability (ATP-content, CellTiter-Glo). Cell confluency and spheroid size was additionally quantified in 2D- and 3D-cultured cells, respectively.

Synergistic drug combinations are more frequently observed in 2D cultures. Next, the drugs were combined in all possible pairwise combinations across all doses in a 5 × 5 matrix (Supplementary Methods: Table II). Drug combination effects were evaluated using the Bliss independence model[22], where Bliss excess values below and above 0 were classified as synergy and antagonism, respectively. The choice of the Bliss independence model as synergy metric was based on that it is, alongside Loewe additivity and the extension of Combination Indexes, one of the most widely used synergy metrics[23,24].

Out of all tested combinations in both 2D- and 3D-cultured cells, we observed that approximately 36% (369 of 1,008 data points, 2D) and 35% (351 of 1,008 data points, 3D) showed a greater than expected combination response (viability), i.e. Bliss excess < 0. Of the 21 pairwise drug combinations, 13 and 8 further showed an average Bliss excess < 0 across the whole dose–response matrix in at least one cell line in 2D and 3D, respectively (Fig. 3a). The combinations found to be synergistic included the well-documented combination effect of co-targeting PI3K and MEK[25–27] as well as combined application of the PI3K inhibitor with the TAK1 inhibitor, previously reported by us[28] and later also by others[29]. The clinically approved combination of oxaliplatin (OXA) with 5-fluorouracil (5-FU)[30] was found to be synergistic at low doses of oxaliplatin across all cell lines, albeit with low efficacy of

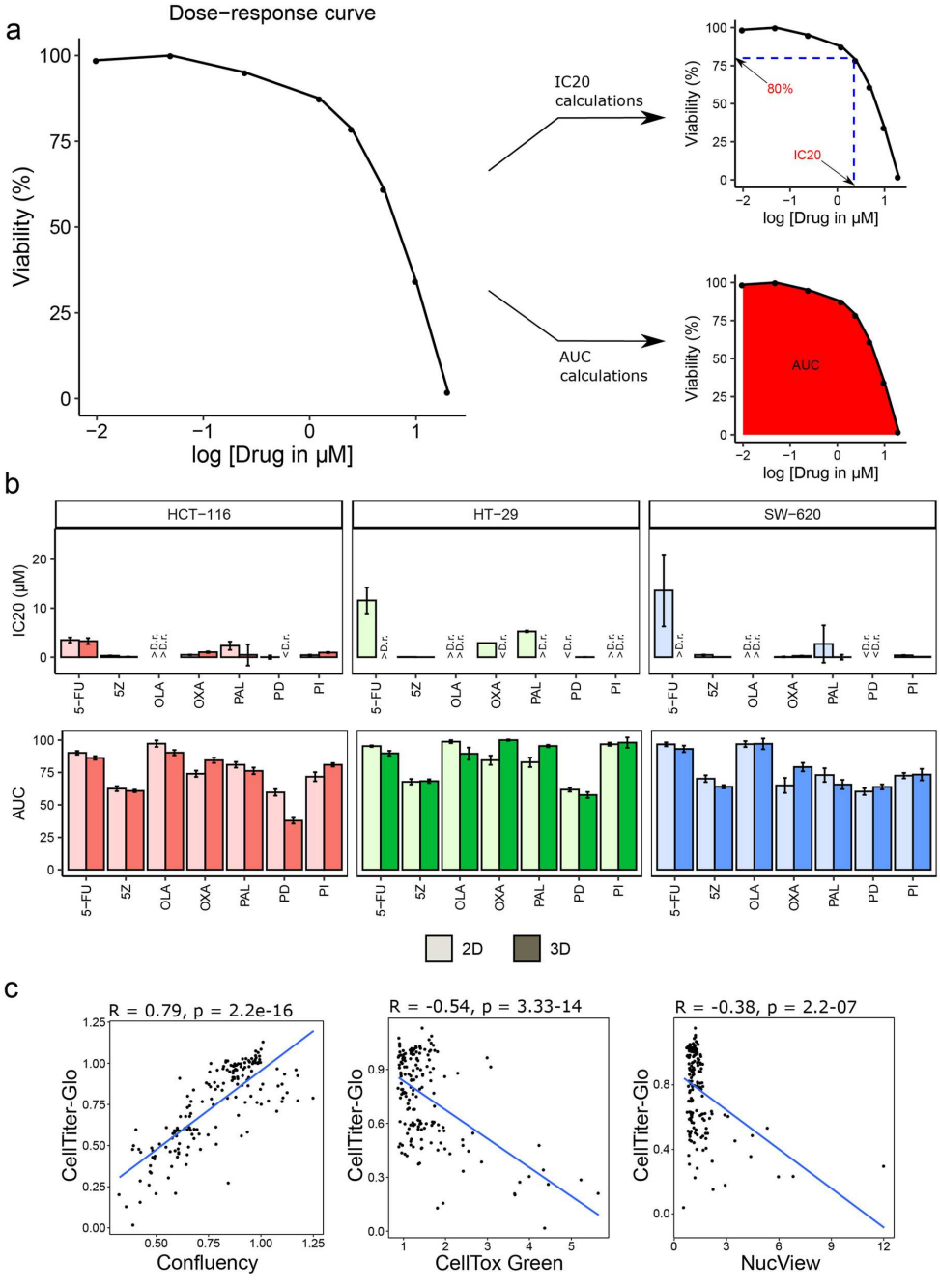

Figure 2. Single-drug screen data. (**a**) Principle: IC20 and AUC values were estimated from viability-based dose–response curves per cell line, culture format and drug. (**b**) Bar plots of IC20 and AUC values, where < D.r. and > D.r. indicate values below and above the tested dose range (0.01–20 µM), respectively. NA indicates that no IC20 could be calculated. Error bars represent standard error of the mean (SEM) of four technical replicates. (**c**) Correlation between CellTiter-Glo (viability) and other responses (confluency, CellTox Green and NucView) in 2D cultures following 48 h of incubation with single-drugs.

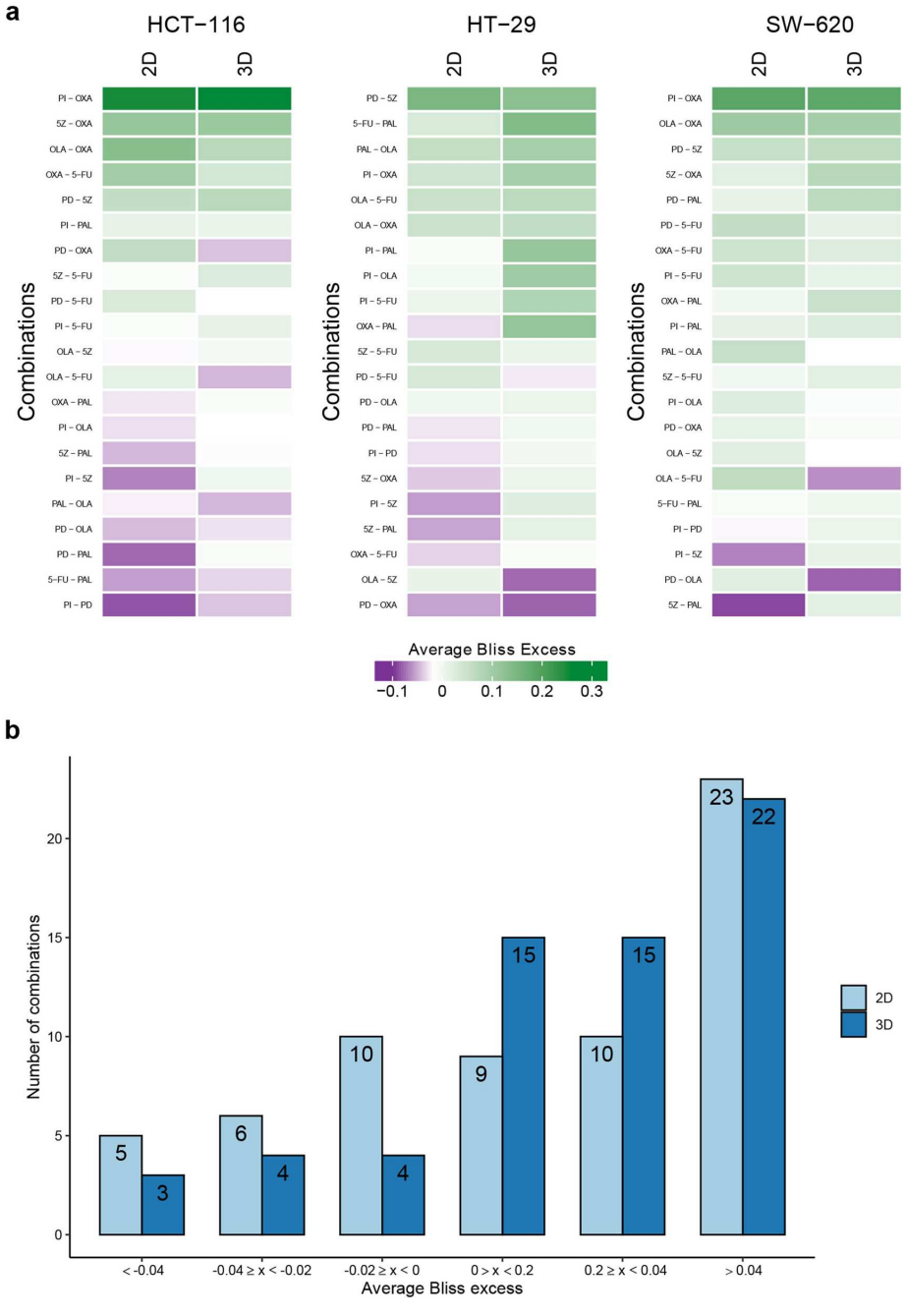

Figure 3. Drug combination effects of tested compounds in 2D and 3D cultured cell lines. (**a**) Heatmaps of Bliss excess averaged across the matrix per combination, cell line and culture format, within cell line comparison of 2D and 3D cultures. Rows are sorted based on Euclidean distance. (**b**) Number of drug combinations showing Bliss excess within given intervals. Combinations with Bliss excess < 0 are classified as synergistic.

only reducing viability to < 0.5 in 2D-cultured HCT-116 cells. Other drug combinations deemed to be synergistic include palbociclib with either the TAK1 inhibitor, oxaliplatin and the MEK inhibitor (Fig. 3). As can be seen in Fig. 3b, in general fewer combinations were observed to be synergistic when cells were assayed in 3D as compared to 2D. While in 2D, six combinations were identified to be synergistic in more than one cell line, in 3D, only three combinations—olaparib with 5-FU, and the MEK inhibitor with either of olaparib and oxaliplatin, displayed synergistic action in more than one cell line. This may indicate that cell line-dependency of combination effects is more pronounced in 3D or may be attributed to a generally lower overall number of synergistic combinations in 3D. Interestingly, none of the combinations identified as synergistic in more than one cell line in 3D were among the combinations identified as synergistic in more than one cell line in 2D-cultured cells.

Together, these results indicate that not only is cell line dependency of drug combination effects more pronounced in 3D, but it is even more profoundly different. In summary, our findings indicate that the drug combination effects vary depending on whether planar or spheroid cultures are studied, and that frequently, for a given cell line, one specific combination can be found to act synergistically in only one of the culture formats.

Synergy-viability plots identify MEK inhibitor combinations as more synergistically effective in 3D cultures. Synergy scores give an estimate of the interaction effect of drugs, but do not inform about the magnitude of remaining viability of cells following treatment. Hence, two different combinations might score as equally synergistic, even though both single-drugs and the combination, affect viability considerably more in one pair compared to the other pair and may thus be of higher interest for further characterisation. To take this into account, we introduced two additional measures of combination effects; one by which effect on viability was assessed *without* taking synergy scores into account (effective combination = combination that strongly compromises viability), and one by which combinations were evaluated jointly based on their effect on viability *and* synergistic properties. We use the term 'synergistically effective combination' for combinations that act synergistically *and* strongly compromise viability (i.e. ≤ 50% for one or several doses). To evaluate the absolute combination treatment effect on viability, we averaged viability data over the whole matrix per cell line and drug combination. We found that combinations involving the MEK inhibitor most strongly reduced this viability score in both 2D- and 3D-cultured cells, with significantly increased sensitivity in 3D compared to 2D for several combinations (Fig. 4a, Supplementary Fig. S8). Although 2D cultures were generally found to be more sensitive when assessed across all drug combinations, 3D cultures tended to be more sensitive to combinations involving the MEK inhibitor. For HCT-116 the higher sensitivity of spheroids was significant for all combinations involving the MEK inhibitor, whereas in HT-29 and SW-620 cells, it was evident for three and two combinations, respectively (Fig. 4a, Supplementary Fig. S8). Although strongly effective in both culture formats, the synergistic effect of MEK inhibitor combinations, compared to non-MEK inhibitor combinations, was generally weaker in 2D compared to 3D (Fig. 3a). This was also reflected in number of 'synergistically effective combination' concentrations (Fig. 4b,c). Here, five out of six MEK inhibitor combinations were among the most synergistically effective combinations in 3D, whereas only two of these combinations were among the five most synergistic and effective combinations in 2D (Fig. 4c). These results indicate that whereas in 2D cultures high sensitivity towards MEK inhibition alone most likely accounts for the strong reduction in viability observed upon treatment with MEK inhibitor combinations, the viability reduction in 3D cultures is a synergistic effect that can to a larger extent be ascribed to both drugs in the pairwise combinations involving the MEK inhibitor. Overall, the landscape of synergistically effective combinations appears to be more diverse in 2D cultures, with four different drugs (PD, PAL, PI and 5Z) involved more than once in the top five combinations (Fig. 4c), compared to only two different drugs (PD and PI) in 3D cultures.

In summary, by implementing the definition 'synergistically effective combinations' we were able to identify drug combinations with viability-compromising, as well as synergistic, properties. This strategy further allowed us to identify MEK inhibitor combinations as more synergistically effective in 3D compared to 2D cultures. Several of the combinations classified as synergistically effective have been tested in clinical trials (including the MEK inhibitor with either PI3K inhibitor or palbociclib), alluding the potential clinical value of this scoring metric.

Synergistic combinations show high agreement within culture formats. After studying differences in drug combination response between 2D and 3D-cultured cells by standard viability readout, we further investigated whether imaging-based readouts can provide us with additional distinct information regarding the combinatorial effect of drugs. For this we studied overall Bliss excess scores for synergy classification per combination, cell line and readout. None of the observed synergies were called based on data from all readouts across all cell lines and in common between both 2D- and 3D-cultured cells (Supplementary Fig. S9, Supplementary Table S2). In 2D-cultured HCT-116 and SW-620 cells, synergistic combinations identified by confluency were also identified as synergistic based on viability, while synergy by viability did not necessarily imply synergy by confluency (Supplementary Table S2). In HT-29 cells three combinations were classified as synergistic based on confluency but not by any other readout (Fig. 5a, Supplementary Fig. S9). These combinations showed significantly stronger synergistic response when assessed by confluency compared to the viability readout (Fig. 5b), however, none of the combinations showed strong effect on growth inhibition (Additional file 5). While the largest number of synergistic combinations was called by viability and confluency readouts of 2D-cultured cells, additional distinct synergistic combinations were captured by the two different 3D readouts (Fig. 5a). In total four combinations were only observed using the 3D viability readout (Fig. 5a), out of which one combination (PD + OXA in HCT-116) showed synergistically effective doses within the tested dose range (Fig. 4c).

These results imply that for 2D-cultured HCT-116 and SW-620 cells there is a strong resemblance in the synergistic landscape uncovered by confluency measures compared to the synergies we see based on cell viability (Supplementary Table S2). While in general drug combinations show a lower effect on confluency than on 2D

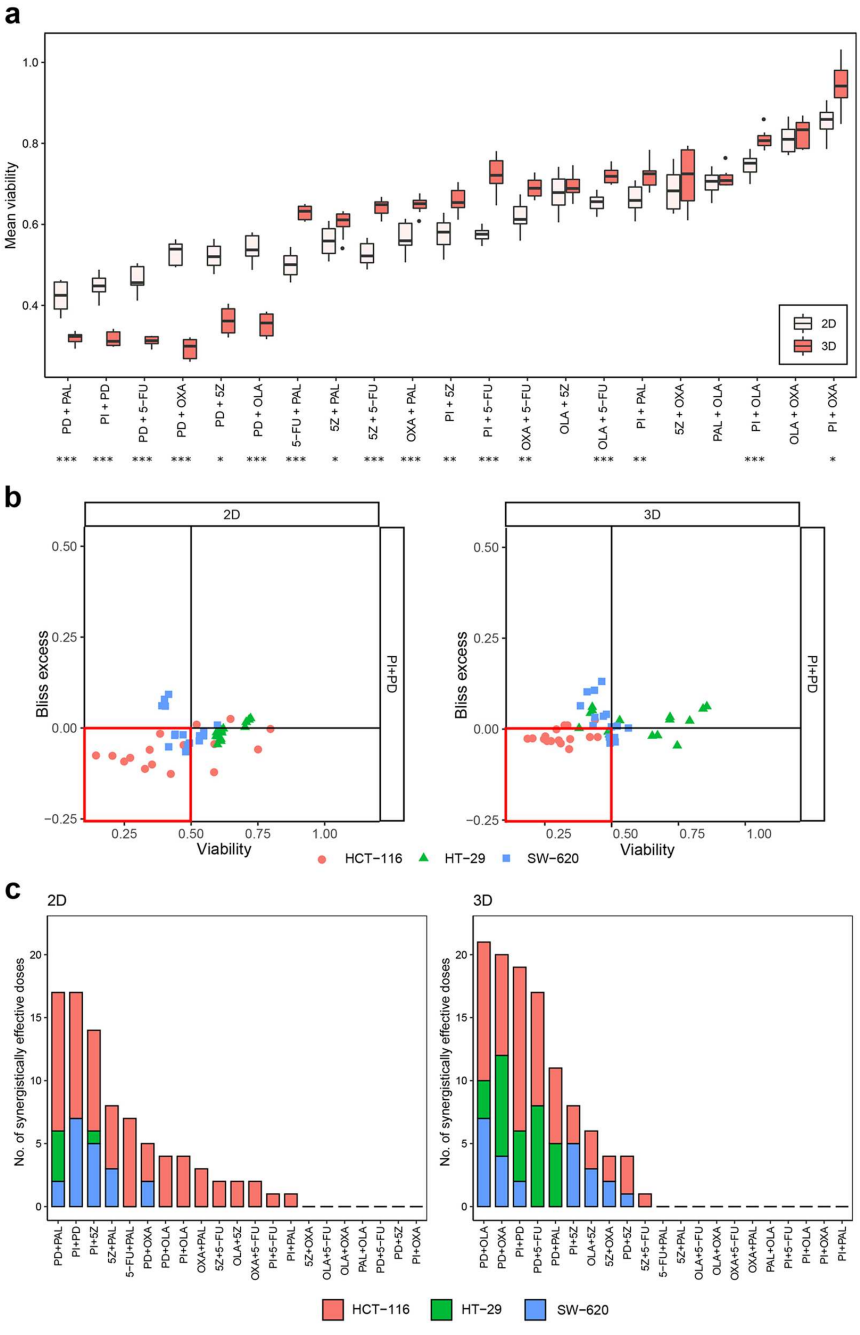

Figure 4. Drug combination effects judged by combined synergy-viability assessments. (**a**) HCT-116 viability averaged across the matrix per drug combination and culture format (2D, 3D). Asterisks (*) indicate a statistically significant difference in average viability between 2D- and 3D-cultured cells per drug combination, with $p \leq 0.05$, $p \leq 0.01$ and $p \leq 0.001$ for *, ** and ***, respectively. (**b**) Bliss excess versus viability plots for 2D- and 3D-cultured cells treated with PI3K inhibitor and MEK inhibitor (PI + PD). Red boxes enclose data points considered to be synergistically effective according to the definition (Bliss excess < 0, viability < 0.5). (**c**) Number of synergistically effective doses per combination, cell line and culture format. Empty positions along the x axis indicate combinations for which no synergistically effective doses were observed (alphabetically per culture format).

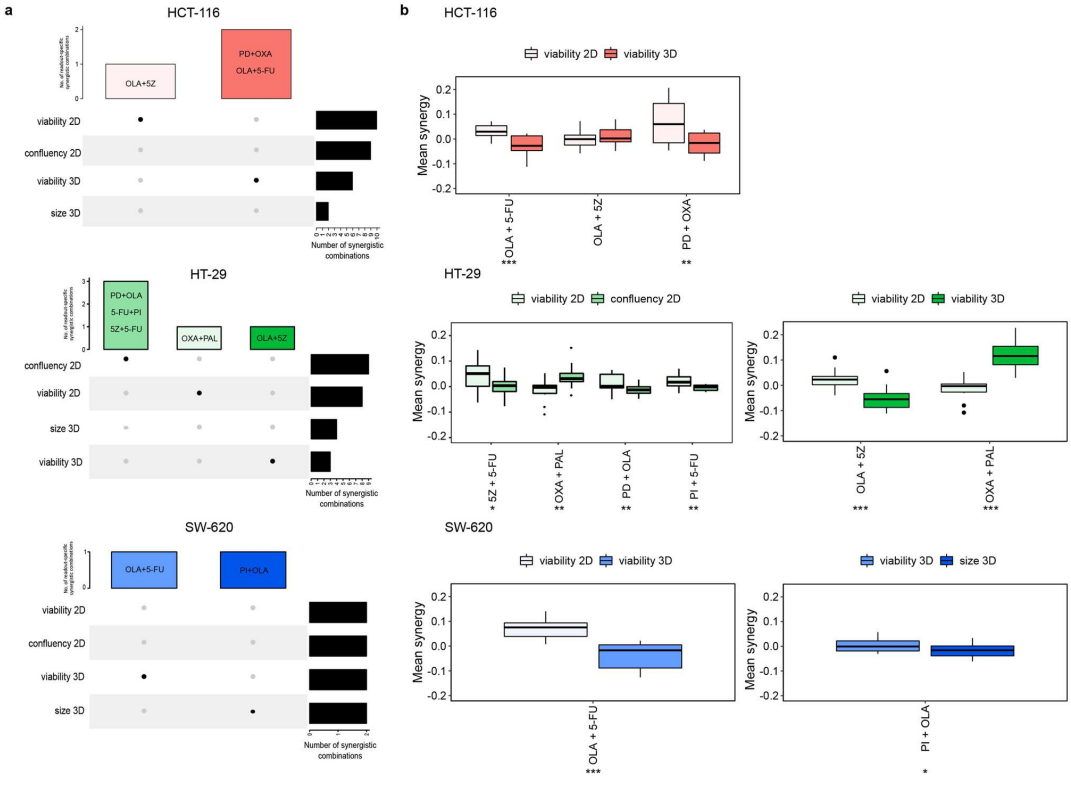

Figure 5. Differences in synergy calling per readout. (**a**) Total number of synergistic drug combinations called per readout (black bars), and total number of readout-specific synergistic combinations (coloured bars), where filled data-points highlight the readout by which synergistic drug combination(s) shown in the coloured bars are uniquely called. (**b**) Differences in synergy strength between indicated readouts per cell line. Asterisks (*) indicate a statistically significant difference in synergy strength, with $p \leq 0.05$, $p \leq 0.01$ and $p \leq 0.001$ for *, ** and ***, respectively.

viability (Additional file 1 & 5), combinations found to be synergistically effective in reducing relative viability (Fig. 4c), were also found to be synergistically effective in reducing relative confluency (Supplementary Fig. S10a). The same trend can be observed when comparing synergistic combinations that show an effect on spheroid viability (Fig. 4c) and size (Supplementary Fig. S10b). To summarise, while different readouts within the same culture format overall show high agreement in synergy calling, additional synergistic combinations of potential interest are revealed by screening in 3D cultures, in addition to standard 2D cultures.

Prolonged drug exposure alters drug combination effects and induces apoptosis upon MEK inhibition. As several drug combinations were found to potently affect viability, we next explored whether also apoptosis was induced and if observed drug effects were reversible or increased with longer exposure time. For this, we continuously monitored apoptosis in addition to cell confluency (2D) and spheroid size (3D) and increased incubation time to 96 h. Viability was included as endpoint measurement for both 2D- and 3D-cultured cells. Three combinations were selected for this follow-up screen based on (1) their synergistic effectiveness (viability ≤ 50% and Bliss excess < 0) in both 2D and 3D at 48 h (5Z + PI, Fig. 4c), or (2) their stronger synergistic effect (Bliss excess) in 3D versus 2D culture at 48 h (PD + OXA, Fig. 3a), or (3) the observation of few synergistic and effective doses across all tested conditions at 48 h (PI + 5-FU, Fig. 4c), but with clinically relevant targets[31,32].

While in general little to no apoptotic response was observed in any of the cell lines and culture formats upon treatment with the PI3K inhibitor combinations, MEK inhibitor treatment alone induced apoptosis at all concentrations in HCT-116 spheroids (Additional file 9). At high concentrations of oxaliplatin, a further increased apoptotic effect was observed by combination treatment (Fig. 6d,e). This effect was not observed in 2D-cultured HCT-116 cells, in contrast here HT-29 cells showed increased apoptosis under MEK inhibitor treatment, which was also weakly observed in HT-29 spheroids (Additional file 10).

Overall, the correlation between combination drug responses at 48 h and 96 h was strong, with a correlation coefficient (R) ranging from 0.74 to 0.89, and from 0.81 to 0.96 in 2D and 3D cultures, respectively (Fig. S11). When comparing mean viability and combination effect (Bliss excess) at the two time points (48 h and 96 h),

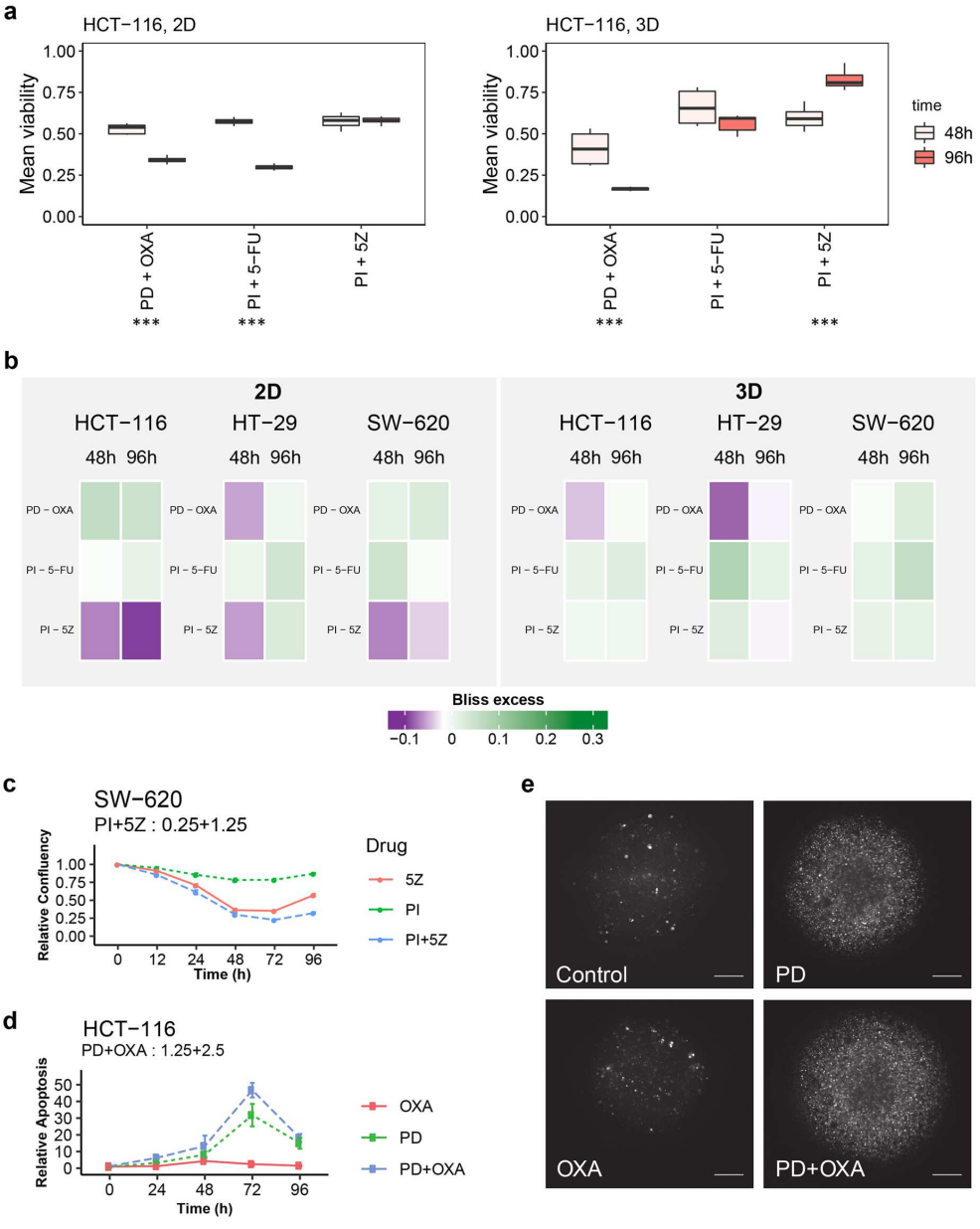

Figure 6. Readout and synergy scoring data upon 48 h and 96 h incubation with drugs. (**a**) Comparison of mean viability at 48 h (combination screen) versus 96 h (96 h screen) for HCT-116 cells cultured in 2D and 3D. Asterisks (*) indicate statistically significant difference in average viability between 48 and 96 h per drug combination, with $p \leq 0.05$, $p \leq 0.01$ and $p \leq 0.001$ for *, ** and ***, respectively. (**b**) Mean Bliss excess at 48 h (combination screen) versus 96 h (96 h screen). (**c**) Relative confluency compared to 0 h and vehicle control in 2D-cultured SW-620 cells exposed to PI and 5Z at the indicated concentrations. (**d**) Relative apoptosis compared to 0 h and vehicle control in 3D-cultured HCT-116 cells treated with the MEK inhibitor PD0325901 (PD), oxaliplatin (OXA), or combination (PD + OXA) at 1.25 (PD) + 2.5 (OXA) μM. (**e**) Representative 72 h-image of apoptotic cells in HCT-116 spheroids treated with vehicle control, 1.25 μM PD, 2.5 μM OXA or combination (PD + OXA). Scale—100 μm. (**c**,**d**) represent the average of three biological replicates with standard deviation.

we found that although response on average was stronger at 96 h (Fig. 6a, Supplementary Fig. S12), likely due to increased exposure time, combination effects overall decreased across all cell lines (Fig. 6b). This was also reflected in the decreased number of synergistically effective doses in 3 out of 6 conditions (Supplementary Fig. S13). Most striking was the strong effect of MEK inhibition alone, with the highest dose of single PD (1.25 μM) being able to reduce viability to less than 25% across all cell lines, while the combination effect of this inhibitor with oxaliplatin was considerably lower at 96 h compared to 48 h (Fig. 6b). Contrary to the general reduction in mean viability at 96 h compared to 48 h, we observed a significant increase in mean viability of HCT-116 spheroids and SW-620 planar-cultured cells when treated with the PI3K inhibitor in combination with the TAK1 inhibitor (Fig. 6a, Supplementary Fig. S12). This was also reflected by an increase in relative confluency/size in both cell lines, albeit weaker in HCT-116 cells (Fig. 6c).

In summary, these results demonstrate that whereas longer incubation time with drugs not unexpectedly further reduces viability compared to 48 h, the synergistic effect of the tested drug combinations overall tends to be weaker and sometimes even reversed at 96 h. This might be due to already strongly compromised viability at 96 h for each single drug at selected doses, and therefore a much smaller viability range for any synergistic combination response observations. Results from the 96 h exposure screen further support our previous findings of the MEK inhibitor PD0325901 (PD) as a strongly potent inhibitor, which also in single application was able to induce considerable apoptosis in several of the tested conditions (Fig. 6e).

Discussion

Advances in high-throughput screening and high-content imaging have accelerated testing and discovery of anti-cancer drugs in vitro. However, despite demonstrating efficiency in vitro, only a small fraction of putative treatments has been found to display similar effects in in vivo experiments, and yet fewer in human clinical trials[7,33]. The insufficient ability of in vitro 2D-cultures to recapitulate treatment responses in vivo is believed to be one among many other possible explanations for the slow developmental progress. 3D cell culture models may more closely mimic the architecture of solid tumours and are being anticipated to enable identification of more clinically relevant drug treatments[34]. As a step towards mapping differences and similarities between the two culture formats, we here systematically examined response and combination effects of 7 single-drugs and 21 pairwise combinations in three 2D- and 3D-cultured CRC cell lines (HCT-116, HT-29 and SW-620). While single drug responses have previously been compared in 2D and 3D cultures[9,35,36], only two other studies have, to our knowledge, compared effects of drug combinations between the two culture formats. The number of combinations tested in these studies has, however, been low (three[37] and ten[38] drug combinations, respectively). Furthermore, while Yan et al.[39] tested 56 drug combinations in 3D cell line cultures, none of these combinations were tested in 2D cultures. To our knowledge, our study represents the largest published comparison of 2D and 3D cultures and their response to cancer-relevant drug combinations.

Altogether, our high-throughput drug screening platform enabled effective identification of single and combination responses in both culture formats. Differences in drug combination responses were observed both between 2D and 3D culture models, readouts and cell lines. This demonstrates the value of including additional readouts and, more so, the use of spheroid-based models for drug combination studies to allow for detection of synergistic effects in different phenotypes and culture formats.

Several studies have reported on altered drug responses in comparisons of spherical versus planar cultures[8,35,37,40–42]. Alterations manifest both as increased and decreased effect of the same drug or drug combination[12]. We too observe culturing mode-related differences in drug sensitivity for some of the tested compounds, with no clear trends pointing towards one of the culture formats as being more sensitive than the other. Consistent with findings by others, we observed reduced sensitivity to the chemotherapeutic agent oxaliplatin in 3D cultures. Riedl et al. previously reported reduced cell cycle progression in several CRC cell lines including HCT-116, HT-29 and SW-620 cells when cultured as spheroids compared to planar cultures[8], similar to what has also been shown for other cancer types[40]. This accords with our observations of reduced sensitivity of HT-29 spheroids to the cell cycle progression inhibitor palbociclib.

Although the number of studies reporting on differences in single-drug responses between 2D and 3D cultures has been on the rise during the last years, high-throughput drug combination studies are still scarce, with only a few pioneering studies published so far[38,39]. We show that several synergistic drug combinations identified in 2D cultures are not rediscovered in 3D cultures, but also that some synergistic combinations are solely identified in spheroid cultures. In contrast to the observed trend of weaker effect of drug combinations in spheroids, we found that combinations involving the MEK inhibitor PD0325901 exerted a stronger inhibitory effect in 3D cultures. This supports the notion that spheroids show increased dependency on the MEK pathway for their survival[41]. Combinations involving 5Z-7-oxozeanol, which in addition to being a TAK1 inhibitor also has been reported to inhibit MEK1 and ERK2[43], did in general not show stronger effect in 3D compared to 2D, which could indicate that the inhibitory effect of the TAK1 inhibitor on MEK is considerably weaker than that of PD0325901, in line with other reports[44,45].

Overall, our results indicate that 2D screening identifies a higher number of positive hits compared to screens of spheroid cultures. This is in contrast to findings by Mathews Griner et al.[38] who reported a generally higher number of synergistic combinations observed in 3D compared to cells cultured in 2D. Overall, this indicates that there is no general trend in which of the two culture systems appears to be more sensitive to combination treatment. These results thus highlight that when using both culture formats additional interesting combination effects can be observed, that are distinct to one of the culture systems and that would have been missed in screening efforts applying only one of them.

In concordance to findings by Gautam et al.[13], we notice that readout method matters, underpinned by the fact that we observed several differences in identified drug synergies, synergy strength and combination effect

between the different readouts used in this study. The generally high compliance of identified synergies between viability and confluency measurements in 2D cultures can be expected as both assays can be considered as proxies for the number of live cells. The lower compliance of identified synergies between 3D viability and spheroid size might be explained by the generally lower number of observed synergistic effects. Alternatively, differences might be explained by loosening of spheroid structure upon certain treatments, as observed by others[46] and which might be interpreted as an increase in size, or low effect on cell death by our treatments.

Although synergistic drug combinations called by different readouts (viability vs. confluency/size) overall showed high agreement within culture formats in our screen, the use of imaging-based readouts might still be of high value for assuring technical validity of drug screens, especially when performing drug screens in 3D cultures. While progress in 3D cultivation technologies has simplified the production and handling of spheroids, many cultivation techniques still suffer from limitations associated with generation of uniform spheroids[47], something that might affect reproducibility of data originating from these models. In our screen, technical as well as biological variability in viability was on average slightly higher in 3D compared to 2D cultures (Supplementary Table S3, Supplementary Fig. S2). As shown by Zanoni et al., both volume and shape of spheroids might affect the response to treatment, in particular when using agents aimed to target proliferating cells[47]. Imaging might allow for pre-selection of optimal spheroids for drug screens by enabling selection of those spheroids meeting specific criteria in terms of e.g. size and morphology[47,48]. By constituting a non-invasive readout method, also real-time monitoring of phenotypic and cellular events is possible[19], as demonstrated by the continuous measurements of apoptosis (2D, 3D), confluency (2D) and size (3D) in our 96 h screen. Similar to the study by Zanoni et al.[47], viability data showed relatively high correlation with data from brightfield imaging in our screen (Supplementary Fig. S14), indicating the power of using imaging not only as a backup to the standard viability readout, but also as a possible complement allowing for non-invasive continuous monitoring of drug response.

Today, drug combination screens are commonly performed on large panels of carefully characterised cell lines[6,49], where combinations considered as clinically relevant often are those classified as synergistic either across the whole panel, or across cell lines in certain mutational-driven clusters. Here, by implementing an approach where drug combinations were mapped according to synergy scores (doses classified as synergistic for Bliss excess < 0) as well as viability response (doses classified as effective for viability ≤ 50%) in 2D and 3D in vitro cultures, we show that the highest scoring drug combinations comprise a sizable number of combinations that are in clinical testing. These results point to the importance of using assessment of cellular phenotype such as viability in addition to synergy score as metrics when evaluating drug combination effects, similarly to what was shown by Meyer et al.[50]. Interestingly, the fourth most synergistically effective drug combination in 3D cultures, 5-FU with the MEK inhibitor, did not demonstrate any synergistically effective doses in 2D cultures, and hence would have been left unidentified if screening in 2D cultures exclusively. The same is true for the two combinations comprising the TAK1 inhibitor with either oxaliplatin or the MEK inhibitor, which were synergistically effective at multiple doses in 3D-cultured HCT-116 and SW-620 cells, but not in 2D-cultured cells. Altogether these results suggest that future screening platforms ideally should encompass monitoring of both conventional ATP-based and additional readouts, as well as more complex culture models, in order to cover as large part of the therapeutic synergy landscape as possible.

Methods

Cell lines, drugs and reagents. Human CRC cell lines used in this study were HCT-116 (CVCL_0291), HT-29 (CVCL_0320) and SW-620 (CVCL_0547). The cell lines were directly obtained from NCI. No mycoplasma testing was done in-house. Cells were routinely cultured in 1X RPMI-1640 medium (Thermo Fisher Scientific) supplemented with 10% fetal bovine serum (FBS, Sigma Aldrich), 2 mM L-Glutamine (Sigma Aldrich) and 100 U/mL Penicillin–Streptomycin (Thermo Fisher Scientific). All cells were maintained at 37 °C with 5% CO_2 and 80% relative humidity and passaged according to in-house protocols (see Supplementary Methods). Cells used in experiments never exceeded passage 21.

Drugs used in screens were olaparib (Selleckchem), oxaliplatin (Selleckchem), palbociclib (Selleckchem), PI-103 (Selleckchem), PD0325901 (Sigma Aldrich), 5-fluorouracil (5-FU, Sigma Aldrich) and 5Z-7-Oxozeaenol (Enzo Life Sciences). Assay reagents used in screens were CellTiter-Glo 2.0 Assay (Promega), CellTiter-Glo 3D Cell Viability Assay (Promega), CellTox Green Cytotoxicity Assay[17] (Promega) and NucView 488 Caspase-3 Substrate[18] (Biotium).

Drug screens. *Cell seeding procedure.* For screening in planar (2D) and spheroid (3D) cultures, cells were plated with 30 µL complete growth medium in 384-well black tissue culture treated plates (Corning) and 384-well black round-bottom ultra-low attachment plates (Corning), respectively. Seeding densities and plating setups are described in Supplementary Methods: Table I. In the 96 h follow-up screen, seeding numbers were reduced for 2D cultures to ensure that controls did not reach full confluency before the endpoint readout. Following seeding, 2D plates were shaken (1,600 rpm, 30 s) to ensure uniform sedimentation of cells. 3D plates were shaken (1,600 rpm, 30 s) and centrifuged (200G, 5 min) to allow aggregation of single cells into spheroids. Before drug addition, cells in 2D and 3D were allowed to adhere/aggregate for 24 h and 72 h, respectively.

Drug treatment. Drug compounds and doses used in screens are summarised in Fig. 1a and Supplementary Methods: Table II. For the combination screen, four of the original eight doses screened in single applications were selected (see Supplementary Methods). Drugs in single, combination, vehicle (DMSO, water, DMSO + water 1:1) and positive controls (staurosporine, digitonin) were added in four technical replicates per condition to the wells using a Tecan Freedom EVO robotic system (5 µL/well). For measurement of apoptosis in the 96 h screen, 3 µL of NucView 488 Caspase-3 Substrate (final reagent concentration: 3.43 µM) and 2 µL of drug solution were

added to the wells. DMSO concentration never exceeded 0.5%. Cells were incubated (37 °C with 5% CO_2, 80% relative humidity) with drugs, vehicle, or positive controls for 48 h (single-drug and combination screens) or 96 h (96 h screen).

The single-drug screen was performed with four technical replicates and one biological replicate. The drug combination screen was performed with four technical replicates and two biological replicates per condition. The drug combination PD + 5Z at doses 0.05 μM + 0.01 μM was excluded from biological replicate 1 as no drug was added to the wells due to a robotic error. The 96 h screen was performed with 2–4 technical replicates and three biological replicates.

Readouts. All readouts are listed in Supplementary Methods: Table III. Shortly, for 2D-cultured cells confluency was assessed based on brightfield imaging. Apoptosis was assessed using NucView 488 Caspase-3 Substrate and fluorescence imaging (excitation: 456 nm, emission: 541 nm). Cell death (membrane integrity) was monitored using CellTox Green Cytotoxicity Assay by reading fluorescence at 535 nm. Cell viability was measured by reading luminescence after 10 min incubation with CellTiter-Glo 2.0 reagent (20 μL/well, mixed 1:1 with PBS prior to addition). A SpectraMax i3x reader equipped with a MiniMax 300 Imaging Cytometer (Molecular Devices) was used for all 2D readouts and image analysis.

Spheroid viability was measured by reading luminescence (Tecan infinite M200 Pro) after 60 min incubation with CellTiter-Glo 3D reagent (20 μL/well). Preceding addition of the CellTiter-Glo 3D reagent, images (× 4 magnification) were captured using an EVOS 1 imaging system (single-drug screen) or an ImageXpress Micro Confocal High-Content Imaging System (Molecular Devices). Apoptosis in spheroids was monitored using NucView 488 Caspase-3 Substrate and confocal fluorescence imaging. Fluorescent Z stack images (five planes per stack and 50 μm separation between planes at 0-72 h; ten planes per stack and 10 μm separation between planes at 96 h) were captured continuously. At each time point, spheroid size was estimated using brightfield imaging of mid-planes.

Data processing and statistical analysis. Confluency and apoptosis (2D) were estimated by re-analysing brightfield and fluorescence images using the SoftMax Pro 6 software. For each well, percentage of covered area (confluency) and number of fluorescent objects (apoptosis) were estimated. Spheroid size was quantified by high-throughput size measurement using SpheroidSizer[51] in Matlab (The MathWorks Inc., Natick, Massachusetts) version 2017a (single-drug screen) or 2015a (combination and 96 h screen). Apoptosis in spheroids was quantified by estimating the number of fluorescent cells in imaged sections using the MetaXpress software. All treatment effects are normalised to the internal vehicle control per plate and reported as average ± standard deviation. Pearson's correlation coefficient (R) has been used to quantify the association between variables.

R versions 3.5.1 and 3.5.3 were used for data processing and graphics, respectively. Packages are summarised in Supplementary Methods: Table IV. For statistical analyses, a two-tailed Student's *t* test (with $p < 0.05$ being considered significant) has been used when comparing two groups.

Synergy scoring. The Bliss independence reference model[22] was used to estimate synergy. The Bliss expectation ($E_{AB,\ Bliss}$) is calculated for drugs A and B from effect (E) as $E_{AB,\ Bliss} = E_A + E_B - E_A E_B$, and synergy is called if the observed effect of the combination is larger than the expectation. Synergy scores were calculated per biological replicate, followed by calculation of mean synergy scores across biological replicates as presented in[52]. We report both average and standard deviation of Bliss excess values per dose and biological replicate, as well as across the matrix.

Screen reproducibility. Inter- and intra-experiment reproducibility of response was assessed by comparing data points (doses) common for the different setups (Pearson correlation). The correlation coefficients for single-drug responses (viability data) in the single-drug screen and the combination screen were 0.78 and 0.77, for 2D and 3D cultures, respectively (Supplementary Fig. S1). The intra-experiment reproducibility for the combination screen was assessed based on the two biological replicates. Correlation coefficients were 0.97, 0.92, 0.93 and 0.95 for 2D viability, 2D confluency, 3D viability and spheroid size, respectively (Supplementary Fig. S2). The intra-experiment reproducibility for the 96 h screen was assessed based on three biological replicates. Correlation coefficients (viability data) ranged from 0.96 to 0.99 (Supplementary Fig. S3). Technical variability was assessed by computing the Coefficient of Variation (CV) per condition (treatment), biological replicate and readout. An overall CV was calculated by averaging the CV values per biological replicate and readout (Supplementary Table S3).

Data availability

All data supporting the conclusions of this article are available in the Figshare repository (https://figshare.com/s/b2b0726049f10a763e39).

Received: 15 January 2020; Accepted: 19 June 2020
Published online: 14 July 2020

References

1. IARC. *World Cancer Report 2014* (WHO Press, Geneva, 2014).
2. Bujanda, L. *et al.* Colorectal cancer prognosis twenty years later. *World J. Gastroenterol.* **16**, 862–867 (2010).
3. Tong, C. W. S., Wu, W. K. K., Loong, H. H. F., Cho, W. C. S. & To, K. K. W. Drug combination approach to overcome resistance to EGFR tyrosine kinase inhibitors in lung cancer. *Cancer Lett.* **405**, 100–110 (2017).

4. Al-Lazikani, B., Banerji, U. & Workman, P. Combinatorial drug therapy for cancer in the post-genomic era. *Nat. Biotechnol.* **30**, 679–692 (2012).
5. Holbeck, S. L. *et al.* The National Cancer Institute ALMANAC: A comprehensive screening resource for the detection of anticancer drug pairs with enhanced therapeutic activity. *Cancer Res.* **77**, 3564–3576 (2017).
6. O'Neil, J. *et al.* An unbiased oncology compound screen to identify novel combination strategies. *Mol. Cancer Ther.* **15**, 1155–1162 (2016).
7. Langhans, S. A. Three-dimensional in vitro cell culture models in drug discovery and drug repositioning. *Front. Pharmacol.* **9**, 14 (2018).
8. Riedl, A. *et al.* Comparison of cancer cells in 2D vs 3D culture reveals differences in AKT–mTOR–S6K signaling and drug responses. *J. Cell Sci.* **130**, 203–218 (2017).
9. Breslin, S. & O'Driscoll, L. The relevance of using 3D cell cultures, in addition to 2D monolayer cultures, when evaluating breast cancer drug sensitivity and resistance. *Oncotarget* **7**, 45745–45756 (2016).
10. Edmondson, R., Broglie, J. J., Adcock, A. F. & Yang, L. Three-dimensional cell culture systems and their applications in drug discovery and cell-based biosensors. *ASSAY Drug Dev. Technol.* **12**, 207–218 (2014).
11. Zhang, J. *et al.* Research progress on therapeutic targeting of quiescent cancer cells. *Artif. Cells Nanomed. Biotechnol.* **47**, 2810–2819 (2019).
12. Tung, Y.-C. *et al.* High-throughput 3D spheroid culture and drug testing using a 384 hanging drop array. *The Analyst* **136**, 473–478 (2011).
13. Gautam, P. *et al.* Identification of selective cytotoxic and synthetic lethal drug responses in triple negative breast cancer cells. *Mol. Cancer* **15**, 34 (2016).
14. Tomska, K. *et al.* Drug-based perturbation screen uncovers synergistic drug combinations in Burkitt lymphoma. *Sci. Rep.* **8**, 12046 (2018).
15. Gottschalk, P. G. & Dunn, J. R. The five-parameter logistic: A characterization and comparison with the four-parameter logistic. *Anal. Biochem.* **343**, 54–65 (2005).
16. *Technical Manual: CellTiter-Glo 2.0 Assay* (2018).
17. Promega Corporation. *Technical Manual: CellTox Green Cytotoxicity Assay* (2019).
18. Biotium. *Product Information: NucView 488 Caspase-3 Substrate* (2017).
19. Sirenko, O. *et al.* High-content assays for characterizing the viability and morphology of 3D cancer spheroid cultures. *ASSAY Drug Dev. Technol.* **13**, 402–414 (2015).
20. Mittler, F. *et al.* High-content monitoring of drug effects in a 3D spheroid model. *Front. Oncol.* **7**, 293 (2017).
21. Acuña, U. M., Wittwer, J., Ayers, S., Pearce, C. J. & Oberlies, N. H. Effects of (5Z)-7-oxozeaenol on the oxidative pathway of cancer cells. *Anticancer Res.* **32**, 2665–2672 (2012).
22. Bliss, C. I. The toxicity of poisons applied jointly. *Ann. Appl. Biol.* **26**, 585–615 (1939).
23. Greco, W. R., Bravo, G. & Parsons, J. C. The search for synergy: A critical review from a response surface perspective. *Pharmacol. Rev.* **47**, 331–385 (1995).
24. Yadav, B., Wennerberg, K., Aittokallio, T. & Tang, J. Searching for drug synergy in complex dose-response landscapes using an interaction potency model. *Comput. Struct. Biotechnol. J.* **13**, 504–513 (2015).
25. Clarke, P. A. *et al.* Dissecting mechanisms of resistance to targeted drug combination therapy in human colorectal cancer. *Oncogene* **38**, 5076–5090 (2019).
26. Haagensen, E. J., Kyle, S., Beale, G. S., Maxwell, R. J. & Newell, D. R. The synergistic interaction of MEK and PI3K inhibitors is modulated by mTOR inhibition. *Br. J. Cancer* **106**, 1386–1394 (2012).
27. Haagensen, E. J. *et al.* Enhanced anti-tumour activity of the combination of the novel MEK inhibitor WX-554 and the novel PI3K inhibitor WX-037. *Cancer Chemother. Pharmacol.* **78**, 1269–1281 (2016).
28. Flobak, Å *et al.* Discovery of drug synergies in gastric cancer cells predicted by logical modeling. *PLOS Comput. Biol.* **11**, e1004426 (2015).
29. Morris, M., Clarke, D., Osimiri, L. & Lauffenburger, D. Systematic analysis of quantitative logic model ensembles predicts drug combination effects on cell signaling networks: Systematic analysis of quantitative logic model. *CPT Pharmacomet. Syst. Pharmacol.* **5**, 544–553 (2016).
30. Mármol, I., Sánchez-de-Diego, C., Pradilla Dieste, A., Cerrada, E. & Rodriguez Yoldi, M. Colorectal carcinoma: A general overview and future perspectives in colorectal cancer. *Int. J. Mol. Sci.* **18**, 197 (2017).
31. Bahrami, A. *et al.* Therapeutic potential of targeting PI3K/AKT pathway in treatment of colorectal cancer: Rational and progress. *J. Cell. Biochem.* **119**, 2460–2469 (2018).
32. Fang, L. *et al.* Determining the optimal 5-FU therapeutic dosage in the treatment of colorectal cancer patients. *Oncotarget* **7**, 81880–81887 (2016).
33. Mak, I. W., Evaniew, N. & Ghert, M. Lost in translation: Animal models and clinical trials in cancer treatment. *Am. J. Transl. Res.* **6**, 114–118 (2014).
34. Booij, T. H., Price, L. S. & Danen, E. H. J. 3D cell-based assays for drug screens: Challenges in imaging, image analysis, and high-content analysis. *SLAS Discov. Adv. Sci. Drug Discov.* **24**, 615–627 (2019).
35. Imamura, Y. *et al.* Comparison of 2D- and 3D-culture models as drug-testing platforms in breast cancer. *Oncol. Rep.* **33**, 1837–1843 (2015).
36. Souza, A. G. *et al.* Comparative assay of 2D and 3D cell culture models: Proliferation, gene expression and anticancer drug response. *Curr. Pharm. Des.* **24**, 1689–1694 (2018).
37. Zoetemelk, M., Rausch, M., Colin, D. J., Dormond, O. & Nowak-Sliwinska, P. Short-term 3D culture systems of various complexity for treatment optimization of colorectal carcinoma. *Sci. Rep.* **9**, 7103 (2019).
38. Mathews Griner, L. A. *et al.* Large-scale pharmacological profiling of 3D tumor models of cancer cells. *Cell Death Dis.* **7**, e2492–e2492 (2016).
39. Yan, X. *et al.* High throughput scaffold-based 3D micro-tumor array for efficient drug screening and chemosensitivity testing. *Biomaterials* **198**, 167–179 (2019).
40. Laurent, J. *et al.* Multicellular tumor spheroid models to explore cell cycle checkpoints in 3D. *BMC Cancer* **13**, 73 (2013).
41. Sahu, N. *et al.* Cotargeting of MEK and PDGFR/STAT3 pathways to treat pancreatic ductal adenocarcinoma. *Mol. Cancer Ther.* **16**, 1729–1738 (2017).
42. Senkowski, W. *et al.* Three-dimensional cell culture-based screening identifies the anthelmintic drug nitazoxanide as a candidate for treatment of colorectal cancer. *Mol. Cancer Ther.* **14**, 1504–1516 (2015).
43. Wu, J. *et al.* Mechanism and in vitro pharmacology of TAK1 inhibition by (5Z)-7-oxozeaenol. *ACS Chem. Biol.* **8**, 643–650 (2013).
44. Bain, J. *et al.* The selectivity of protein kinase inhibitors: a further update. *Biochem. J.* **408**, 297–315 (2007).
45. Ninomiya-Tsuji, J. *et al.* A resorcylic acid lactone, 5Z-7-oxozeaenol, prevents inflammation by inhibiting the catalytic activity of TAK1 MAPK kinase kinase. *J. Biol. Chem.* **278**, 18485–18490 (2003).
46. Brüningk, S. C., Rivens, I., Box, C., Oelfke, U. & ter Haar, G. 3D tumour spheroids for the prediction of the effects of radiation and hyperthermia treatments. *Sci. Rep.* **10**, 1–13 (2020).
47. Zanoni, M. *et al.* 3D tumor spheroid models for in vitro therapeutic screening: A systematic approach to enhance the biological relevance of data obtained. *Sci. Rep.* **6**, 19103 (2016).

48. Kondo, J. *et al.* High-throughput screening in colorectal cancer tissue-originated spheroids. *Cancer Sci.* **110**, 345–355 (2019).
49. Horn, T. *et al.* High-order drug combinations are required to effectively kill colorectal cancer cells. *Cancer Res.* **76**, 6950–6963 (2016).
50. Meyer, C. T. *et al.* Quantifying drug combination synergy along potency and efficacy axes. *Cell Syst.* **8**, 97-108.e16 (2019).
51. Chen, W. *et al.* High-throughput image analysis of tumor spheroids: A user-friendly software application to measure the size of spheroids automatically and accurately. *J. Vis. Exp.* https://doi.org/10.3791/51639 (2014).
52. Flobak, Å *et al.* A high-throughput drug combination screen of targeted small molecule inhibitors in cancer cell lines. *Sci. Data* **6**, 1–10 (2019).

Acknowledgements

We would like to thank Torkild Visnes for valuable discussions and assistance with confocal microscopy. We also would like to thank Andrea Draget Hoel for assistance during robotic screening. The NCI DTP 60 cell lines were provided by the NCI-DCTD Repository in Frederick, MD (MTA #1-5578-17). The funding was provided by the Liaison Committee between the Central Norway Regional Health Authority (Samarbeidsorganet) and the Norwegian University of Science and Technology (NTNU) and The NTNU Strategic Research Area NTNU Health.

Author contributions

Conceived and designed the experiments: E.F., B.N., V.N., L.T., G.K., A.L. and Å.F. Performed the experiments: E.F. and B.N. Wrote robot scripts: V.N. and G.K. Analysed the data: E.F. and B.N. Contributed reagents/materials/analysis tools: E.F., B.N., V.N., L.T., G.K., A.L. and Å.F. Wrote the paper: E.F., B.N., V.N., L.T., G.K., A.L. and Å.F. All authors read and approved the final manuscript.

Competing interests

The authors declare no competing interests.

Additional information

Supplementary information is available for this paper at https://doi.org/10.1038/s41598-020-68441-0.

Correspondence and requests for materials should be addressed to Å.F.

Reprints and permissions information is available at www.nature.com/reprints.

Publisher's note Springer Nature remains neutral with regard to jurisdictional claims in published maps and institutional affiliations.

Supplementary Material

High-throughput screening reveals higher synergistic effect of MEK inhibitor combinations in colon cancer spheroids

Evelina Folkesson[1†], Barbara Niederdorfer[1†], Vu To Nakstad[3], Liv Thommesen[4], Geir Klinkenberg[3], Astrid Lægreid[1], Åsmund Flobak[1,2*]

[1] Department of Clinical and Molecular Medicine, Norwegian University of Science and Technology, Trondheim, Norway

[2] The Cancer Clinic, St Olav's University Hospital, Trondheim, Norway

[3] SINTEF Materials and Chemistry, Department of Biotechnology, Trondheim, Norway

[4] Department of Biomedical Laboratory Science, Norwegian University of Science and Technology, Trondheim, Norway

†These authors contributed equally to this work

*asmund.flobak@ntnu.no

Additional file 1

Supplementary Methods

Cell passaging

Long-term stored in liquid nitrogen, HCT-116, HT-29 and SW-620 cells were thawed and passaged for at least two weeks (split twice a week) before entering experiments. The standard splitting procedure included i) aspiration of old medium, ii) PBS wash (1-2 á 12 mL), iii) trypsinization (Thermo Fisher Scientific), 5 minutes at 37°C, iv) resuspension in complete growth medium (RPMI Medium 1640 (1X) supplemented with 10% fetal bovine serum (FBS), 2 mM L-Glutamine and 100 U/mL Penicillin-Streptomycin). A fraction of cells (1:10, 1:8 and 1:6 for HCT-116, HT-29 and SW-620 cells, respectively) was transferred to a new T75 flask. Final volume in T75 flask: 15 mL. Cells were passaged twice per week.

Selection of doses

Doses for the combination screen were guided by the IC20 for each single-drug observed with CellTiter-Glo in 2D and 3D cultures. IC20 calculations were performed in R (version 3.3.3) using the drc package version 3.0.1 and a five-parameter log-logistic dose-response model[1]. In cases where the lowest drug concentration used in the single-drug screen reduced viability with more than 20%, the four lowest screened doses from the single-drug screen were selected for the combination screen. In cases where the highest drug concentration reduced viability with less than 20%, the four highest screened doses from the single-drug screen were selected. In remaining cases, we selected the 4-points dose range that covered as many of the calculated IC20 values as possible for that specific drug. Note that for each drug, the same doses were selected for all cell lines in 2D and 3D.

*Table I. Seeding numbers and assay reagent concentrations (at plating). Setup 1 = cells in medium, Setup 2 = cells in medium + CellTox Green, Setup 3 = cells in medium + NucView 488 Caspase-3 Substrate. * Cells (2D, 3D) seeded in medium (Setup 1) - NucView 488 Caspase-3 Substrate added at drug addition.*

	Seeding density (cells/well); assay reagent concentration							
	Single-drug screen				**Combination screen**		**96 hours screen***	
	2D			**3D**	**2D**	**3D**	**2D**	**3D**
Cell line	**Setup 1**	**Setup 2**	**Setup 3**	**Setup 1**	**Setup 1**	**Setup 1**	**Setup 1**	**Setup 1**
HCT-116	1200; -	1200; 1:1000	1200; 3.43 µM	1200; -	1200; -	1200; -	300; -	1200; -
HT-29	3750; -	3750; 1:1000	3750; 3.43 µM	4800; -	3750; -	4800; -	900; -	4800; -
SW-620	3000; -	3000; 1:1000	3000; 3.43 µM	600; -	3000; -	600; -	900; -	600; -

Table II. Compounds and doses used in the single-drug (SDS), combination (CS) and 96 hours screen (96h).
** Primary target according to manufacturer.*

Compound	Abbreviation	Primary target*	Solvent	Doses (µM)			PubChem CID
				SDS	CS	96h	
Olaparib	OLA	PARP1, PARP2	DMSO	0.01, 0.05, 0.25, 1.25, 2.5, 5.0, 10, 20	2.5, 5, 10, 20	Not included	23725625
Palbociclib	PAL	CDK4, CDK6	Water		0.25, 1.25, 2.5, 5	Not included	11478676
PD0325901	PD	MEK1, MEK2	DMSO		0.01, 0.05, 0.25, 1.25	0.01, 0.05, 0.25, 1.25	9826528
PI-103	PI	PI3K (p110α/β/γ/δ)	DMSO		0.01, 0.05, 0.25, 1.25	0.01, 0.05, 0.25, 1.25	9884685
5Z-7-Oxozeanol	5Z	TAK1	DMSO		0.01, 0.05, 0.25, 1.25	0.01, 0.05, 0.25, 1.25	9863776
5-Fluorouracil	5-FU	Thymidylate synthase	DMSO		2.5, 5, 10, 20	2.5, 5, 10, 20	3385
Oxaliplatin	OXA	DNA synthesis	Water		0.05, 0.25, 1.25, 2.5	0.05, 0.25, 1.25, 2.5	4609

Table III. Readouts per culture format in single-drug (SDS), combination (CS) and 96 hours screen (96h). Assays, as well as readout time points, are indicated. Confluency and apoptosis were assessed by imaging two views per well.

Culture format	**Readout**	**Assay reagent**	**Detection method**	**Time point (h)**		
				SDS	**CS**	**96h**
2D	Viability	CellTiter-Glo 2.0	Luminescence	48	48	96
	Confluency	-	Brightfield imaging	0, 6, 12, 18, 24, 30, 36, 48	48	0, 12, 24, 48, 72, 96
	Cell death	CellTox Green	Fluorescence	0, 6, 12, 18, 24, 30, 36, 48	-	-
	Apoptosis	NucView 488	Fluorescence imaging	0, 6, 12, 18, 24, 30, 36, 48	-	0, 12, 24, 48, 72, 96
3D	Viability	CellTiter-Glo 3D	Luminescence	48	48	96
	Size	-	Brightfield imaging	0, 48	48	0, 24, 48, 72, 96
	Apoptosis	NucView 488	Fluorescence imaging	-	-	0, 24, 48, 72, 96

Table IV. R packages used for data processing and graphics.

Execution	Package	Version	Comment
Data processing	tidyr	0.8.3	R version 3.5.1
	dplyr	0.8.1	R version 3.5.1
	lattice	0.20.38	R version 3.5.1
	PharmacoGx	1.12.0	R version 3.5.2
Graphics	ggplot2	3.2.0	R version 3.5.3
	ComplexHeatmap[2]	1.20.0 2.3.2	R version 3.5.3
	ggpubr	0.2	R version 3.5.3
	gridExtra	2.3	R version 3.5.3
	ggrepel	0.8.1	R version 3.5.3
	grid	3.5.3	R version 3.5.3
	UpsetR[3]	1.4.0	R version 3.5.3

References

1. Gottschalk, P. G. & Dunn, J. R. The five-parameter logistic: A characterization and comparison with the four-parameter logistic. *Anal. Biochem.* **343**, 54–65 (2005).
2. Gu, Z., Eils, R. & Schlesner, M. Complex heatmaps reveal patterns and correlations in multidimensional genomic data. *Bioinformatics* **32**, 2847–2849 (2016).
3. Lex, A., Gehlenborg, N., Strobelt, H., Vuillemot, R. & Pfister, H. UpSet: Visualization of Intersecting Sets. *IEEE Trans. Vis. Comput. Graph.* **20**, 1983–1992 (2014).

Additional file 2

Supplementary Tables

Table S1 - IC20 (µM) values estimated from viability data (single-drug screen). Non-computable IC20 values are indicated by NaN in the table. Estimated IC20 values outside screening range (0.01-20 µM) are indicate by < D.r. and > D.r..

	IC20 (µM)					
Drug	**HCT-116**		**HT-29**		**SW-620**	
	2D	**3D**	**2D**	**3D**	**2D**	**3D**
OLA	NaN	NaN	NaN	< D.r.	NaN	NaN
PAL	2.33 ± 0.85	0.47 ± 2.13	5.26 ± 0.17	NaN	2.70 ± 3.78	0.013 ± 0.47
PD	0.02 ± 0.33	< D.r.	< D.r.	0.01 ± 0.02	< D.r.	< D.r.
PI	0.41 ± 0.11	0.93 ± 0.12	> D.r	NaN	0.38 ± 0.05	0.10 ± NA
5Z	0.29 ± 0.06	0.07 ± 0.04	0.06 ± NA	0.01 ± NA	0.45 ± 0.09	0.06 ± NA
5-FU	3.49 ± 0.52	3.28 ± 0.62	11.58 ± 2.65	NaN	13.60 ±7.34	NaN
OXA	0.47 ± 0.07	1.01 ± 0.16	2.90 ± NA	< D.r.	0.06 ± 0.09	0.26 ± 0.05

Table S2 – Synergistic drug combinations (x) per readout and cell line. Average Bliss score per 5x5 matrix was calculated for all drug combinations per readout and cell line. Imaging corresponds to assessment of confluency and size in 2D and 3D cultures, respectively.

Synergistic drug combinations	HCT-116				HT-29				SW-620			
	Viability		Imaging		Viability		Imaging		Viability		Imaging	
	2D	3D	2D	3D	2D	3D	2D	3D	2D	3D	2D	3D
5Z + PAL	X		X	X	X		X		X		X	
5Z + PI	X		X		X		X	X	X		X	
PD + OLA	X	X	X				X			X		X
PD + PI	X	X	X		X		X	X				
5-FU + PAL	X	X	X	X								
PD + OXA		X			X	X		X				
PD + PAL	X		X		X		X					
OLA + 5Z	X					X	X					
OXA + PAL	X		X		X							
PAL + OLA	X	X	X									
PI + OLA	X		X									X
5Z + OXA					X			X				
OLA + 5-FU		X								X		
OXA + 5-FU					X		X					
5-FU + PD						X						
5-FU + PI							X					
5Z + 5-FU							X					

Table S3 – Average Coefficient of Variation (%) per biological replicate and readout. Average CV values were calculated by averaging those per condition (treatment) within each biological replicate and readout.

Readout	**Average CV (%)**	
	Rep 1	**Rep 2**
Viability 2D	6.01	6.90
Confluency 2D	3.03	4.95
Viability 3D	9.59	9.55
Size 3D	4.19	3.88

Supplementary Figures

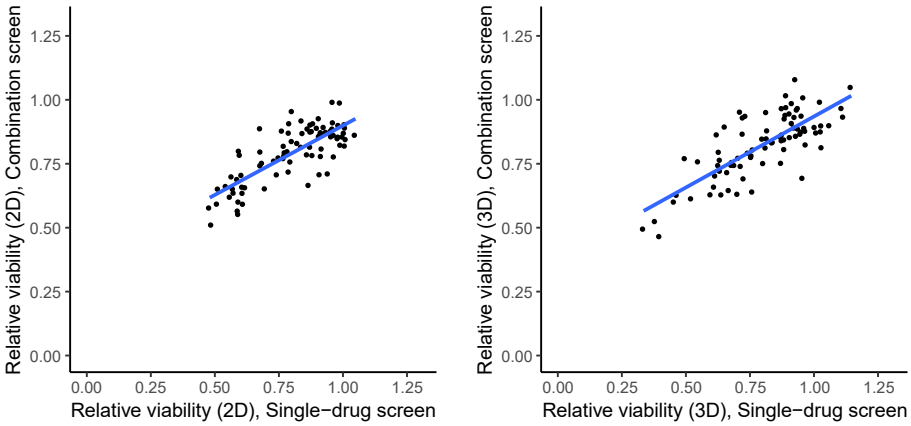

Figure S1 - Inter-experiment reproducibility for single-drug and combination screens. (a) Correlation plots showing Pearson's correlation between data points (viability) common for the single-drug dose-response screen and the combination screen in 2D and (b) 3D.

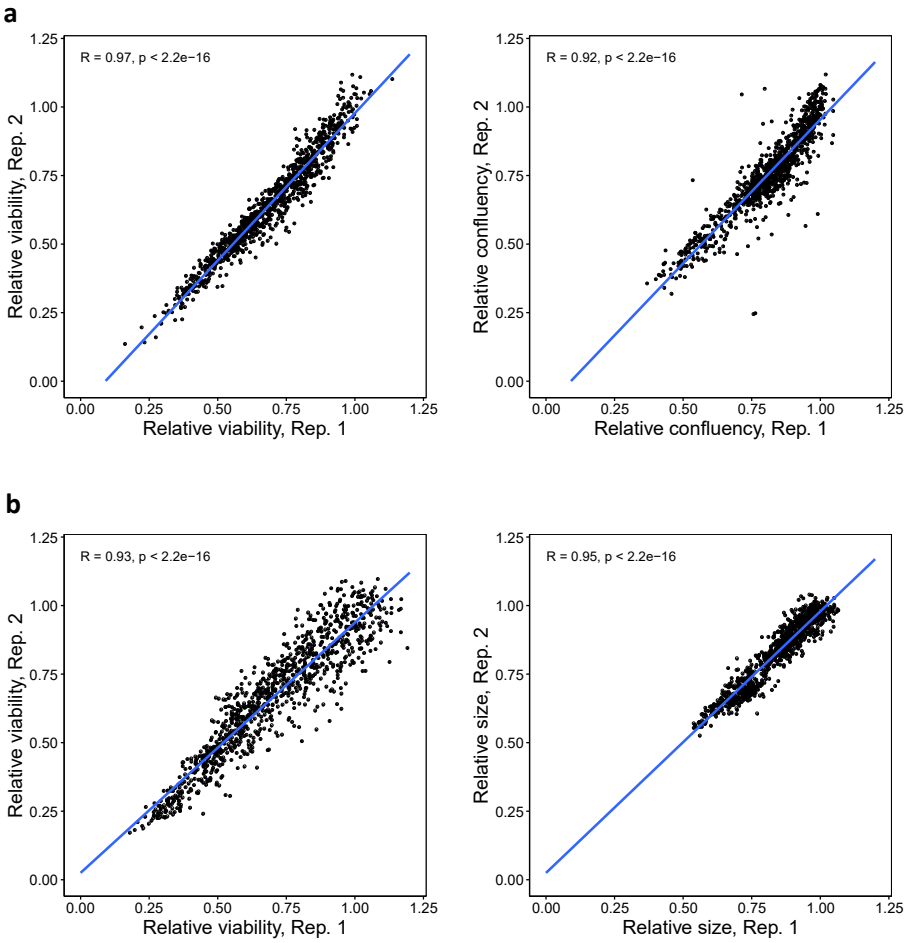

Figure S2 - Intra-experiment reproducibility for the combination screen. (a) Correlation plots showing Pearson's correlation between replicates per readout in 2D and (b) 3D.

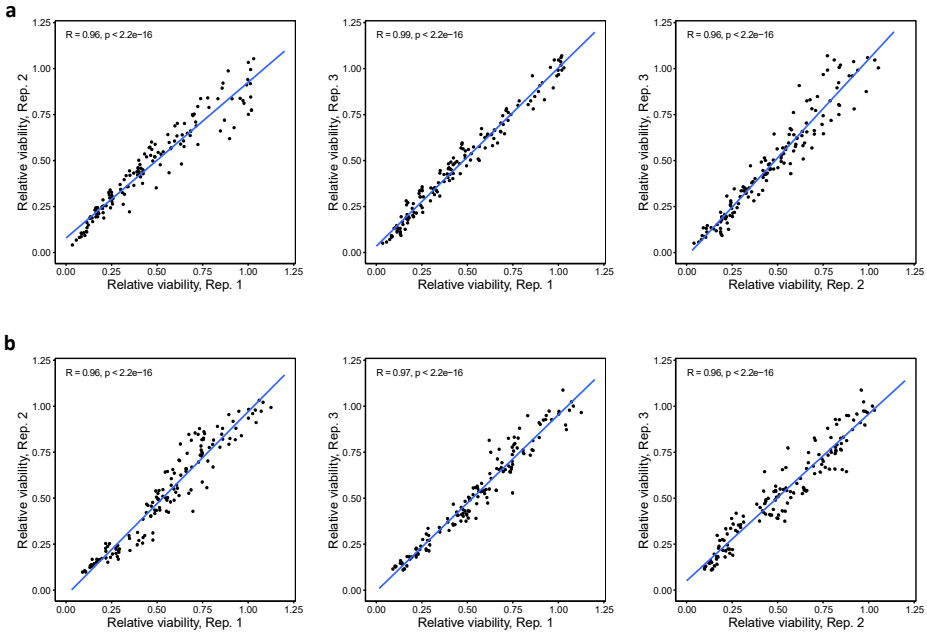

Figure S3 - Intra-experiment reproducibility for the 96 hours screen. (a) Correlation plots showing Pearson's correlation between replicates (viability) in 2D and (b) 3D.

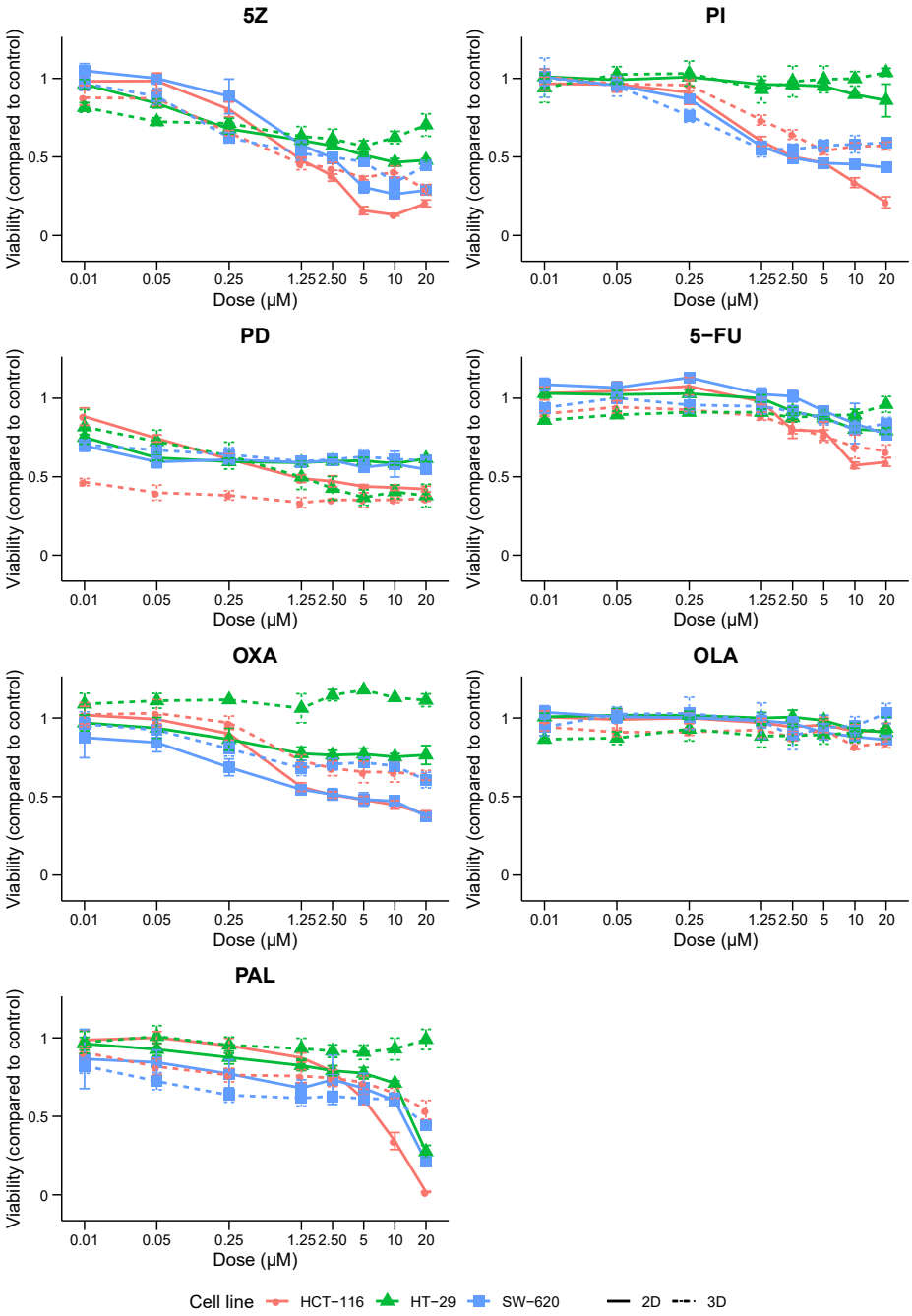

Figure S4 - Single-drug dose-response viability data (endpoint, 48h). Relative viability of HCT-116, HT-29 and SW-620 cells upon exposure to seven single compounds as measured by CellTiter-Glo.

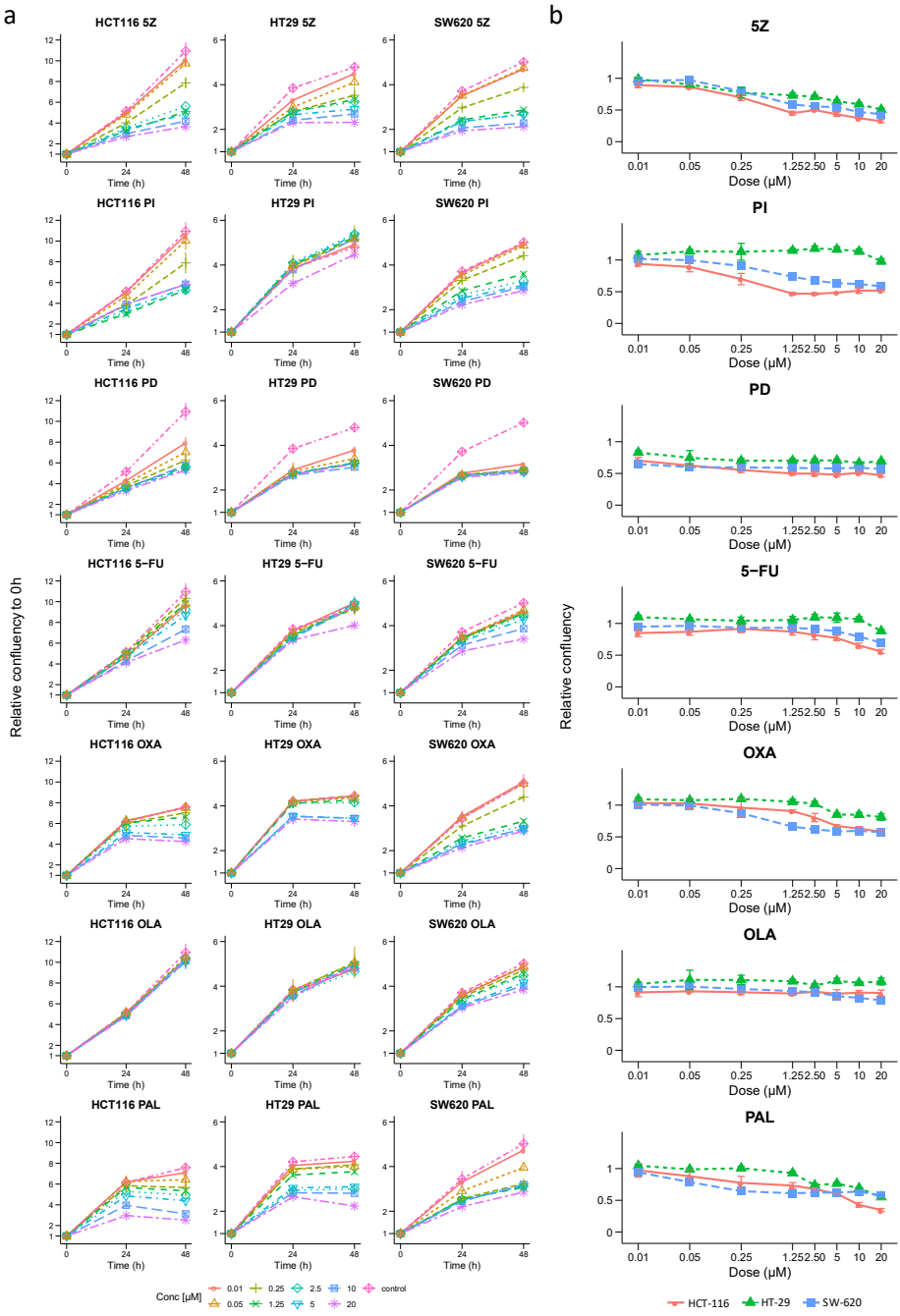

Figure S5 - Single-drug dose-response confluency data. Cellular confluency of HCT-116, HT-29 and SW-620 cells upon exposure to seven single-compounds as measured by brightfield imaging. (a) Continuous confluency compared to 0h. Control shows cell growth of internal plate control. (b) Relative confluency at endpoint (48h) compared to vehicle control and 0h.

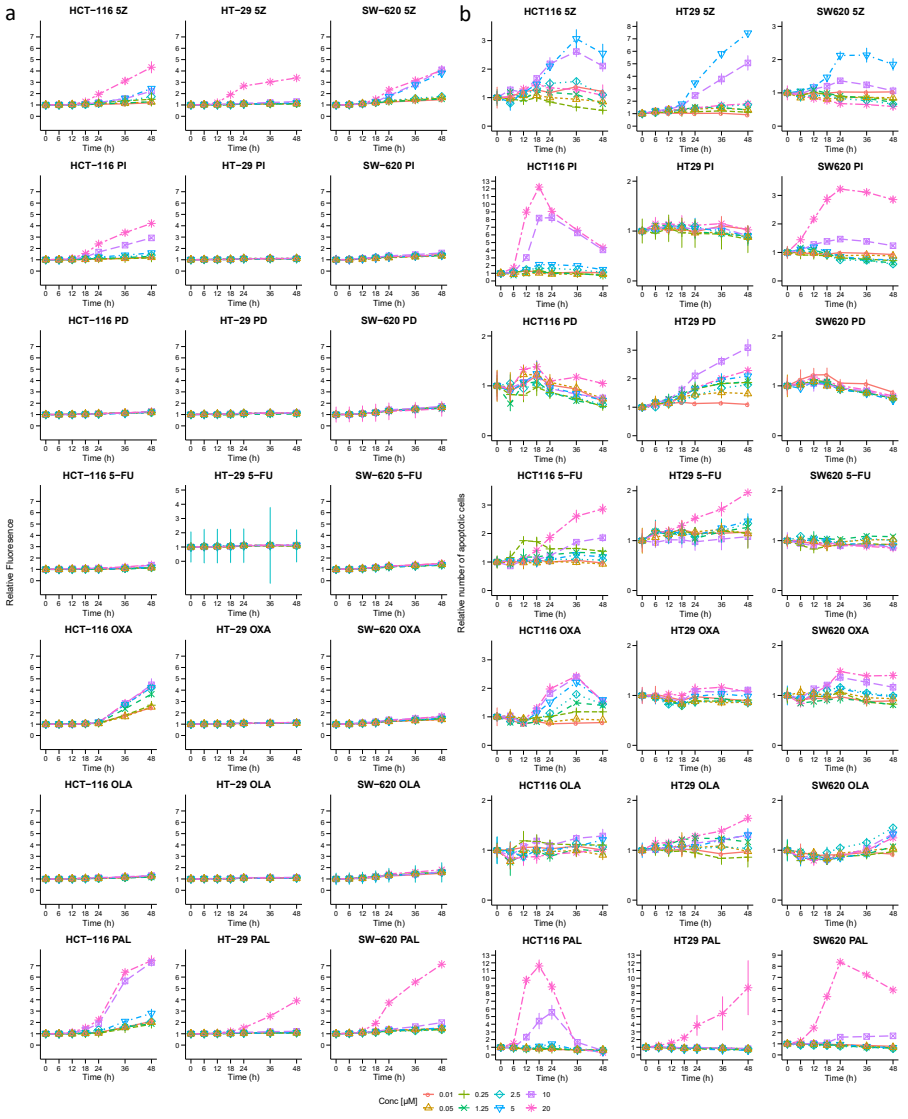

Figure S6 - Single-drug dose-response cell death data (continuous). (a) Relative cell death of HCT-116, HT-29 and SW-620 cells upon exposure to seven single-compounds at doses 0.01 – 20 μM, as measured by CellTox-Green (cell membrane integrity) and (b) NucView (apoptosis).

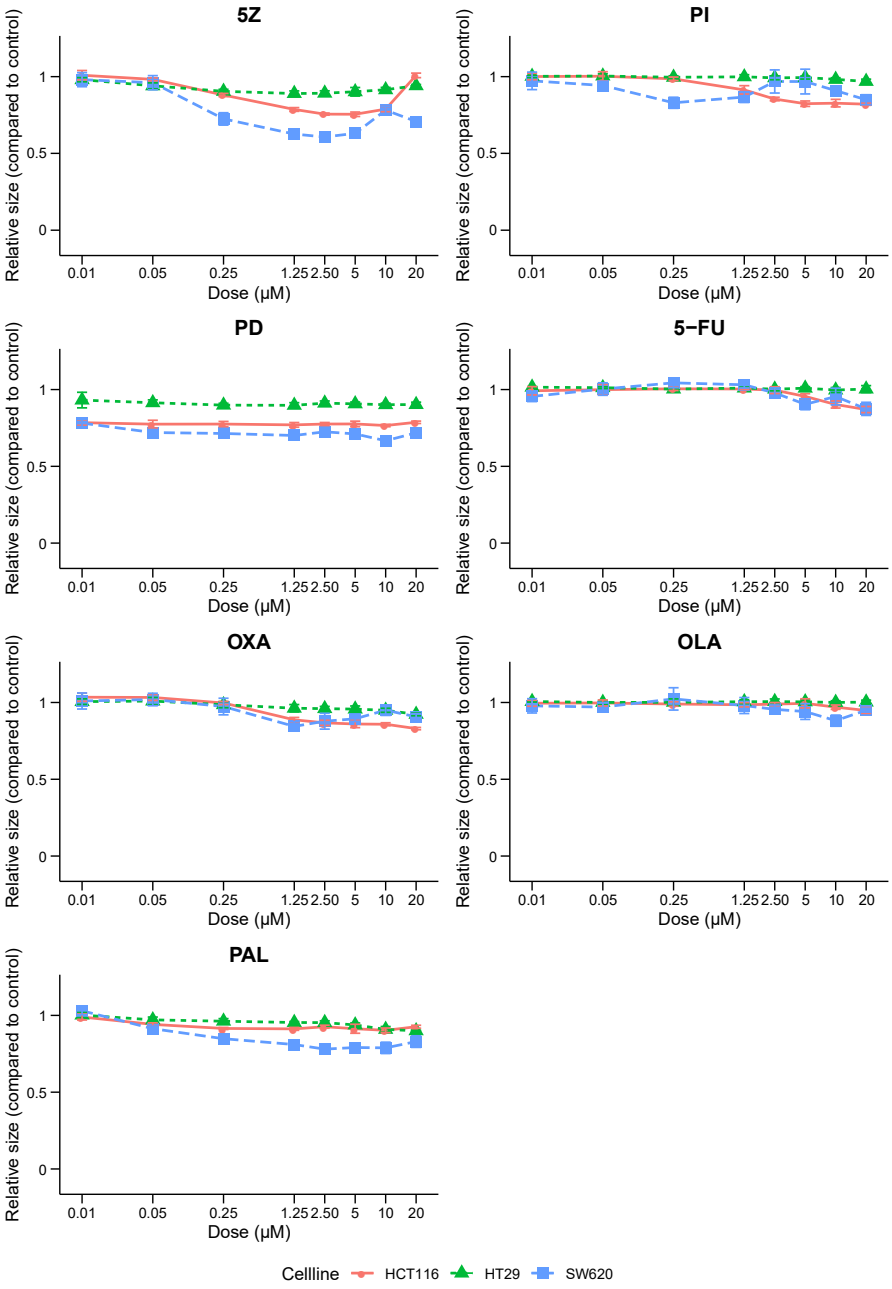

Figure S7 - Single-drug dose-response spheroid size data (endpoint, 48h). Relative spheroid size of HCT-116, HT-29 and SW-620 spheroids upon exposure to seven single-compounds as measured by brightfield imaging.

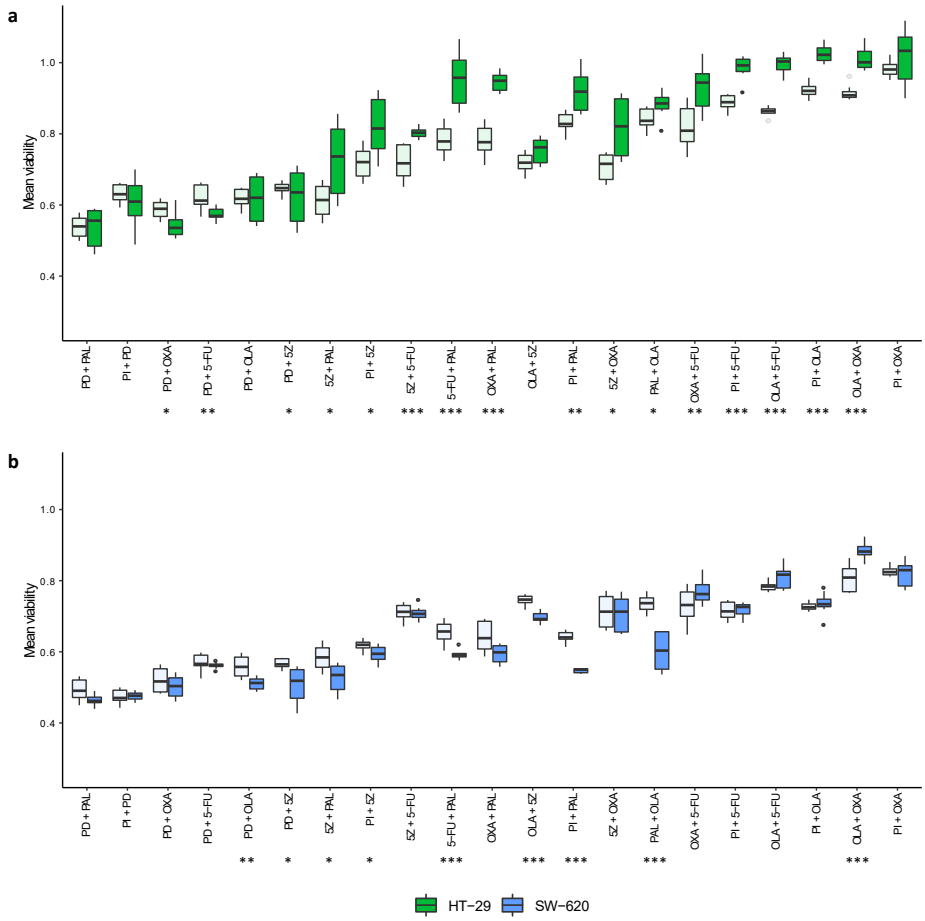

*Figure S8 - Average viability in the combination screen (endpoint, 48h). (a) Viability averaged across the matrix per drug combination and culture format (2D = light, 3D = dark) in HT-29, and (b) SW-620 cells. Asterisks (*) indicate statistically significant difference in average viability between 2D and 3D cultured cells per drug combination, with $p \leq 0.05$, $p \leq 0.01$ and $p \leq 0.001$ for *, ** and ***, respectively.*

HCT-116

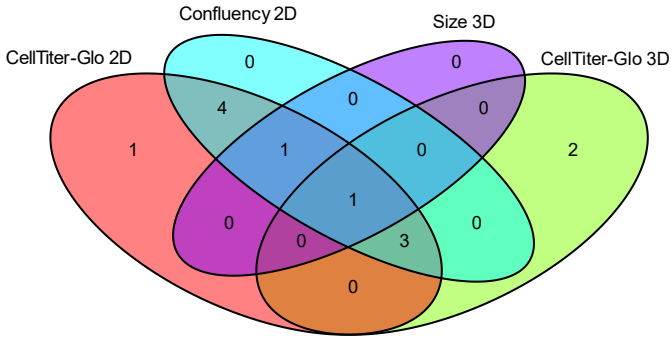

HT-29

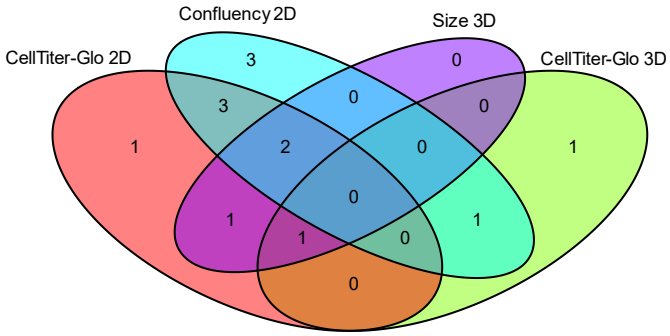

SW-620

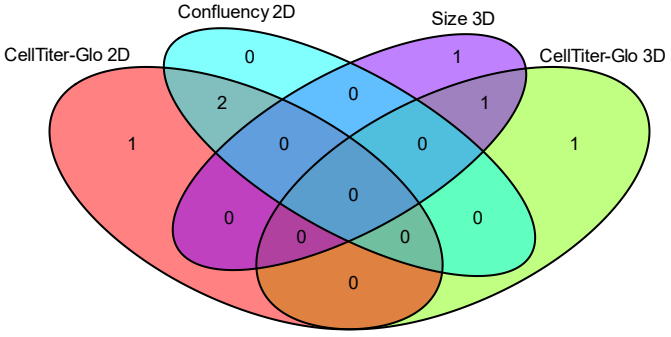

Figure S9 - Venn diagrams showing the number of synergistic drug combinations identified by one or more readouts. Here, synergy is defined as an overall Bliss excess < 0 when data points are averaged over the 5x5 matrix per cell line and drug combination.

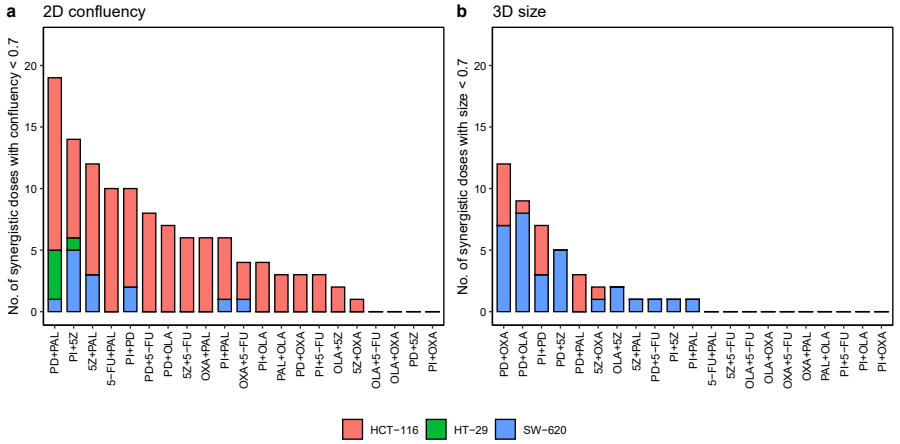

Figure S10 - Number of synergistic doses per combination, cell line and culture format, which reduce confluency or spheroid size to < 0.7. Empty positions along the x-axis indicate combinations for which no doses were observed to fulfil this (alphabetically per culture format).

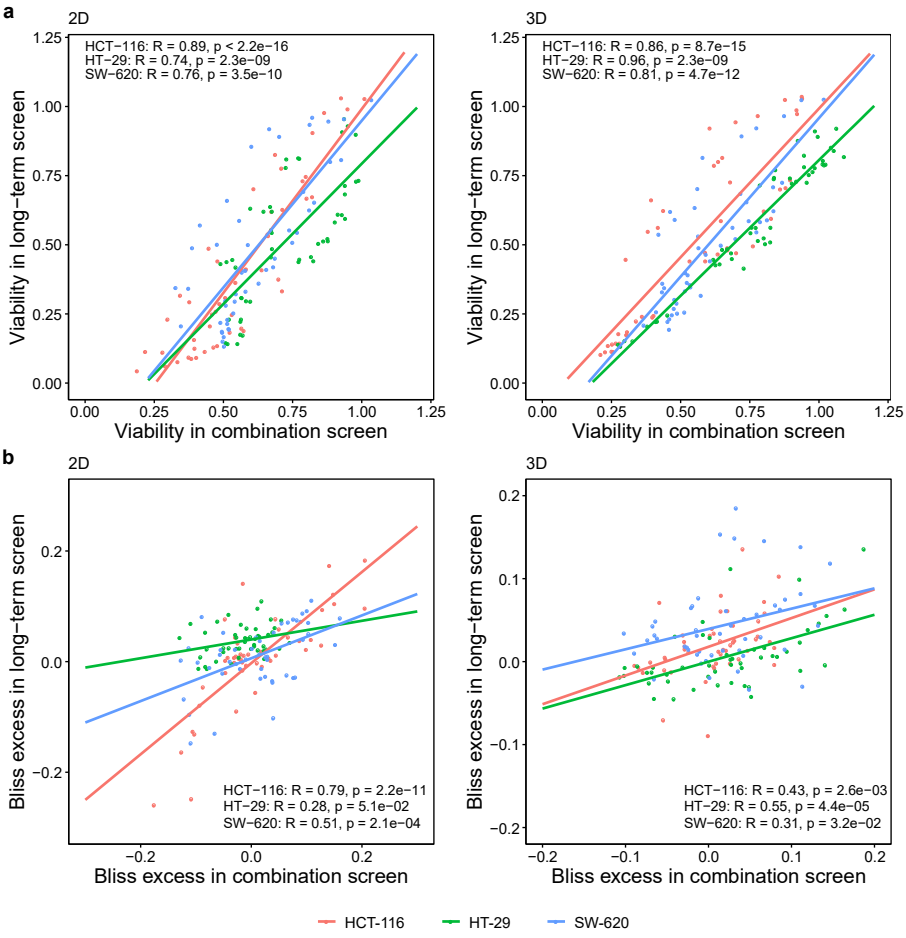

Figure S11 - Combination and 96 hours (here referred to as long-term) screen viability and Bliss excess correlation. (a) Pearson's correlation between viability at 48h (combination screen) and 96h (long-term screen) in 2D (left) and 3D (right), and (b) Bliss excess scores at 48h (combination screen) and 96h (long-term screen) in 2D (left) and 3D (right).

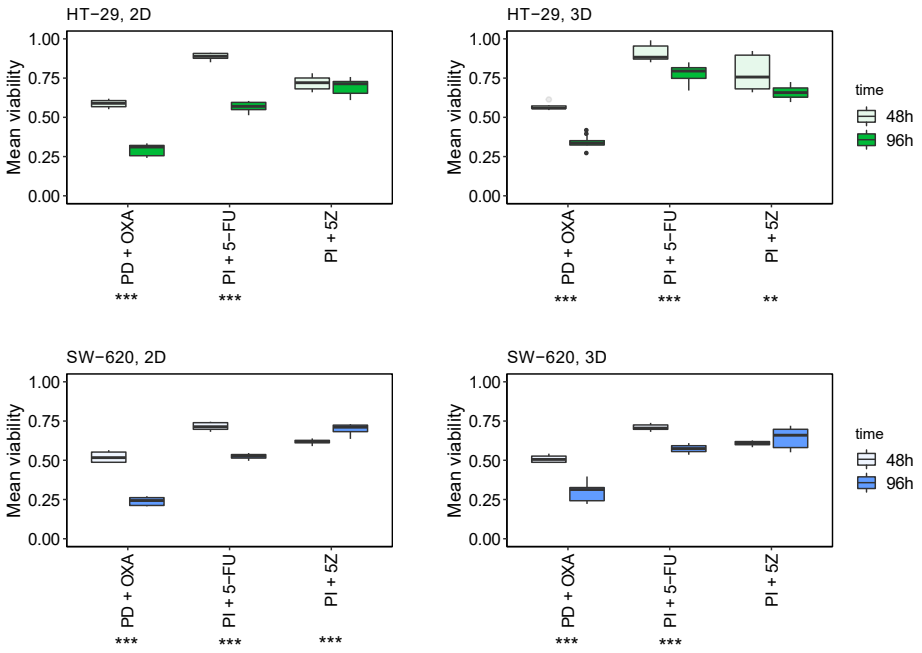

*Figure S12 - Average viability per combination in the combination and 96 hours screens. Viability of 2D (left) and 3D (right) cultured HT-29 and SW-620 cells in the combination screen (48h = light) and 96 hours screen (96h = dark). Viability was averaged across the matrix per drug combination, culture format and time-point. Asterisks (*) indicate statistically significant difference in average viability between 48h and 96h per drug combination, with p ≤ 0.05, p ≤ 0.01 and p ≤ 0.001 for *, ** and ***, respectively.*

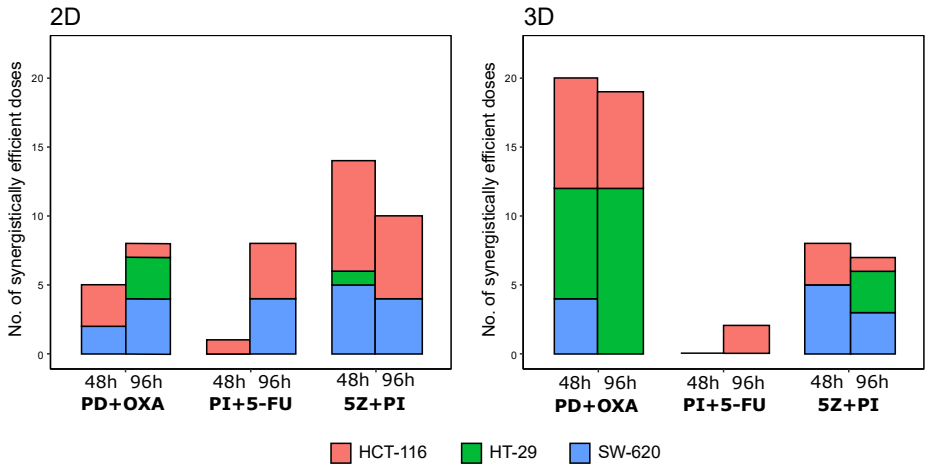

Figure S13 - Number of synergistically effective doses per combination, cell line and culture format at 48h (high-throughput screen) and 96h (96 hours screen).

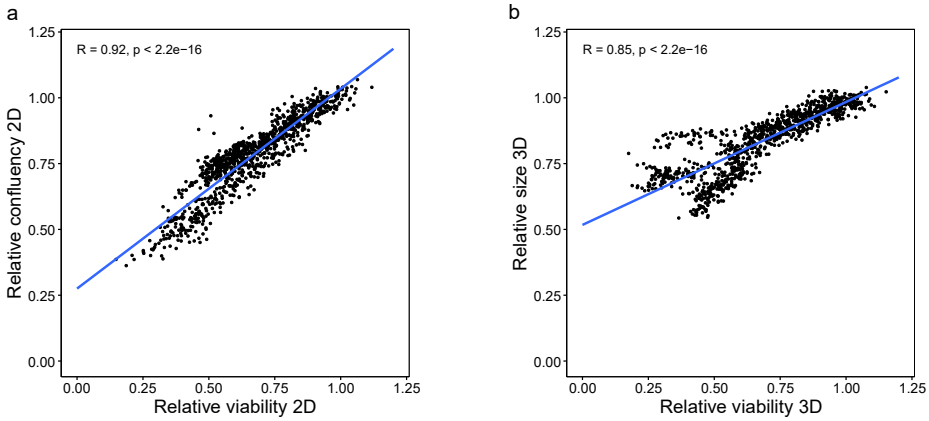

Figure S14 - Correlation between relative readout response in the combination screen in a) 2D, and b) 3D-cultured cells.

Paper II

Synergistic effects of complex drug combinations in colorectal cancer cells predicted by logical modelling

Evelina Folkesson[1], B. Cristoffer Sakshaug[1], Andrea D. Hoel[2], Geir Klinkenberg[2], Åsmund Flobak[1,3]

1. Department of Clinical and Molecular Medicine, Norwegian University of Science and Technology, Trondheim, Norway
2. Department of Biotechnology, SINTEF Materials and Chemistry, Trondheim, Norway
3. The Cancer Clinic, St Olav's University Hospital, Trondheim, Norway

Keywords: colorectal cancer, logical modelling, drug combinations, synergy

Funding: This project was funded by the Liaison Committee between the Central Norway Regional Health Authority (Samarbeidsorganet) and the Norwegian University of Science and Technology (NTNU).

Corresponding author:
Åsmund Flobak
Address: Prinsesse Kristinas gate 1, 7030 Trondheim, Norway
E-mail: asmund.flobak@ntnu.no,
Phone: +47 72 57 37 17

Conflict of interest: The authors declare no conflicts of interest.

Paper III

Growth and drug responses of patient-derived colorectal tumour spheroids evaluated with imaging

Evelina Folkesson[1,2✢], Baard Cristoffer Sakshaug[1✢], Tonje Husby Haukaas[2], Margrét Sylvía Sigfúsdóttir[2], Torkild Visnes[2], Arne Wibe[3], Liv Thommesen[4], Astrid Lægreid[1], Geir Klinkenberg[2], Åsmund Flobak[1,5]

1. Department of Clinical and Molecular Medicine, Norwegian University of Science and Technology, Trondheim, Norway
2. Department of Biotechnology, SINTEF Materials and Chemistry, Trondheim, Norway
3. Department of Surgery, St Olav's University Hospital, Trondheim, Norway
4. Department of Biomedical Laboratory Science, Norwegian University of Science and Technology, Trondheim, Norway
5. The Cancer Clinic, St Olav's University Hospital, Trondheim, Norway

✢ These authors contributed equally: Evelina Folkesson and Cristoffer Sakshaug

Keywords: colorectal cancer, patient-derived tumour spheroids, chemotherapy, imaging

Funding: This project was funded by The Research Council of Norway, The Liaison Committee between the Central Norway Regional Health Authority (Samarbeidsorganet) and the Norwegian University of Science and Technology (NTNU).

Corresponding author:
Åsmund Flobak
Address: Prinsesse Kristinas gate 1, 7030 Trondheim, Norway
E-mail: asmund.flobak@ntnu.no,
Phone: +47 72 57 37 17

Conflict of interest: The authors declare no conflicts of interest.

ISBN 978-82-326-6092-6 (printed ver.)
ISBN 978-82-326-5440-6 (electronic ver.)
ISSN 1503-8181 (printed ver.)
ISSN 2703-8084 (online ver.)

NTNU
Norwegian University of
Science and Technology